

A Thesis Submitted for the Degree of PhD at the University of Warwick

Permanent WRAP URL:

<http://wrap.warwick.ac.uk/111069>

Copyright and reuse:

This thesis is made available online and is protected by original copyright.

Please scroll down to view the document itself.

Please refer to the repository record for this item for information to help you to cite it.

Our policy information is available from the repository home page.

For more information, please contact the WRAP Team at: wrap@warwick.ac.uk



Modeling From a Trader's Perspective

by

Jun Maeda

Thesis

Submitted to the University of Warwick

for the degree of

Doctor of Philosophy

Department of Statistics

August 2018

THE UNIVERSITY OF
WARWICK

Contents

| | |
|---|-------------|
| List of Tables | iv |
| List of Figures | vi |
| Acknowledgments | viii |
| Declarations | ix |
| Abstract | x |
| Chapter 1 Introduction | 1 |
| 1.1 New Model | 1 |
| 1.1.1 Autocallables | 1 |
| 1.1.2 Problem with Autocallable Trades | 4 |
| 1.1.3 A Solution | 8 |
| 1.2 Approximating the Solution of Semilinear PDE with PIA | 11 |
| 1.3 Technical Analysis | 12 |
| Chapter 2 Modeling via Market Driver | 16 |
| 2.1 Introduction | 16 |
| 2.2 The Market Driver Model | 19 |
| 2.3 Partial Differential Equations | 22 |
| 2.4 Control Problem | 24 |
| 2.5 Policy Improvement Algorithm | 25 |
| 2.6 Numerical Simulation | 30 |
| 2.6.1 First Example | 30 |
| 2.6.2 Second Example | 35 |
| 2.6.3 PIA on the Example in Subsection 2.6.1 | 37 |
| 2.7 Conclusions | 39 |

| | |
|---|-----------|
| Chapter 3 Quadratic Local Convergence of the PIA | 40 |
| 3.1 Introduction | 40 |
| 3.2 Setup | 41 |
| 3.3 Main Results | 43 |
| 3.4 Numerical Example | 44 |
| 3.4.1 First Example | 44 |
| 3.4.2 Second Example | 49 |
| 3.5 Conclusion and Open Questions | 52 |
| | |
| Chapter 4 Modeling Technical Analysis | 54 |
| 4.1 Introduction | 54 |
| 4.2 Setup | 58 |
| 4.3 Selling Problem | 59 |
| 4.3.1 The Case Where $m \leq L$ | 62 |
| 4.3.2 $m \geq L$ Case | 62 |
| 4.3.3 Solving the Optimal Stopping Problem | 63 |
| 4.3.4 Maximizer in the Case of $m \leq L$ | 63 |
| 4.3.5 Maximizer in the Case where $m \geq L$ | 68 |
| 4.3.6 Optimal Stopping Problem | 72 |
| 4.4 Optimal Timing of Buying | 74 |
| 4.5 Conclusions | 76 |
| | |
| Bibliography | 77 |
| | |
| Appendix A Derivation of Heston's PDE (2.3) | 84 |
| | |
| Appendix B Lemmas for Chapter 2 | 86 |
| | |
| Appendix C Numerical Calculations on Autocallables under Market Driver Model | 91 |
| C.1 Pricing Autocallable as the Market Driver | 91 |
| C.2 Pricing Straddle under the Concentration in Autocallable | 93 |
| C.3 Pricing Another Autocallable under the Concentration in Autocallable | 93 |
| C.4 Summary | 94 |
| | |
| Appendix D Proof of Theorem 3.3.1 | 96 |
| | |
| Appendix E Arbitrage-free Markets | 99 |
| E.1 Introduction | 99 |

| | | |
|-------|--|-----|
| E.2 | No Arbitrage for the New Model | 99 |
| E.3 | No Arbitrage in the Technical Analysis Setup | 100 |
| E.3.1 | Technical Analysis Setup | 100 |
| E.3.2 | No Arbitrage | 101 |

List of Tables

| | | |
|-----|--|----|
| 1.1 | An example of the detail of the autocallable structure. | 5 |
| 2.1 | Parameters for numerical simulation. | 30 |
| 2.2 | Summary for 120 call at $S = 98.255$ and $v = 0.030049$ | 31 |
| 2.3 | Summary for at-the-money (ATM) call at $S = 98.255$ and $v = 0.030049$ | 31 |
| 2.4 | Implied volatility calculated based on the risk calculated in the Heston model. | 32 |
| 2.5 | Summary for 120 call at $S = 98.255$ and $v = 0.030049$ | 35 |
| 2.6 | Summary for at-the-money (ATM) call at $S = 98.255$ and $v = 0.030049$ | 36 |
| 2.7 | Implied volatility calculated based on the risk calculated in the Heston model. | 36 |
| 2.8 | Largest differences in absolute value between the numerical solutions of the approximated linear PDE and the original semilinear PDE. The figures could be regarded as the differences in percentage against the initial price of the stock as it is set to 100. | 37 |
| 3.1 | Parameters we use for the numerical calculation. | 45 |
| 3.2 | Calculation load comparison for successful convergence. One calculation here means solving the difference equation (3.25) once at one point. | 47 |
| 3.3 | Detail of the calculations in the PIA. | 48 |
| 3.4 | Parameters we use for the numerical calculation. | 50 |
| 3.5 | Calculation load comparison for successful convergence. One calculation here means solving the difference equation (3.37) once at one point. | 51 |
| 3.6 | Detail of the calculations in the PIA. | 52 |
| C.1 | Detail of the autocallable structure in concentration. | 91 |

| | | |
|-----|---|----|
| C.2 | Summary for the autocallable that is the market driver at $S = 98.255$ and $v = 0.030001$ | 92 |
| C.3 | Detail of the straddle we price. | 93 |
| C.4 | Summary for the straddle given the existence of the autocallable described in Section C.1 as the market driver at $S = 98.255$ and $v = 0.030001$ | 93 |
| C.5 | Detail of a different autocallable to be priced given the concentration of the structure given in Table C.1. | 93 |
| C.6 | Summary for the autocallable in Table C.5 given another autocallable described in Section C.1 as the market driver at $S = 98.255$ and $v = 0.030001$ | 94 |
| C.7 | Implied volatilities calculated based on the risk figures from the Heston model. | 95 |

List of Figures

| | | |
|-----|---|----|
| 1.1 | Graph showing how vega moves with respect to the underlying price. Note that the minimum vega is obtained around the average of the barrier levels, which is at 95. | 5 |
| 1.2 | Graph showing how vega moves with respect to the implied variance. | 6 |
| 1.3 | Graph showing the Nikkei 225 index level (in solid line) and 3 year implied volatility level (in dotted line) between the years 2011 and 2013. We see that the sharp fall in the volatility around the end of the year 2012 with the Nikkei 225 level staying around the level 8,500. We also see a sharp increase in the index and its volatility around the beginning of the year 2013. | 8 |
| 1.4 | With larger supply, the mean variance \bar{v} comes lower to \bar{v}' | 10 |
| 1.5 | The positive region is the region $[SR - \delta_1, \infty)$ where the price process takes the positive regime. Similarly, the negative region is the region $(0, SR + \delta_2]$ where the price process takes the negative regime. $[SR - \delta_1, SR + \delta_2]$ is where the underlying price process can be in either regimes. | 15 |
| 2.1 | Simulation of the SDEs (2.4) for the first 6 months starting from $S = 100$ and $v = 0.04$ with F being the value of the 2Y 120 call in (a) Heston model and (b) the new model. The difference in the values of the two prices is shown in (c) where the largest difference in absolute value is 1.3248, which corresponds to 132.48 basis points to the initial stock price. We used the drift $\mu = 0.05$. (d) shows how the vega of the call in the new model changes over time. | 33 |
| 2.2 | The volatility processes on the same simulation as in Figure 2.1 in (a) Heston model and (b) the new model. The difference in values shown in (c). | 34 |

| | | |
|-----|--|----|
| 2.3 | Risks of the calls; Top 3 charts are for the 120 call and the bottom 3 are for the ATM call. The solid lines indicate the risks calculated in the new model and the dotted lines the corresponding risks calculated in the Heston model. | 35 |
| 2.4 | The differences plotted between the values in the new model and the Heston model from Figure 2.3. | 36 |
| 2.5 | PIA results for the 120 call. Dotted line is the solution using Finite Difference Method (FDM) directly on the semilinear PDE. v is taken as $v = 0.040048$ | 37 |
| 2.6 | Magnification around at-the-money of Figure 2.5. We see that the first iteration already approximates well the numerical solution to the semilinear PDE. | 38 |
| 3.1 | Graphs of the data in Table 3.3. (a) the maximum of $ \pi_i - \pi_{i-1} $ in each step, (b) the maximum of $ V^{\pi_i} - V^{\pi_{i-1}} $ in each step, and (c) the number of calculations in each step. | 48 |
| 3.2 | Graphs of the data in Table 3.6. (a) the maximum of $ \pi_i - \pi_{i-1} $ in each step, (b) the maximum of $ V^{\pi_i} - V^{\pi_{i-1}} $ in each step, and (c) the number of calculations in each step. | 52 |
| 4.1 | Example of (a) the support and (b) the resistance levels. Note that the levels are not hard limits, and the price can fluctuate around the levels. | 55 |
| 4.2 | An example of a line being both the support and resistance level. . . | 56 |
| C.1 | Premiums and risks of the concentrated autocallable at time $t = 0$. Solid lines indicate those in the new model and dotted lines those in the Heston model. | 92 |
| C.2 | Premiums and risks of the straddle under the risk concentration in the autocallable. Solid lines indicate those in the new model and dotted lines those in the Heston model without any assumptions on risk concentration. | 94 |
| C.3 | Premiums and risks of the autocallable described in Table C.6 under the concentration of another autocallable specified in Table C.1. Solid lines indicate those in the new model and dotted lines those in the Heston model without any concentrations. | 95 |

Acknowledgments

First of all, I would like to thank my supervisor, Professor Saul D. Jacka for his guidance, support, and advice during my studies at the University. I spent more than eight years away from the academia, so it was, of course, not easy to recall mathematics in the field of quantitative finance. However, I believe it was even more difficult for him to supervise me over my research. Even when he was short of time, he scheduled a meeting with me every week. I learned many important things from him.

Secondly, I want to thank people at the Department of Statistics who supported me in my research in every aspect. With available fundings from the Department, I was able to visit many conferences and to present our work outside of the University. Research from other students and faculties in the Department stimulated my interest and I was able to even learn something outside of my field of research.

Thirdly, I want to thank people with whom I have worked in the industry prior to coming to Warwick. Starting as an analyst in the equity derivatives trading desk at an investment bank, I received much support in gaining trading and programming skills that are helpful even in my academic career. I want to also thank people who supported me in coming back to academia. Without their support, I could not have accomplished the research I worked on during my stay in Warwick.

Finally, I want to thank my family, especially my wife, Kumi, for her support during our stay in Warwick.

Declarations

This thesis is submitted to the University of Warwick in support of my application for the degree of Doctor of Philosophy. It has been composed by myself and has not been submitted in any previous application for any degree. All the works are joint works with my supervisor Professor Saul D. Jacka. The content of the chapters are in preparation for publications and uploaded in the arXiv as preprints:

- J.Maeda and S. D. Jacka, *A market driver volatility model via policy improvement algorithm*, [arXiv: 1612.00780].
- J.Maeda and S. D. Jacka, *Modeling technical analysis*, [arXiv: 1707.05253].
- J.Maeda and S. D. Jacka, *Evaluation of the rate of convergence in the PIA*, [arXiv: 1709.06466].

Abstract

I was trading professionally in the years 2006–2014 in the equity derivatives market. This thesis deals with two of the ideas inspired by my experience as a professional trader.

The first topic deals with the pricing of a derivatives product in the market with a specific risk concentration. We call the product that causes the concentration a market driver. When the market driver exists, not only the market driver itself, but any derivatives product will not be priced fairly. We introduced a new model based on the Heston model that accounts for the concentration. The model leads to a pair of partial differential equations (PDEs): one semilinear parabolic PDE to price the market driver and one linear parabolic PDE to price all the other products.

In solving the semilinear PDE, we use the policy improvement algorithm (PIA) to approximate the solution with those of linear PDEs. We show that the approximated solutions satisfy quadratic local convergence (QLC) which explains the efficiency of the algorithm. This efficiency of the algorithm is proved in a more general setup.

The other idea sparked by my experience that is explored in the last chapter of the thesis concerns modeling technical analysis. Technical analysis is a family of methods that traders use to make decisions to purchase/sell assets. There is no mathematical proof that shows that they are correct as far as I am aware. We focus on one of the methods, the method of support and resistance levels, and used the optimal stopping argument to show the validity of the method. As far as I know, this is one of the first results to mathematically prove the effectiveness of a method in technical analysis.

Chapter 1

Introduction

1.1 New Model

Japan is currently the third largest economy in terms of Gross Domestic Product (GDP), and its derivatives market is one of the biggest in the world. Due to the low interest rate in the country, investors seek high coupons that are paid for a long period of time. Because of this, the product called autocallable is very popular and indeed has become the most traded derivatives product in the country.

1.1.1 Autocallables

The product is an equity-linked structured product with a form of bond or swap. There are several variations, but let us introduce the most popular one.

Let us define the following variables:

- S_0 : initial price of the underlying asset
- T : maturity
- $t_i = (i/N)T$: observation dates; $i = \{0, \dots, N\}$
- S_i : price of the underlying asset at time t_i
- K : periodical knock-out barrier (%)
- k : continuous knock-in barrier (%)
- c : periodical coupon barrier (%)
- h : high coupon (%)

- l : low coupon (%)
- $q = N/T$: frequency of the observation dates (*i.e.* how many observation dates a year the structure has)
- P : invested amount (notional)

The payment of the product is made only on the observations dates, and is as follows:

1. At $t = t_1$,
 - Coupons:
 - if $S_1/S_0 \geq c$, then it pays $(h/q) \times P$;
 - otherwise, it pays $(l/q) \times P$.
 - Redemption:
 - if $S_1/S_0 \geq K$, then it pays P back and terminates;
 - otherwise, it survives, and wait for the next observation date t_2 .
2. At $t = t_i$ ($2 \leq i < N$), unless the structure was already terminated in the previous observation dates,
 - Coupons:
 - if $S_i/S_0 \geq c$, then it pays $(h/q) \times P$;
 - otherwise, it pays $(l/q) \times P$.
 - Redemption:
 - if $S_i/S_0 \geq K$, then it pays P back and terminates;
 - otherwise, it survives, and wait for the next observation date t_{i+1} .
3. At $t = t_N$, unless the structure was already terminated in the previous observation dates,
 - Coupons:
 - if $S_N/S_0 \geq c$, then it pays $(h/q) \times P$;
 - otherwise, it pays $(l/q) \times P$.
 - Redemption (Expiry):
 - if $\min_{t \in [0, T]} S(t) > kS_0$ or $S_N \geq S_0$, then it pays P back;
 - otherwise, it pays $(S_N/S_0) \times P$.

An important point to note is that the products tend to have long maturities. This feature matches with the investors' goal as they want to receive high coupons for a long period of time. The high coupons are generated by shorting the knock-in put with Bermudan (periodical) knock-outs. The high coupons are not possible with shorter maturities since the premiums of corresponding knock-in puts are not high enough. Therefore, the product is usually feasible with long maturities.

Remark 1. *There are some varieties of type on this structure:*

- *K could be dependent on i , i.e. K could be different on every observation. On the autocallables traded in South Korea, K tends to start high and gradually comes down every time the structure survives an observation date. The barrier level can even become sub par (100%) as the structure gets near its maturity (the structure is sometimes called a 'step-down' autocallable).*
- *The payout upon breaching the knock-out barrier could be more than 100% (for example, 105%) of the initial investment P . In other words, there may be a bonus coupon on top of regular coupons upon knock out. This bonus coupon may accumulate as it survives the observation dates (the structure is sometimes referred to as a 'snowball' autocallable).*
- *It is possible not to have down-and-in put, hence a capital-guaranteed version. This type is called an 'enman', and used to be popular as it guarantees the return of the capital (initial invested amount). However, with low interest rates in Japan, in order for the structure to have attractive returns for the investors, it needs to have the maturity longer than 10 years and some had 30 years in maturity.*
- *The coupon could be fixed, i.e. c could be 0%.*
- *The $\min_{t \in [0, T]} S(t)$ could be observed continuously or daily.*
- *In the knock-in forward type of the structure, the last redemption given that the knock-in barrier had been breached is $(S_N/S_0) \times P$ instead of $\min(S_N/S_0, 100\%) \times P$. This means that it is possible to get a greater return at maturity with the activation of the knock-in barrier than without.*

1.1.2 Problem with Autocallable Trades

With autocallables, investors earn high coupons with a "relatively" low risk of losing the initial capital* and banks earn some margin on the large notional, so the trade is a win-win where both parties are satisfied with the trade.

However, there is a particular feature of this trade. Investors purchase autocallables in the form of bonds, and they seek the (potentially) high coupons that the equity linked bonds pay. Therefore, they do not want to hedge the position. If they hedge their position, it would make their return lower which would conflict with their initial motivation. In contrast, the banks who sold the autocallables seek the margin they receive at the time of the trade and their goal is not to make, or rather not to lose money on taking the risk. From this perspective, they want to hedge out the risk as much as possible. From now on, we will focus on the vega risk[†].

In general, if two parties, a buyer and a seller, are in the same market, the trade does not affect the market overall in the sense that the net risk after the trade neither increases nor decreases. In other words, the risk as a whole in the market is conserved. However, in the autocallable trade, only one of them, the seller, is active in the over-the-counter (OTC) market and hedges the position. The sellers of the autocallables are long the vega[‡], hence they need to sell volatility in order to hedge their portfolio. The vega profile at time $t = 0$ of an autocallable with parameters shown in Table 1.1 with respect to the underlying asset and the implied variance calculated in the Heston model are shown in Figures 1.1 and 1.2. Here, *vanna* refers to the risk that is equal to the derivative of vega with respect to the underlying price and *volga* the risk that is equal to the derivative of vega with respect to the underlying variance.

In an idealised Black-Scholes model, one can trade the underlying asset for infinite size at the current price without affecting the market, but we all know that this is not the case in the actual market. Only limited amounts may be traded at the current bid and offer prices, so if one needs to instantly sell more than what is on the current bid, for example, then she needs to trade some at the second

*Of course, if the underlying price breaches the knock-in barrier and stays low until the maturity, the investor will only receive low coupons and the low performance of the underlying asset, hence ends with a loss. However, the underlying price has to cross the knock-in barrier first for that to happen and usually the barrier is around 40% away from the initial level.

[†]Vega usually refers to the risk of the product with respect to the implied volatility, but in the thesis, we rather define it to be the risk of the product with respect to the implied variance.

[‡]The buyer of autocallables is selling the put to boost the coupons that they potentially receive in the future. On the other hand, the seller is purchasing the put from the buyer, therefore the sellers of the autocallables are long the vega.

| Parameter | Value |
|-----------|----------|
| K | 105% |
| c | 85% |
| k | 70% |
| T | 3 Years |
| h | 3% |
| l | 0.01% |
| q | 3 months |

Table 1.1: An example of the detail of the autocallable structure.

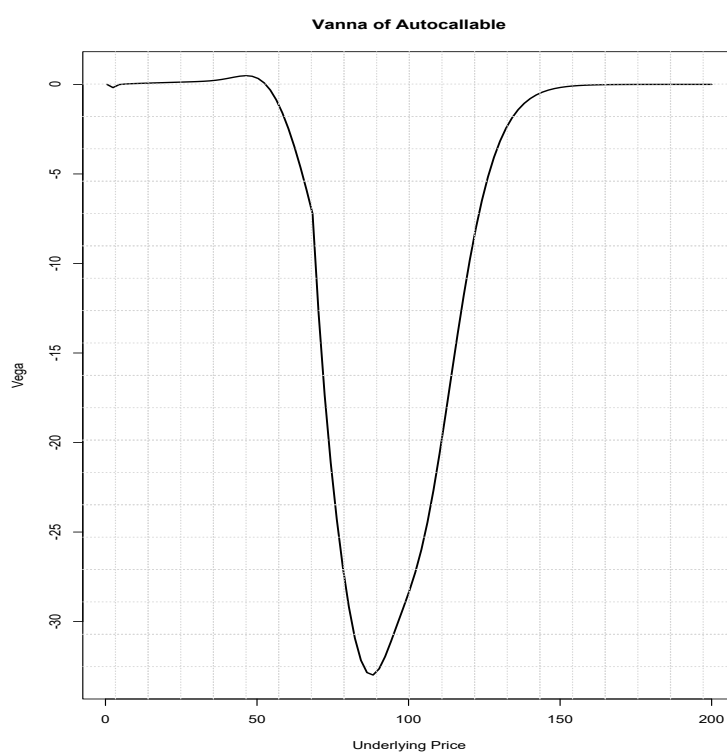


Figure 1.1: Graph showing how vega moves with respect to the underlying price. Note that the minimum vega is obtained around the average of the barrier levels, which is at 95.

best bid. This transaction will lower the current tradable price in the market. The same argument goes for the autocallable trades. Since banks have bought the vega from trading autocallables, they want to sell the risk in the market by selling plain vanilla options. When the size of the traded autocallables increases, the banks will need to sell options at lower prices than the current bids. The selling pressure on plain vanilla options will lower the prices of the options and therefore will lower the

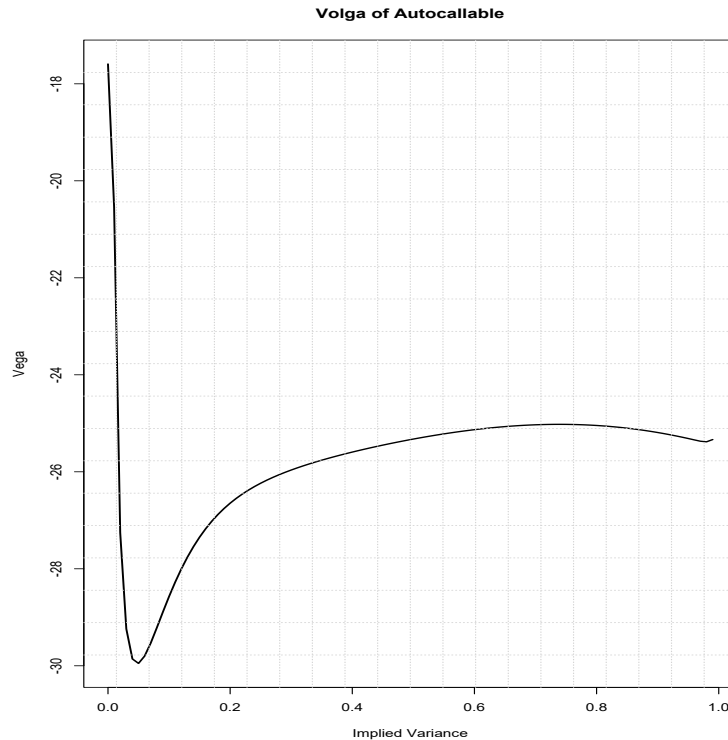


Figure 1.2: Graph showing how vega moves with respect to the implied variance.

current (implied) volatility.

If the risk of the autocallable does not change over the life of the trade, then the risk affects the volatility only when the product is traded. However, the risk of the autocallable dynamically changes with the market due to the complex structure of the product as seen in Figures 1.1 and 1.2.

Our explanation of why we should see the risk profile as shown in the Figures 1.1 and 1.2 is as follows: Roughly speaking, the vega increases with the expected maturity (which is called the *duration*). If the implied volatility decreases, since it will be more difficult for the underlying asset price process to breach the knock-out and knock-in barriers, the duration increases and the vega increases. When the underlying asset price process moves further away from both barriers, since it will now have lower probability of hitting them, the duration becomes longer and the vega of the autocallable increases. Therefore, the average of the knock-out and knock-in barriers is roughly the level where the duration, hence the vega, becomes the largest from the bank's perspective.

Remark 2. Note that the traders are the ones who sold the autocallables, hence their vanna profile is the opposite of what is shown in Figure 1.1. The same applies

to its volga profile as shown in Figure 1.2.

From this rough sketch of the dynamics of the vega with respect to the implied variance and the underlying asset price, we can conclude that the vega grows larger as the asset price gets closer to the average of the barriers and as the implied variance decreases.

This is what happened in the Japanese equity market in the year 2012. A lot of trades on autocallables had been made in the previous years on Nikkei 225 and they had not knocked out nor knocked in. The index decreased to the level around 8,500, around the level where the vega of autocallables becomes the largest with respect to the index level. To make things worse, the implied volatility kept decreasing as the traders tried to sell the vega that they had gained from the autocallables already in issue and as the realized volatility became low. Even when the vega of the autocallables increased, they were not able to hedge what they gained because:

- Banks all had the same vega profile and no one in the market was willing to buy the vega.
- The vega which banks wanted to sell was that with long maturities where the market was illiquid. The market was not liquid enough to absorb the huge supply of vega introduced by the existing autocallables.

After banks suffered a huge loss from the index pinned around the average of the barriers and with the low implied volatility, circumstances drastically changed around the end of the year . With a new prime minister presenting his plan on focusing on making the economy in Japan better with "Abenomics", the market surged. The sudden spike in the market made the Nikkei 225 and its volatility go up and knocked out most of the existing autocallables. With autocallables vanishing from their portfolio, the sellers were now left with the hedges they sold against the autocallables, hence they suddenly became short large quantities of vega. They now wanted to buy the volatility back to rebalance their portfolios. The outcome was that it sent the volatility even higher and made the traders lose their money again from the increased volatility on their short position. The story is well described in the articles [11; 12; 52; 55; 74; 75; 76; 77; 78; 80; 81; 82][§]. The level of the Nikkei

[§]Sometimes, autocallables are called *uridashi*, which is a Japanese word for "launching" or "marketing" new trades/products. This term is used to specify a special type of autocallables which are sold through public auctions and we call them *public trades*. The other type of traded autocallables are called *private trades* and they are traded between the client and the bank, and the information of the trade is not publicly announced. Sometimes the word *uridashi* is used to

225 index and its implied volatility level in 2011-2013 are shown in Figure 1.3 [¶].

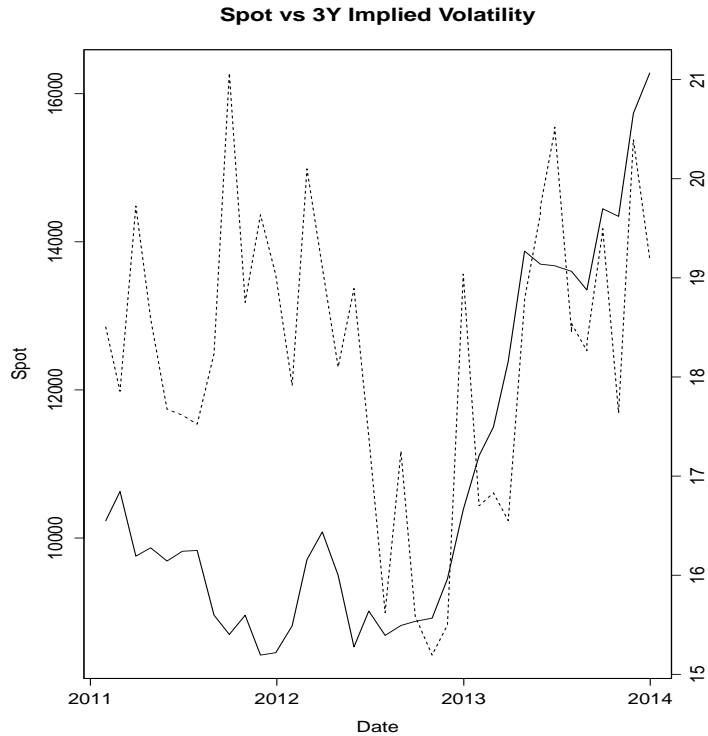


Figure 1.3: Graph showing the Nikkei 225 index level (in solid line) and 3 year implied volatility level (in dotted line) between the years 2011 and 2013. We see that the sharp fall in the volatility around the end of the year 2012 with the Nikkei 225 level staying around the level 8,500. We also see a sharp increase in the index and its volatility around the beginning of the year 2013.

1.1.3 A Solution

The huge losses of banks on autocallables in 2012 was largely caused by traders ignoring the fact that all the banks had similar preferences in vega and volatility from their huge position in autocallables, and this risk preference impacted the volatility to move against itself as traders wanted to hedge the risk. Our goal is to construct a model that correctly captures the extra dynamics of the volatility process caused by the existence of the market driver (e.g. autocallables).

specify both types of the autocallables as in [78]. Uridashi trades trade less but each trade tends to be large in notional (can be as large as 300 million U.S. dollars). Private trades trade a lot but each notional tends to be small (can be as little as 1 million U.S. dollars)

[¶]The graph is based on the dataset of Nikkei 225 end of the month evaluations on plain vanilla options, kindly provided by Markit Totem.

We first base our model on that of Heston [26]. The Heston SDEs that determine the dynamics of the underlying asset price process and its variance process are

$$\begin{cases} dS = \mu S dt + \sqrt{v} S dW^1 \\ dv = \kappa(\bar{v} - v) dt + \eta \sqrt{v} dW^2 \\ \langle dW^1, dW^2 \rangle = \rho dt. \end{cases} \quad (1.1)$$

Here, S denotes the underlying stock price and v the variance of the underlying. W^1 and W^2 are Wiener processes with correlation ρ , μ is the drift of the stock, $\kappa > 0$ is a constant which expresses the intensity of the mean reversion of the variance, \bar{v} is the mean variance, and η is the volatility of the variance.

We focus on the variance dynamics^{||}. From the drift of the SDE (1.1) on the variance process, we see that the process tries to revert to the level \bar{v} . In this sense, the level \bar{v} is the equilibrium point of the variance or the mean variance. The variance process should move around the mean variance. If the demand and supply curves of the vega cross at a unique point, then the variance coordinate of the point should be equal to \bar{v} .

We now think of the case when the traders are short the market driver whose vega is negative. In this market, the supply of vega increases and results in a parallel shift of the supply curve of vega. Therefore, assuming that the demand curve of vega is unchanged, the variance coordinate of the equilibrium point (which is the point where the demand and the supply curves meet) will be shifted by some amount proportional to the vega of the market driver. This is shown in Figure 1.4.

Remark 3. *In our model, we assume that we know the structure of the market driver. This is true in our motivated example because:*

- *Traders see it in their portfolios.*
- *The public trades (the uridashis) are announced with the detail of the trades, so we know which and in what quantity each structured product traded.*

It would be an interesting research topic to ascertain or estimate how much detail of the market driver we can obtain by only observing the market dynamics.

^{||}We can similarly think of taking into account the impact of the market driver on the underlying asset price process. However, the impact of the market driver is large when the market is illiquid and closed. Usually, the underlying asset is fairly liquid, especially when one needs to think of derivatives products on it, and has more variety in types of the market participants. For example, derivatives market is somewhat restricted since there are more regulations in order to trade derivatives in the OTC market than to trade stocks. Therefore, the impact of the market driver is usually larger in the derivatives market than in the underlying asset. We therefore focus on the impact of the market driver on the variance process.

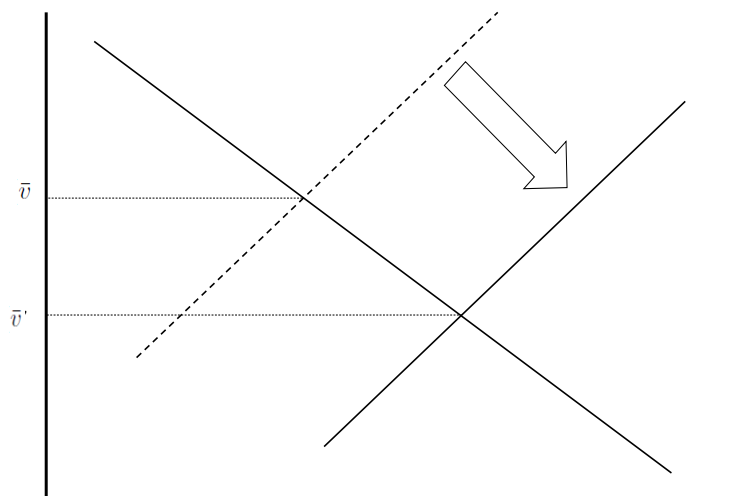


Figure 1.4: With larger supply, the mean variance \bar{v} comes lower to \bar{v}' .

Remark 4. *Credit Suisse introduced a new way of hedging the product by trading a corridor variance swap spread[60; 79]. In this trade, the banks sell Nikkei 225 corridor variance swap and buy the same structure on S&P500 both contingent on the levels of Nikkei 225 index. The premium of the spread looked attractive to hedge funds so the bank was able to trade the product in large size. The corridor variance swap has similar vega profile to that of the autocallables, hence the bank was able to hedge the vanna and volga effects from the autocallables with the product. The trade works well in the Japanese market because the banks already have the long vega position from autocallables and because the S&P 500 volatility market is liquid enough. The trade helped relax the concentration of vega in the Japanese derivatives market caused by the autocallables.*

The new model we introduce in Chapter 2 is similar to the feedback models proposed in the late 90's as in, for example, [21; 61; 70]. The difference of our model from the classical feedback models is that the effect of the feedback is known in our case, hence we are able to directly formalize the effect of the concentration using the risk of the concentrated position. The previous models generally have more parameters and generates quasilinear PDEs which are more challenging to solve. From our model, we get nonlinearity up to the first derivatives and not on the second derivatives, which is beneficial in approximating the solution as discussed in the next subsection.

The new model is also similar to the stock pinning models as in [4; 34]. The

stock pinning effect occurs when traders hedge their deltas around specific strike. The delta hedging makes the stock less volatile around the strike. As the delta difference below and above the strike gets larger as it gets closer to the maturity, the pinning effect becomes stronger. Similar to the feedback models, the main driver for the pinning effect is the delta hedging. On the other hand, we incorporate the vega concentration effect directly in the variance process of the underlying asset.

1.2 Approximating the Solution of Semilinear PDE with PIA

The Heston model on which we based our market driver model requires one to solve a linear PDE to calculate the price of a derivatives product. On the other hand, our model requires us to solve two PDEs and one of them is nonlinear. From a practitioner's point of view, this is a little bit troublesome as they may not have a solver for nonlinear PDEs and may have to create one from scratch. They may not be able to allocate enough resource to do that even if the pricing under the new model is beneficial for the banks. To help overcome the difficulty, we apply the policy improvement algorithm (PIA) to approximate the solution to the semilinear PDE with those of linear PDEs.

The policy improvement algorithm is an iterative algorithm in a control problem where one solves for the optimal control in each step and is very efficient. It is a well-established algorithm and the general theory is explained in, for example, [30; 31; 32].

If the solution to the semilinear PDE can be approximated by those of linear PDEs, it is a great improvement because it enables one to use our improved model with the solver for linear PDEs (e.g. the one to solve the Heston PDEs), but only if the convergence is fast. If it takes too long before it shows convergence, the approximation is not useful from a practitioner's point of view since the calculation using the approximation will be too slow for the fast dynamics of the market. Thankfully, in our experience it generally only takes a few iterations before the approximations reach the convergence. To the best of my knowledge, there is no general proof that it only takes a few iterations to obtain sufficiently close approximation to the original solution. In this specific problem of the market driver model, we are able to show quadratic local convergence (QLC) of the PIA approximated solution to the original problem under a norm using Schauder's boundary estimate. This partially explains the fast convergence in the iteration under the PIA.

Remark 5. *This result is very much like that of the Newton method in numerical*

analysis, where one can show that the approximated solutions show QLC, but nothing stronger than this in general.

We are able to show the QLC in this specific model, but a natural question to ask is whether this applies generally to any PIA-approximated solutions. To answer this, we show that the PIA-approximated solutions indeed show QLC under a few additional assumptions. We will see some examples in Chapter 3.

1.3 Technical Analysis

Traders' decisions depend on various elements, for example, financial information of companies, expectations of some events in the future, information from financial analysts, and rumors. Further information that they could rely on is that of the technical analysis.

Technical analysis refers to a family of methods that derive the expected future dynamics of the underlying asset price from the graph of the historical prices. In this field, the graph is called a *chart*. This is why sometimes technical analysis is called 'charting'. There is still a big debate on the effectiveness of the analysis, but many traders continue to believe in the information it provides. Reasons why the analysis may be effective include:

- The dynamics of the underlying asset price depend on many factors and it is impossible to follow all of them. Many traders who believe in technical analysis also believe in the efficient market hypothesis (EMH). Even if investors try to follow all the information available to them, they cannot get all of the information that determines the future dynamics of the underlying asset price. For example, if there is some insider information on a company's earning, since it is not publicly available, there is no way one can get the information before it is published. If the information is so critical that it may push the company into bankruptcy, it definitely will impact the future stock price of the company. Traders who follow technical analysis believe that even this kind of information is taken into account in the current asset price. In the case of insider information that will potentially make the stock price decline, some people might already be aware of the information before it is published in public. In order to take advantage of knowing the information ahead of others, the only way they can profit from this is to sell the stock. The selling of the stocks will push the stock price lower and the movement will be reflected in the chart of the stock price. This way, the technical analysts believe they

can still capture the dynamics without the actual information that causes the decline in price.

- When people make decisions, it is not always easy to sap the right ones. For example, given the same information, one makes different decisions depending on whether one is ahead or behind his budget target. Decisions by humans are not always consistent, and this inconsistency makes the trading very difficult. On the other hand, the technical analysis is consistent. One comes up with the rule by observing the charts, and whether it's a buy or a sell is determined only by the rule (of course, whether the trader decides to follow the outcomes of the technical analysis is something else). The analysis is free from human inconsistency.

Technical analysis is somewhat easier for amateur traders as it does not require many sophisticated financial and economic ideas, but only the techniques to discover the chart patterns. It is also easy in the sense that one needs to look at only the chart and nothing else to decide on trading.

One of the reasons why technical analysis is not popular in academia is because it lacks mathematical support. There may be some explanation rooted in the field of behavioral finance, but as far as we know, there is no mathematical proof on the validity of any of the methods. A concern in introducing technical analysis in the field of mathematical finance is the existence of arbitrage opportunities. If the methods of technical analysis were true, then there will be an arbitrage opportunity by following what they indicate. The idea of our research is to try to prove and justify the methods of the technical analysis mathematically in an incomplete market.

The most basic method in the field is that of support/resistance levels. The *support level* is a level which the underlying asset price process is reluctant to cross from above. The *resistance level* is defined similarly as a level which the price process is reluctant to cross from below. We refer to the horizontal line drawn at the support level as the *support line* and the horizontal line at the resistance level as the *resistance line*. These levels may be defined separately, i.e., the support level could be the support level but not the resistance level and vice versa. However, the levels are regarded as separating the two regimes; the positive regime where the expected return of the asset is better and the negative regime where the expected return is worse than in the other regime. Therefore, we consider the levels to be the same and always think of the resistance level as the support level and vice versa. In other words, we can consider the level to be the support level when the asset price is in the positive regime and consider it to be the resistance level when the asset price

is in the negative regime. The level switches between the support and the resistance levels. This is in line with what the practitioners consider the levels.

In investigating the method of support/resistance levels, the difficulty is that they are not exactly the levels where the regime transitions occur. For example, when the asset price is in the positive regime and touches the support level, the regime will not switch right away. In other words, the price process can fluctuate around the level within the current regime without switching the regimes. With this observation in mind, we define the region in space where the price process takes the positive regime as the positive region and the space in which the process takes the negative regime as the negative region. We assume that there is some non-empty region that is the intersection of the positive and negative regions where the process can be in either regime (*cf.* Figure 1.5). Let us call the support/resistance level SR . We define the rule of the regime transition as follows:

- From the positive regime to the negative regime, the transition occurs when the price process hits the level $SR - \delta_1$, where $\delta_1 > 0$ is some fixed value.
- From the negative regime to the positive regime, the transition occurs when the price process hits the level $SR + \delta_2$, where $\delta_2 > 0$ is some fixed value.

When $\delta_1 + \delta_2$ are sufficiently big, the rule prevents the regime transition from happening with high frequency.

Under this setup, we first consider the problem of optimally stopping to optimize the discounted stock price $\mathbf{E}[e^{-rt}S_t]$ to solve for the optimal stopping time to sell the stock. With this solution in the optimal selling problem, we then solve for the optimal stopping time to purchase the stock that maximizes our expected profit.

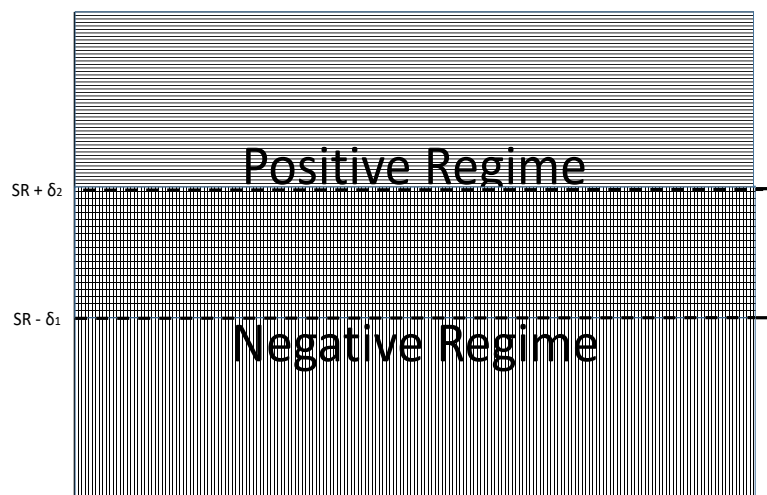


Figure 1.5: The positive region is the region $[SR - \delta_1, \infty)$ where the price process takes the positive regime. Similarly, the negative region is the region $(0, SR + \delta_2]$ where the price process takes the negative regime. $[SR - \delta_1, SR + \delta_2]$ is where the underlying price process can be in either regimes.

Chapter 2

Modeling via Market Driver

2.1 Introduction

Japan has one of the largest equity derivatives markets in the world. According to the Bank for International Settlements, Japan had \$378 billion in face value of equity-linked contracts out of the worldwide total of \$5,445 billion as of September 13, 2015 [6]. A common underlying for equity-linked derivatives products in the country is the price-weighted Nikkei Stock Average Index (Nikkei 225) published by Nikkei Inc. Since the country is the world's third largest economy by GDP, people generally assume that the market is liquid enough to trade freely any desired position. However, from my own experience, this is not quite true. Long-dated volatility (especially between 2 and 5 years) is generally priced low due to the fact that most of the traders in the market already own vega (sensitivity to volatility) from selling (usually in significant sizes) a structured product called autocallable to their clients. Therefore it is generally difficult to sell vega in the market. We will give some numerical examples for this exotic case in Appendix C, and for now, we will focus on explaining our model in a simpler context in this chapter. The important fact to note is that there is a position that affects the pricings and risks of all the existing and potential derivatives products in the market.

In order to understand the background of our model, we first formulate a toy example.

Assume that there are only 2 traders, A and B, in the over-the-counter (OTC) market. If A wants to buy volatility, A needs to buy it from B and vice versa. If A buys \$10 million of vega from B, the vega that B holds is decreased by the same amount. Generally, traders do not want to own so much risk on one side, so they might want to hedge the risk a little. Since the only market participants are A and

B, they need to reverse what they previously traded in order to hedge themselves. This does not make much sense in this case, as there are only 2 market participants, but even if we assumed more participants in the market, this is still essentially what is happening: overall, the market vega is maintained and does not change whatever A and B do. Whatever A gains, B loses and vice versa.

Now introduce a new market participant C. Let us assume that C is not a participant in the OTC market but only buys vega from A and B as their client to hedge against market risk, and does not otherwise hedge the position (we could think of C as an insurance company, for example). If C buys \$10 million of vega from A, then A is now short the risk, so may want to buy some back in the market to hedge himself. A needs to buy it from B, of course, as C does not sell any vega. The important point is that the OTC market whose only participants are A and B is now short \$10 million of vega overall. The market now would like to buy some vega back. This generally drives the volatility of the underlying security or index higher.

We elaborate this point in more detail. The demand and supply of vega could be, in general, directly converted to the supply and demand of volatility. It is easier to think of this in the Black-Scholes framework. If there is more demand for vega than supply, more people want to buy vega. The way they accomplish this is to buy plain vanilla calls and puts, which are positive vega products. If more people buy these products, the prices of the products move higher. Given other parameters are fixed, this price increase could only be explained by the increase in the underlying volatility. This is why the actual market participants refer to 'buying (selling) volatility' when they are actually buying (selling) vega. These phrases will be used with the same meanings hereafter.

Remark 6. *The corresponding volatility level is implied volatility as opposed to realized (or historical) volatility.*

Up to this point, volatility movement is just a matter of demand and supply. Now suppose that the derivative product that C bought has big second order risks, like vanna (the derivative of vega with respect to stock price) and volga (the derivative of vega with respect to volatility). For example, if the product is long vanna, vega increases when the underlying stock moves higher. In this case, A gets shorter vega just from the market movement and he needs to buy it in the market to re hedge himself. However, if B has the same position, B gets shorter vega as well, so neither of them are interested in selling any more vega. This will make the volatility even higher. Note that in this situation, what is moving the volatility is

just the change in the risk of the product that was already traded, not a new trade. We call the special product (of which the risks affect the dynamics of supply and demand of the volatility) the *market driver*.

In order to model the example above, we posit a simple and easy-to-use model which is an extension of the Heston model, one of the most popular stochastic volatility models. The core of our model is a semilinear parabolic partial differential equation (PDE) that we retrieve to price the market driver. Once we obtain the valuation of the market driver, we use a *linear* parabolic PDE, which is very similar to those of Black-Scholes and Heston, to price other derivatives products.

As mentioned earlier, we are more interested in the case where the market driver is of a specific exotic type because we think its risk feedback effect is more prominent in practice. We will handle this problem numerically in Appendix C and concentrate now on the case when it is of plain vanilla type.

The problem statement so far may remind some readers of the 'feedback effect' of options which is now a somewhat mature field. The Black-Scholes model with a feedback effect models the prices of derivative products affected by delta hedging executed by program traders [21; 61; 70]. It was a field which attracted a lot of interests in the 1990s. We have also seen more recently the stock pinning models [4; 34] which we can consider as one type of feedback models, but not much work has been done since then. Although the research in this paper was done separately from the studies done in the field, our ideas are very similar in the sense that some trade affects other option pricing. We are (in a way) incorporating the feedback effect in a stochastic volatility framework. The key difference, however, is that we are not applying the feedback effect of the underlying asset (stock), but instead, *that of the underlying volatility*. In the earlier models, the effect impacts the volatility passively via program traders trading the underlying asset. On the other hand, our model incorporates the effect directly in the dynamics of the volatility.

It may not look natural to incorporate a feedback effect in the volatility as it is not a tradable asset. However, from my experience, supply and demand effects of the volatility do exist in the actual market and we think our model reflects, at least qualitatively, the actual market dynamics with the market driver. We believe that our model is more in line with market practitioners' perspectives than the classical feedback model.

One of the difficulties in the earlier feedback models is that they model the realized (historical) volatility rather than the implied volatility. Hedging delta of derivative products by dynamically trading the underlying asset does affect the implied volatility, but only that of short maturity. Behaviour of the current stock

price has little impact over the long-dated implied volatility. Depending on the sign of the vanna of the market driver, it is possible, for example, that even when the realized volatility increases with a large drop in the stock price, the long-dated implied volatility goes lower. This cannot be modelled in the classic feedback model.

One of the benefits of our model is that the nonlinear PDEs that we derive can be approximated by a series of linear ones. The PDEs derived in the classic feedback model are generally of quasilinear type, where the nonlinearity occurs in the highest order of the equations. On the other hand, although we need a pair of PDEs, one for the market driver and the other for a general derivative product, our PDEs are at most of semilinear parabolic type, where the nonlinearity occurs in lower order terms of the equations. This enables us to apply a linear approximation algorithm called the Policy Improvement Algorithm (PIA) in which the approximated solution converges quickly to the actual solution of the semilinear PDE.

The reason why we introduce the PIA is that it enables us to reuse the setup for the Heston model. The Heston model has already been implemented in practice and is widely used. It is convenient to use the existing setup, whenever possible, to calculate the solutions of the new model. We also note that in the course of our research, we encountered some cases where we had a convergence of the numerical solution using the PIA, but not using the finite difference method (FDM): the PIA seems to have better convergence properties than the FDM.

The rest of the chapter is organized as follows: Section 2.2 explains the new model in detail. We will establish the existence and uniqueness of the solution to our PDEs in Section 2.3. In Section 2.4, we transform the nonlinear PDE to an HJB equation. The PIA is then described in Section 2.5. In Section 2.6, we give a numerical example to see how valuations and risks, which are very important for day-to-day hedging for traders, change in our model from those in Heston's model. We also see in this section how PIA-approximated solutions converge to that of the nonlinear PDE. We give our conclusions in Section 2.7.

2.2 The Market Driver Model

We start by briefly reviewing Heston's stochastic volatility model [26]. Let $(\Omega, \mathcal{F}, (\mathcal{F}_t)_{t \geq 0}, \mathbf{P})$ be a filtered probability space satisfying the usual conditions. The stochastic differential equations for the stock price and the variance are:

$$\begin{cases} dS = \mu S dt + \sqrt{v} S dW^1 \\ dv = \kappa(\bar{v} - v) dt + \eta \sqrt{v} dW^2 \\ \langle dW^1, dW^2 \rangle = \rho dt. \end{cases} \quad (2.1)$$

Here, S denotes the underlying stock price and v the variance of the underlying. W^1 and W^2 are Wiener processes with correlation ρ , μ is the drift of the stock, $\kappa > 0$ is a constant which expresses the intensity of the mean reversion of the variance, \bar{v} is the mean variance, and η is the volatility of the variance.

Since v only takes positive values, it is usual to require the model to satisfy Feller's condition for avoiding the origin [37]:

$$2\kappa\bar{v} > \eta^2. \quad (2.2)$$

With this setup, the value V of a derivative product satisfies Heston's PDE:

$$\begin{aligned} \frac{\partial V}{\partial t} + rS \frac{\partial V}{\partial S} + \kappa(\bar{v} - \omega v) \frac{\partial V}{\partial v} \\ + \frac{1}{2} v S^2 \frac{\partial^2 V}{\partial S^2} + \frac{1}{2} v \eta^2 \frac{\partial^2 V}{\partial v^2} + v S \eta \rho \frac{\partial^2 V}{\partial S \partial v} - rV = 0 \end{aligned} \quad (2.3)$$

with appropriate initial (or terminal, if we are calculating backwards in time) and boundary conditions. Here, ω is some constant for volatility risk premium and r is the interest rate. Equation (2.3) is a second order linear parabolic PDE. The derivation of (2.3) is in Appendix A.

Let us now assume that there is some distinguished product (called the market driver) with value denoted by F .

Using this F , our revised model is written as

$$\begin{cases} dS = \mu S dt + \sqrt{v} S dW^1 \\ dv = \kappa(\bar{v} - v + Q \frac{\partial F}{\partial v}) dt + \eta \sqrt{v} dW^2 \\ d\langle W^1, W^2 \rangle_t = \rho dt \end{cases} \quad (2.4)$$

with some coefficient Q .

Note that the only change made to the Heston SDE (2.1) is the term $\kappa Q \frac{\partial F}{\partial v}$ in the second equation. A simple justification for this is that the vega (in this thesis, we use the term 'vega' for the derivative of the valuation with respect to variance, whereas it usually means the derivative of the valuation with respect to volatility) of the market driver impacts supply and demand of the variance and causes the shift in its mean. We are only adding this adjustment to the variance SDE. If we want

to, we could, of course, similarly add 'delta' (derivatives of valuation with respect to the underlying stock price) adjustment in the SDE for the stock price S in (2.4). However, we do not do this since i) deltas of derivatives products are generally low, so in order to have a large impact on the stock price, the face value traded on the position needs to be massive, which is not realistic and ii) the stock market is more liquid than the OTC derivatives market, in the sense that there are more people with different incentives in trading and many more people have access to the market (for example, personal investors can easily trade stocks, whereas they might need to satisfy additional requirements in order to trade derivatives. It is even more difficult for them to be able to trade in the OTC market due to size requirements, credit issues, and other restrictions).

A sufficient condition for the variance not to go negative is derived by comparing the two processes v and v' starting at the same value:

$$\begin{cases} dv = \kappa(\bar{v} - v + Q \frac{\partial F}{\partial v})dt + \eta\sqrt{v}dW^2 \\ dv' = \kappa\{\bar{v} - v' + \min(Q \frac{\partial F}{\partial v})\}dt + \eta\sqrt{v'}dW^2. \end{cases} \quad (2.5)$$

Since we will be working in a bounded domain, Proposition 5.2.18 in [35] shows that $v' \leq v$ almost surely. Applying Feller's condition (2.2) on v' , if

$$2\kappa\left\{\bar{v} + \min\left(Q \frac{\partial F}{\partial v}\right)\right\} > \eta^2, \quad (2.6)$$

then $v' > 0$ almost surely, hence $v > 0$ almost surely. We call condition (2.6) the *positive variance condition*.

If we follow the usual argument, we obtain the following PDE for the value V of a derivative:

$$\begin{aligned} \frac{\partial V}{\partial t} + rS \frac{\partial V}{\partial S} + \kappa\left(\bar{v} - \omega v + Q \frac{\partial F}{\partial v}\right) \frac{\partial V}{\partial v} \\ + \frac{1}{2}vS^2 \frac{\partial^2 V}{\partial S^2} + \frac{1}{2}v\eta^2 \frac{\partial^2 V}{\partial v^2} + vS\eta\rho \frac{\partial^2 V}{\partial S \partial v} - rV = 0. \end{aligned} \quad (2.7)$$

Since F is also the value of a specific derivative, we can substitute $V = F$ in (2.7) and obtain a nonlinear PDE for F :

$$\begin{aligned} \frac{\partial F}{\partial t} + rS \frac{\partial F}{\partial S} + \kappa\left(\bar{v} - \omega v + Q \frac{\partial F}{\partial v}\right) \frac{\partial F}{\partial v} \\ + \frac{1}{2}vS^2 \frac{\partial^2 F}{\partial S^2} + \frac{1}{2}v\eta^2 \frac{\partial^2 F}{\partial v^2} + vS\eta\rho \frac{\partial^2 F}{\partial S \partial v} - rF = 0. \end{aligned} \quad (2.8)$$

Note that given F , the differential equation (2.7) is a second order parabolic PDE that is linear in V as in the Heston model. On the other hand, the differential equation (2.8), is semilinear.

Remark 7. *We have the following proposition:*

Proposition 2.2.1. *The new model (2.4) is arbitrage-free.*

We defer the proof of Proposition 2.2.1 in Section E.2 in Appendix E.

2.3 Partial Differential Equations

We recall some theorems from the theory of PDEs. For more detail, we refer to [40].

We take a bounded, open, and connected domain \mathcal{E} in \mathbb{R}_+^2 which is bounded away from the axes. We further assume that $\partial\mathcal{E}$ is $C^{2+\alpha'}$ for some $\alpha' > 0$. Let $Q_T = \mathcal{E} \times (0, T)$, $\mathcal{D} = \partial\mathcal{E}$, $\mathcal{D}_T = \{(x, y, t) | (x, y) \in \mathcal{D}, t \in [0, T]\}$, $\mathcal{D}_\tau = \mathcal{D}_T \cap \{t : t \leq \tau\}$, and $\Gamma_T = \mathcal{D}_T \cup \{(x, y, t) | (x, y) \in \mathcal{E}, t = 0\}$. We impose ψ as our initial and boundary conditions and assume it satisfies the compatibility condition, i.e. $\psi(x, y, t) \in C(\overline{Q_T})$.

We define the differential operator L by

$$\begin{aligned} -Lu &:= rxu_x + \kappa(v_0 - \alpha y)u_y + \frac{1}{2}x^2yu_{xx} + \frac{1}{2}\eta^2yu_{yy} + \eta\rho xyu_{xy} \\ &= a_{ij}u_{ij} + b_iu_i \end{aligned} \quad (2.9)$$

under the Einstein summation convention.

We reparameterize time-to-go t backwards by replacing $t \rightarrow T - t$ and rewrite (2.8) in general form:

$$u_t + Lu + ru - \kappa Qu_y^2 = 0. \quad (2.10)$$

The PDE (2.10) is uniformly parabolic as it satisfies

$$\nu_1|\xi|^2 \leq a_{ij}\xi_i\xi_j \leq \nu_2|\xi|^2 \quad \forall (x, y) \in \overline{\mathcal{E}}, \quad \forall \xi \in \mathbb{R}^2 \quad (2.11)$$

for some $\nu_1, \nu_2 > 0$.

We introduce the distance between points $P = (x, y, t)$ and $Q = (\bar{x}, \bar{y}, \bar{t})$ as

$$d(P, Q) = [|x - \bar{x}|^2 + |y - \bar{y}|^2 + |t - \bar{t}|^2]^{1/2}. \quad (2.12)$$

For any point $P = (x, y, t) \in \overline{Q_T}$, we define the distance from P to $\Gamma_\tau := \Gamma_T \cup \{t : t \leq \tau\}$ as

$$d_P = \sup_{Q \in \Gamma_\tau} d(P, Q) \quad (2.13)$$

and set

$$d_{PQ} = \min\{d_P, d_Q\}. \quad (2.14)$$

We define a norm

$$\|u\|_{2+\alpha} = \langle u \rangle_\alpha + \langle dD_x u \rangle_\alpha + \langle dD_y u \rangle_\alpha + 2 \langle d^2 D_x D_y u \rangle_\alpha + \langle d^2 D_t u \rangle_\alpha, \quad (2.15)$$

where

$$\begin{aligned} \langle d^m u \rangle_0 &= \sup_{P \in \overline{Q_T}} d_P^m |u(P)|, \\ H_\alpha(u) &= \sup_{P, Q \in \overline{Q_T}} d_{PQ}^{m+\alpha} \frac{|u(P) - u(Q)|}{d(P, Q)^\alpha}, \\ \langle d^m u \rangle_\alpha &= \langle d^m u \rangle_0 + H_\alpha(d^m u). \end{aligned} \quad (2.16)$$

We let $H^{\alpha, \alpha/2}(\overline{Q_T})$ denote the Banach space of functions $u(x, y, t)$ that are continuous in $\overline{Q_T}$ with $\|u\|_{2+\alpha}$ finite (Theorem 4, Section 3.2 [22]).

Theorem 6.2 of Chapter V of [40] shows the existence and uniqueness of the solution to (2.10) with continuous initial and boundary conditions. By the theorem, the solution belongs to the space $H^{\beta, \beta/2}(\overline{Q_T})$ for some $0 < \beta < 1$, it also has bounded first spatial derivatives in $\overline{Q_T}$, and its second order spatial derivatives and first order time derivative belong to $H^{\gamma, \gamma/2}(\overline{Q_T})$ for some nonnegative and nonintegral number γ .

By substituting this solution in the coefficients of the PDE (2.7), Corollary 1 in Section 3.5 on page 74 of [22] affirms the existence and uniqueness of the solution to the linear PDE for suitable initial and boundary conditions.

Remark 8. *We require the positive variance condition (2.6) to be satisfied in order to ensure that v is nonnegative. Theorem 6.2 of Chapter V from [40] affirms that F_y is bounded, but as far as the statement of the theorem goes, we do not have an explicit expression of it. For that reason, it is not easy to show that (2.6) is satisfied in general. In the case where the market driver with value F is of plain vanilla type*

with $Q > 0$, enforcing Feller's condition (2.2) is sufficient for the positive variance condition (2.6) to be satisfied since $\partial F/\partial y \geq 0$, and therefore $Q(\partial F/\partial y) \geq 0$.

2.4 Control Problem

From now on, we focus on solving (2.10). We can apply various numerical methods, for example, the FDM, to calculate the solution numerically. If we were to do this, we would need additional resources to implement it in actual trading and in some cases, it may not be easy to do so*. One of the difficulties may originate from the fact that even though it's semilinear, it's still a nonlinear PDE that we are dealing with. Applying the model to actual trading becomes more straightforward with the help of the Policy Improvement Algorithm (PIA).

It is easy to see that (2.10) can be rewritten as

$$\inf_{\pi \in \mathbb{R}} \left(u_t + Lu + ru - \pi u_y + \frac{\pi^2}{4\kappa Q} \right) = 0. \quad (2.17)$$

Note that this is the HJB equation to minimize

$$V^\pi(x, y, t) = \mathbf{E} \left[\int_0^{\tau \wedge t} e^{-rs} f^\pi(Z_s^{z, \pi}, t-s) ds + e^{-r(\tau \wedge t)} g(Z_{\tau \wedge t}^{z, \pi}, t \wedge \tau) \right] \quad (2.18)$$

under the controlled process $Z_t^{z, \pi} := (X, Y^\pi)^T$ with dynamics given by the SDEs

$$\begin{cases} dX = \mu X dt + \sqrt{Y} X dW^1 \\ dY^\pi = \kappa(\bar{v} - Y^\pi + \pi/\kappa) dt + \eta \rho \sqrt{Y^\pi} dW^1 + \eta \sqrt{Y^\pi} \sqrt{1 - \rho^2} dW^2 \\ d\langle W^1, W^2 \rangle_t = 0 \end{cases} \quad (2.19)$$

with $Z_0^{z, \pi} = z = (x, y)^T$. Here, $f^\pi = \pi^2/4\kappa Q$, $g = \psi$ is the initial and boundary conditions introduced in Section 2.3, and τ is the first hitting time of the boundary of the domain.

Our problem is now converted into the HJB equation for the following controlled initial/boundary problem:

*For example, banks usually have their own quants create special functions implemented in their platform to be used by the employees globally. In order to add a new function, they first need to seek approval from their managers. Once they get the approval, they have to write codes for the function and test it on top of their daily tasks. Chased up by many urgent issues that come up every day, the release of the new function may be delayed or eventually be forgotten.

$$\begin{cases} \inf_{\pi \in \mathbb{R}} \left(u_t + Lu + ru - \pi u_y + \frac{\pi^2}{4\kappa Q} \right) = 0, & (x, y, t) \in \mathcal{E} \times (0, T) \\ u(x, y, t) = \inf_{\pi} V^{\pi}(x, y, t). \end{cases} \quad (2.20)$$

From the positive variance condition (2.6),

$$\pi > \frac{\eta^2}{2} - \kappa \bar{v} \quad (2.21)$$

is sufficient for Y not to go below zero.

2.5 Policy Improvement Algorithm

We now give a detailed formulation of the PIA and the proof of convergence. For more detail, we refer to [31], [32], and [69].

Let $(\Omega, \mathcal{F}, (\mathcal{F}_t)_{t \geq 0}, \mathbf{P})$ be a filtered probability space satisfying the usual conditions that supports a 2-dimensional $(\mathcal{F}_t)_{t \geq 0}$ - Wiener process $W = (W_t)_{t \geq 0}$.

For any process $\mathcal{Y} = (\mathcal{Y}_t)_{t \geq 0}$, define

$$\tau_{\mathcal{E}}(\mathcal{Y}) := \inf\{t \geq 0; \mathcal{Y}_t \in \partial\mathcal{E}\}. \quad (2.22)$$

Let

$$\begin{aligned} \mathcal{A}(z, T) := \{ & \Pi = (\Pi_t)_{t < T}; \Pi \text{ is adapted to } (\mathcal{F}_t)_{t < T}, \Pi_t(\omega) \in \mathbb{R} \\ & \text{for every } t < T \text{ and } \omega \in \Omega, \text{ and there exists a process } Z^{z, \Pi} \\ & \text{that satisfies (2.24) and is unique in law}\}, \end{aligned} \quad (2.23)$$

where

$$Z_t^{z, \Pi} = z + \int_0^t \sigma(Z_s^{z, \Pi}, s, \Pi_s) dW_s + \int_0^t \mu(Z_s^{z, \Pi}, s, \Pi_s) ds, \quad t \leq T \wedge \tau_{\mathcal{E}}(Z^{z, \Pi}). \quad (2.24)$$

A measurable function $\pi : \Omega \times (0, T) \rightarrow \mathbb{R}$ is a *Markov policy* if for every $z \in \mathcal{E}$ and $T > 0$ there exists a process $Z_t^{z, \pi}$ that is unique in law and satisfies the following:

$$\begin{aligned}
Z_t^{z,\pi} &= z + \int_0^t \sigma(Z_s^{z,\pi}, s, \pi(Z_s^{z,\pi}, s)) dW_s + \int_0^t \mu(Z_s^{z,\pi}, s, \pi(Z_s^{z,\pi}, s)) ds \\
&= z + \int_0^t \sigma_\pi(Z_s^{z,\Pi}, s) dW_s + \int_0^t \mu_\pi(Z_s^{z,\Pi}, s) ds, \quad t \leq T \wedge \tau_{\mathcal{E}}(Z^{z,\pi}).
\end{aligned} \tag{2.25}$$

For any domain $Q_T = \mathcal{E} \times (0, T)$ and bounded measurable function g defined on Γ_T , define $V^{g,\mathcal{E},\pi}$ by

$$V^{g,\mathcal{E},\pi}(z, t) = \mathbf{E}_z \left(\int_0^{t \wedge \tau} e^{-rs} f^\pi(Z_s^{z,\pi}, t-s) ds + e^{-r(t \wedge \tau)} g(Z_{t \wedge \tau}^{z,\pi}, t \wedge \tau) \right), \tag{2.26}$$

where f^π is the running cost and τ is the first exit time from Q_T .

Now define

$$V^{g,\mathcal{E}} := \inf_{\pi \in \mathcal{A}} V^{g,\mathcal{E},\pi}. \tag{2.27}$$

Finally, we define the differential operator L^π :

$$L^\pi u := -u_t + \frac{1}{2} \text{Tr} \{ \sigma_\pi^T (Hu) \sigma_\pi \} + \mu_\pi^T \nabla u \quad \text{for } u \in C^{2,1}, \tag{2.28}$$

where Hu denotes the Hessian of the function u .

Proposition 2.5.1. *For any Markov policy π that is Lipschitz on compact sets in \mathbb{R}_+^2 , the following holds: $V^{g,\mathcal{E},\pi} \in C^{2,1}(Q_T)$ and it satisfies*

$$L^\pi V^{g,\mathcal{E},\pi} - rV^{g,\mathcal{E},\pi} + f^\pi = 0. \tag{2.29}$$

Proof. It suffices to prove that $V^{g,\mathcal{E},\pi}$ satisfies (2.29) in every domain $U_T = U \times (0, T)$ with $\overline{U_T} \subset Q_T$, where $U \subset \mathbb{R}_+^2$ is an open ball with centre ζ and radius ℓ . Let $z \in U_T$ and define τ as the first time the process $Z^{z,\pi}$ hits the boundary of U_T . For every $n \in \mathbb{N}$, define U^n as the closed ball with centre ζ and radius $\ell - \frac{1}{n}$. Define U_T^n as $U^n \times (0, T)$, and let τ_n be the first time the process $Z^{z,\pi}$ hits the boundary of U_T^n .

Let $v \in C^{2,1}(U_T) \cap C(\overline{U_T})$ be the unique solution of the initial boundary value problem

$$\begin{cases} L^\pi v - rv + f^\pi = 0 \\ v|_{U_T} = V^{g,\mathcal{E},\pi}|_{U_T}. \end{cases} \tag{2.30}$$

The existence and uniqueness is guaranteed by Corollary 1 on page 71 in [22] and Lemma B.5 in Appendix B. The partial derivatives of v are Hölder continuous by

the same corollary. Let n_0 be large enough such that $z \in U_T^n$, and for every $n \geq n_0$, define the process $(J^n)_{n \geq n_0}$ by

$$J_t^n := \int_0^{t \wedge \tau_n} e^{-rs} f^\pi(Z_s^{z, \pi}, t-s) ds + e^{-r(t \wedge \tau_n)} v(Z_{t \wedge \tau_n}^{z, \pi}, t - t \wedge \tau_n) \quad (2.31)$$

and

$$J_t := \int_0^{t \wedge \tau} e^{-rs} f^\pi(Z_s^{z, \pi}, t-s) ds + e^{-r(t \wedge \tau)} v(Z_{t \wedge \tau}^{z, \pi}, t - t \wedge \tau). \quad (2.32)$$

Itô's formula on $[0, \tau_n]$ and the differential equation for v yield

$$\begin{aligned} J_t^n &= v(z, t) + \int_0^{t \wedge \tau_n} e^{-rs} (f^\pi - rv + L^\pi v)(Z_s^{z, \pi}, t-s) ds + \int_0^{t \wedge \tau_n} e^{-rs} (\nabla v)^T \sigma_\pi dW_s \\ &= v(z, t) + \int_0^{t \wedge \tau_n} e^{-rs} (\nabla v)^T \sigma_\pi dW_s. \end{aligned} \quad (2.33)$$

Hence J^n is a local martingale, and since it is clearly a bounded process, it is a uniformly integrable martingale. Thus the Dominated Convergence Theorem yields

$$v(z, t) = \lim_{n \rightarrow \infty} \mathbf{E}(J_0^n) = \lim_{n \rightarrow \infty} \mathbf{E}(J_t^n) = \mathbf{E}(J_t). \quad (2.34)$$

From the initial and boundary conditions for v , we obtain

$$\begin{aligned} J_t &= \int_0^{t \wedge \tau} e^{-rs} f^\pi(Z_s^{z, \pi}, t-s) ds + e^{-r(t \wedge \tau)} v(Z_{t \wedge \tau}^{z, \pi}, t - t \wedge \tau) \\ &= \int_0^{t \wedge \tau} e^{-rs} f^\pi(Z_s^{z, \pi}, t-s) ds + e^{-r(t \wedge \tau)} V^{g, \mathcal{E}, \pi}(Z_{t \wedge \tau}^{z, \pi}, t - t \wedge \tau) \\ &= \mathbf{E} \left(\int_0^{t \wedge \tau} e^{-rs} f^\pi(Z_s^{z, \pi}, t-s) ds + e^{-r(t \wedge \tau)} g(Z_{t \wedge \tau}^{z, \pi}, t \wedge \tau) \middle| \mathcal{F}_t \right). \end{aligned} \quad (2.35)$$

The last equality in (2.35) follows from Lemma B.1. We conclude:

$$\begin{aligned} v(z, t) &= \mathbf{E} \left(\int_0^{t \wedge \tau} e^{-rs} f^\pi(Z_s^{z, \pi}, t-s) ds + e^{-r(t \wedge \tau)} g(Z_{t \wedge \tau}^{z, \pi}, t \wedge \tau) \right) \\ &= V^{g, \mathcal{E}, \pi}(z, t). \end{aligned} \quad (2.36)$$

□

We now describe the algorithm. Let π_0 be a Markov policy that is Lipschitz on compacts in \mathbb{R}_+^2 . The algorithm is defined as follows:

$$\begin{cases} \mathcal{L}u_i - \pi_i(u_i)_y + f^{\pi_i} = 0 \\ \pi_{i+1}(z, t) = \arg \min_{p \in A} (L^p u_i(z, t) - ru_i(z, t) + f^p(z, t)), \end{cases} \quad (2.37)$$

where the differential operator \mathcal{L} is defined as

$$\mathcal{L} := -\frac{\partial}{\partial t} - L \quad (2.38)$$

using L in (2.9). It is important to note that \mathcal{L} is independent of π_i . In our problem, (2.37) can be further calculated as

$$\begin{cases} \mathcal{L}u_i - \pi_i(u_i)_y + \pi_i^2/4\kappa Q = 0 \\ \pi_{i+1}(z, t) = 2\kappa Q(D_y u_i), \end{cases} \quad (2.39)$$

where D_y denotes the partial differential operator with respect to y .

We already know from Section 2.3 that the solution of the semilinear PDE (2.10) exists uniquely with bounded spatial derivatives, so instead of \mathcal{A} in (2.23), we can take a subset of \mathcal{A} on which the controls are uniformly bounded. Also, note that $D_y u_i$ expresses the vega of the (approximated) market driver which we assumed to be a plain vanilla. As mentioned in Section 2.1, since plain vanilla options are positive vega products and if $Q > 0$, we know that π_i is nonnegative from the definition in (2.39). If we assume that (2.2) is satisfied, then we see that condition (2.21) is also satisfied. This precludes Y^π from becoming negative.

In order to apply the PIA, we need to check if the algorithm (2.39) satisfies the criteria of the PIA. The only criterion needed to be verified is the uniform Lipschitz condition on π_i . The following lemma proves this.

Lemma 2.5.2. *$\{\pi_i\}_i$ defined in (2.39) is uniformly Lipschitz continuous.*

Proof. From the Schauder estimate, we have

$$\|u_{i+1}\|_{2+\alpha} \leq C(\|g\|_{2+\alpha} + \|f^{\pi_n}\|_\alpha), \quad (2.40)$$

where C only depends on the Hölder norms of the coefficients of L^π , the domain Q_T , and ν_1 in (2.11). If g is continuous, we can approximate it uniformly in $2 + \alpha$ norm by the Weierstrass approximation theorem as mentioned on page 71 in [22]. In our specific problem, $f^{\pi_n} = \pi_n^2/4\kappa Q$, so $\|f^{\pi_n}\|_\alpha$ is uniformly bounded thanks to

the uniform boundedness of $\pi_i \in \mathcal{A}$. As the right hand side of (2.40) is uniformly bounded, $(u_i)_i$ is uniformly bounded in $2 + \alpha$ norm, hence π_i is uniformly Lipschitz continuous from the second equation in (2.39). \square

The PIA tells us that the u_i in (2.39) converges and the limit function is $V^{g, \mathcal{E}}$ which is $C^{2,1}$ and satisfies the HJB equation (2.20) in Q_T .

We will see later in the actual numerical example that the convergence to the solution happens fast. In the case of a plain call option as the market driver, we get a numerical solution very close to that of the semilinear PDE with only 1 iteration.

Proposition 2.5.3. $\|u_{i+2} - u_{i+1}\|_{2+\alpha} \leq C\kappa Q \|u_{i+1} - u_i\|_{2+\alpha}^2$

Proof. By definition and Proposition 2.5.1

$$\begin{cases} \mathcal{L}u_{i+2} - \pi_{i+2}(u_{i+2})_y + \pi_{i+2}^2/4\kappa Q = 0 \\ \mathcal{L}u_{i+1} - \pi_{i+1}(u_{i+1})_y + \pi_{i+1}^2/4\kappa Q = 0. \end{cases} \quad (2.41)$$

Subtracting these 2 equations and setting $v_{i+2} := u_{i+2} - u_{i+1}$,

$$\mathcal{L}v_{i+2} - \pi_{i+2}(v_{i+2})_y - (\pi_{i+2} - \pi_{i+1})^2/4\kappa Q = 0. \quad (2.42)$$

Since v_i is 0 on the parabolic boundary, from the Schauder estimate:

$$\|v_{i+2}\|_{2+\alpha} \leq C \left\| \frac{\pi_{i+2} - \pi_{i+1}}{4\kappa Q} \right\|_{\alpha}^2 = C\kappa Q \|(v_{i+1})_y\|_{\alpha}^2 \leq C\kappa Q \|v_{i+1}\|_{2+\alpha}^2 \quad (2.43)$$

\square

Proposition 2.5.3 shows that if the approximation of the solution is close enough to the classical solution of the semilinear PDE, $\{u_i\}_i$ converges quadratically to the solution. In other words, Proposition 2.5.3 shows the quadratic local convergence of the solutions of the PIA to the classical solution.

Corollary 2.5.4.

$$\|u_{i+1} - u_i\|_{2+\alpha} \leq (C\kappa Q \|u_1 - u_0\|_{2+\alpha})^{2^i - 1} \|u_1 - u_0\|_{2+\alpha} \quad (2.44)$$

Proof. Use Proposition 2.5.3 and induction. \square

2.6 Numerical Simulation

2.6.1 First Example

We now numerically investigate how the pricing and risks change with our model. We assume that a large amount of 2 year, 120 strike call is owned by investors outside the OTC market. We first price this structure using (2.8). Then, substituting this solution in (2.7), we price a different derivatives product, a 2 year, 100 strike call. We compare the results with the ones obtained from the Heston model. We used the explicit FDM method. We note that with sufficiently fine mesh in the discretization, the numerical solutions converge to the analytic ones. Hereafter, we refer to the 2 year, 120 strike call as 120 call and 2 year, 100 strike call as 100 call or at-the-money (ATM) call.

We use the parameters in Table 2.1.

| Parameter | Value |
|-----------|---------|
| Q | 0.0003 |
| r | 3.0% |
| ρ | -0.7571 |
| η | 0.3 |
| ω | 1.0 |
| \bar{v} | 0.04 |
| κ | 0.55 |

Table 2.1: Parameters for numerical simulation.

Note that Feller's condition (2.2) is met and $Q > 0$. From Remark 8, the positive variance condition (2.6) is therefore satisfied.

We take our domain \mathcal{E} to be a round rectangle so that the boundary is $C^{2+\alpha}$ and denote by S_{min} , S_{max} , v_{min} , and v_{max} the minimum and maximum values of the variables in the domain. In this example, we took $S_{min} = 0.5$, $S_{max} = 200$, $v_{min} = 0.00005$, and $v_{max} = 1.0$ and took the increments in S direction as $(S_{max} - S_{min})/50 = (200 - 0.5)/50$ and in v direction as $(v_{max} - v_{min})/50 = (1.0 - 0.00005)/50$. For the time interval $[0, 2]$, we discretized it similarly by 30,000 so that the time increment is $2/30000 = 1/15000$ years. We denote by F_H the value F calculated in the Heston model and by F_N the value calculated in the new model. Similarly, we denote by V_H and V_N the corresponding values for an arbitrary V .

As in [26], for the calculation in the Heston model, we use the initial and boundary conditions:

$$\begin{cases} F_H(S, v, 0) = \max(0, S - K)^+ & (S, v) \in \mathcal{E} \\ F_H(S_{min}, v, t) = 0 & (S = S_{min}) \\ \frac{\partial F_H}{\partial S}(S_{max}, v, t) = 1 & (S = S_{max}) \\ \frac{\partial F_H}{\partial t} - rS \frac{\partial F_H}{\partial S} + rF_H - \kappa \bar{v} \frac{\partial F_H}{\partial v} = 0 & (v = v_{min}) \\ F_H(S, v_{max}, t) = S & (v = v_{max}). \end{cases} \quad (2.45)$$

The solution to the initial-boundary problem for Heston's PDE with conditions (2.45) is continuous up to the boundary, so we can use the value of F_H as the boundary condition for F_N . This way, the values of F_H and F_N match on the parabolic boundary.

We use the same conditions as in (2.45) for V .

With the parameters in Table 2.1, the drift in the second SDE of (2.4) is shifted by $\kappa Q \frac{\partial F_N}{\partial v}$, which in this case is calculated as $0.55 \times 0.0003 \times 77.188 = 0.0127$. This is about 58% of the value of $\kappa \bar{v}$.

The result for the 120 call (which in our case is the market driver) is shown in Table 2.2.

| Risks | Value | Delta | Vega | Vanna | Volga |
|-----------|--------|---------|--------|--------|----------|
| Heston | 2.6058 | 35.378% | 70.940 | 3.8766 | 119.001 |
| New Model | 3.5121 | 42.457% | 77.188 | 2.4132 | -535.557 |

Table 2.2: Summary for 120 call at $S = 98.255$ and $v = 0.030049$.

The result for the other derivative product (in our case, an at-the-money call) is shown in Table 2.3.

| Risks | Value | Delta | Vega | Vanna | Volga |
|-----------|--------|---------|--------|---------|----------|
| Heston | 11.299 | 74.117% | 79.238 | -0.5666 | -543.263 |
| New Model | 12.116 | 76.942% | 78.824 | -1.6201 | -961.800 |

Table 2.3: Summary for at-the-money (ATM) call at $S = 98.255$ and $v = 0.030049$.

The results are for $S = 98.255$ and $v = 0.030049$ at time $t = T = 2$. In volatility convention (i.e. standard deviation, as traders usually prefer this over variance), this value of v is equivalent to $\sigma = \sqrt{v} = 17.335\%$.

The obvious result is that the options are priced higher under the new model and we see it from Table 2.2 and Table 2.3. This is due to the current set-up that the 120 call (which is a positive vega product) is held outside of the OTC market. Since the OTC market is then overall short vega, or in other words, short volatility,

the model correctly adjusts the level of the volatility which is now in demand. If we calculate the equivalent volatilities in the Heston model based on the prices we get from the new model, we get the correspondance shown in Table 2.4.

| | 120 Call | ATM Call |
|------------|----------|----------|
| Heston | 17.335% | 17.335% |
| New Model | 20.694% | 20.090% |
| Difference | 3.359% | 2.755% |

Table 2.4: Implied volatility calculated based on the risk calculated in the Heston model.

From Table 2.4, we see that the volatility is higher, and the increments against the Heston volatilities are different for different structures. The result of Table 2.4 shows a skewness of the impact the market driver has on the volatility.

To understand how large this difference in the implied volatility is, we can assume that the vega traders maintain ranges between \pm \$10 million. With 3% difference in volatility as shown in Table 2.4, if they are short \$10 million of vega, their mark-to-market loss would be -\$30 million. If their goal is to raise \$100 million of profit in a year, then this loss already corresponds to 30% of the annual target.

Figure 2.1 and Figure 2.2 show a simulation of the processes of the stock price and the volatility.

As mentioned in Section 2.1, this model prices-in not only the initial impact when some big position is traded with clients, but also the adjusted impact afterwards due to the change in the risk of the market driver. The risks change as the market moves, therefore the way traders hedge options changes under the new model. This is reflected in the graphs of the delta, vanna, and volga risks calculated in the new model compared to the ones calculated in the Heston model in Figure 2.3. The difference in each risk is plotted in Figure 2.4.

For example, when we check the delta on Table 2.2 and Table 2.3, the values are higher in the new model. This is because traders lose money when the stock price goes higher. To explain this in more detail, when the stock price goes higher, the vega of the 120 call gets larger since the stock price gets closer to the strike 120. This makes the traders in the OTC market get shorter in vega, hence they will even be more eager to buy the volatility in the market. This shifts the volatility higher. The consequence of this is that the traders will lose in mark-to-market because the value of the call they are short is greater now due to the spike in volatility. The new model anticipates this and asks the traders to buy more stocks beforehand so that they are hedged from this event.

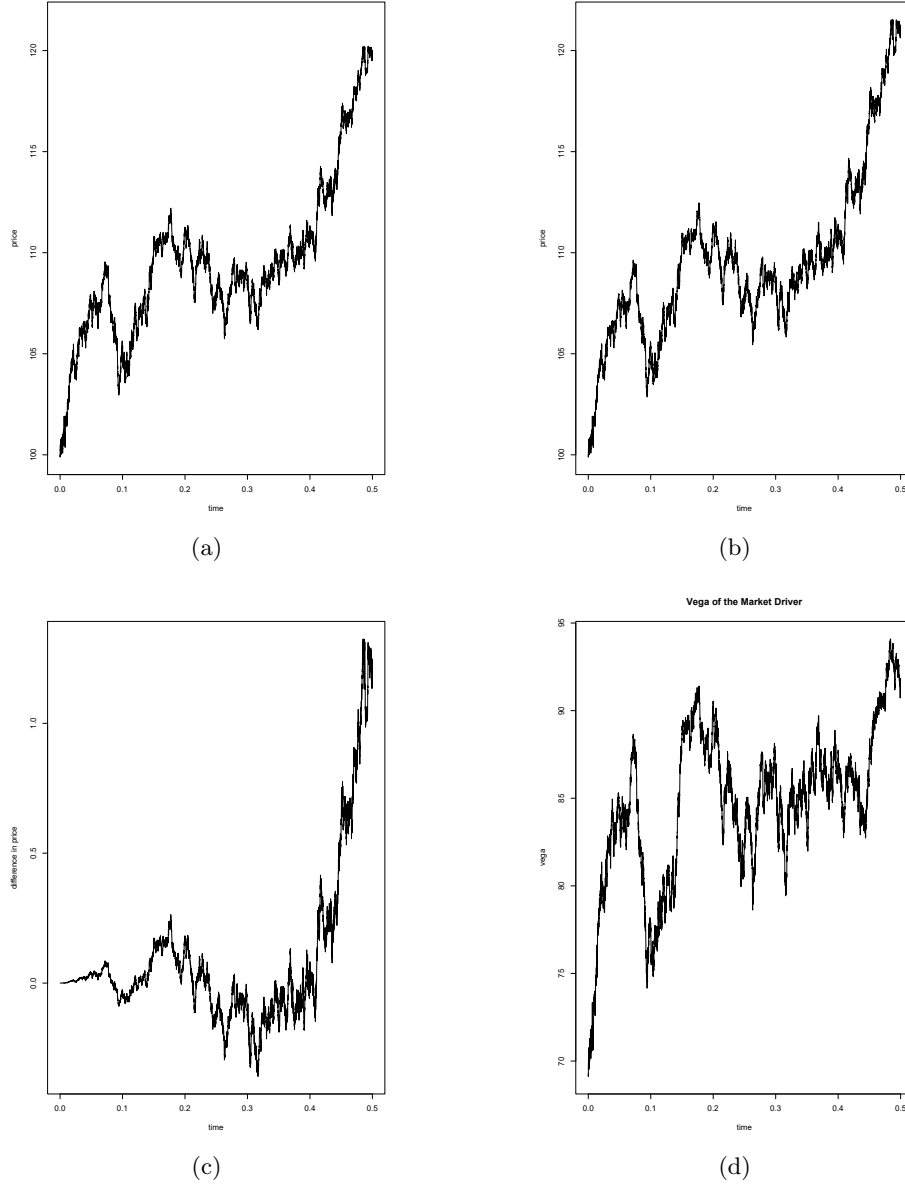
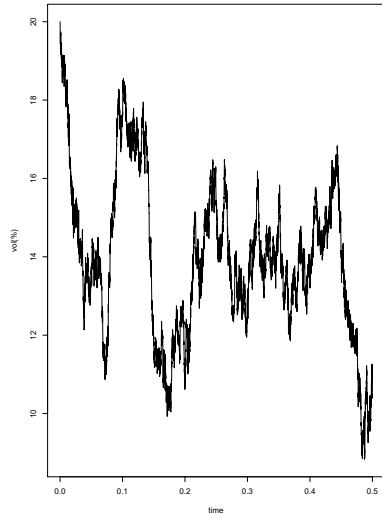
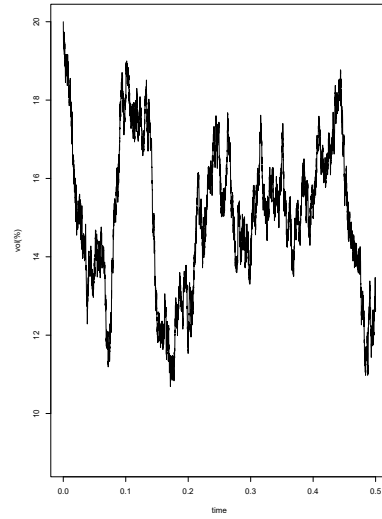


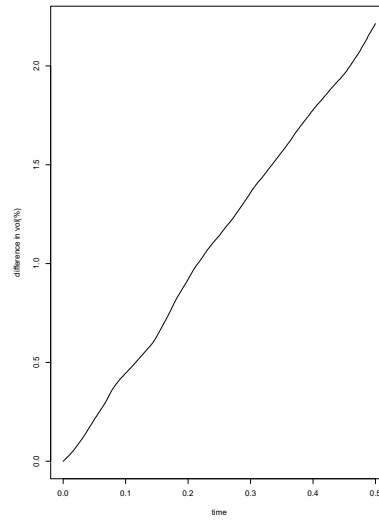
Figure 2.1: Simulation of the SDEs (2.4) for the first 6 months starting from $S = 100$ and $v = 0.04$ with F being the value of the 2Y 120 call in (a) Heston model and (b) the new model. The difference in the values of the two prices is shown in (c) where the largest difference in absolute value is 1.3248, which corresponds to 132.48 basis points to the initial stock price. We used the drift $\mu = 0.05$. (d) shows how the vega of the call in the new model changes over time.



(a)



(b)



(c)

Figure 2.2: The volatility processes on the same simulation as in Figure 2.1 in (a) Heston model and (b) the new model. The difference in values shown in (c).

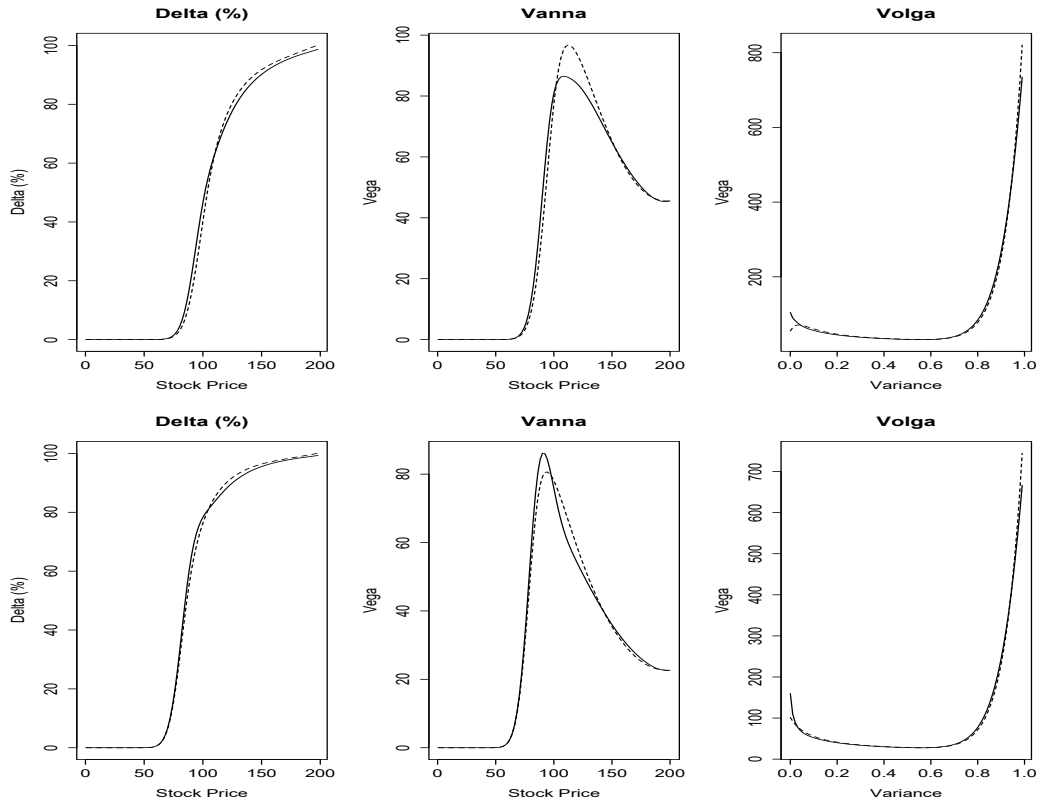


Figure 2.3: Risks of the calls; Top 3 charts are for the 120 call and the bottom 3 are for the ATM call. The solid lines indicate the risks calculated in the new model and the dotted lines the corresponding risks calculated in the Heston model.

2.6.2 Second Example

In the previous subsection, we assumed that the 120 call was the market driver and traders were short of the position such that the volatility was in demand. We saw that it indeed made the prices of plain vanilla options more expensive, hence the implied volatility higher. In this subsection, we keep the same structure as the market driver, but assume now that this is held by the traders, hence the volatility should now be offered. We set $Q = -0.0003$ and keep all the parameters the same as in Table 2.1.

| Risks | Value | Delta | Vega | Vanna | Volga |
|-----------|--------|---------|--------|--------|---------|
| Heston | 2.6058 | 35.378% | 70.940 | 3.8766 | 119.001 |
| New Model | 2.1438 | 30.905% | 60.440 | 3.8553 | 382.287 |

Table 2.5: Summary for 120 call at $S = 98.255$ and $v = 0.030049$.

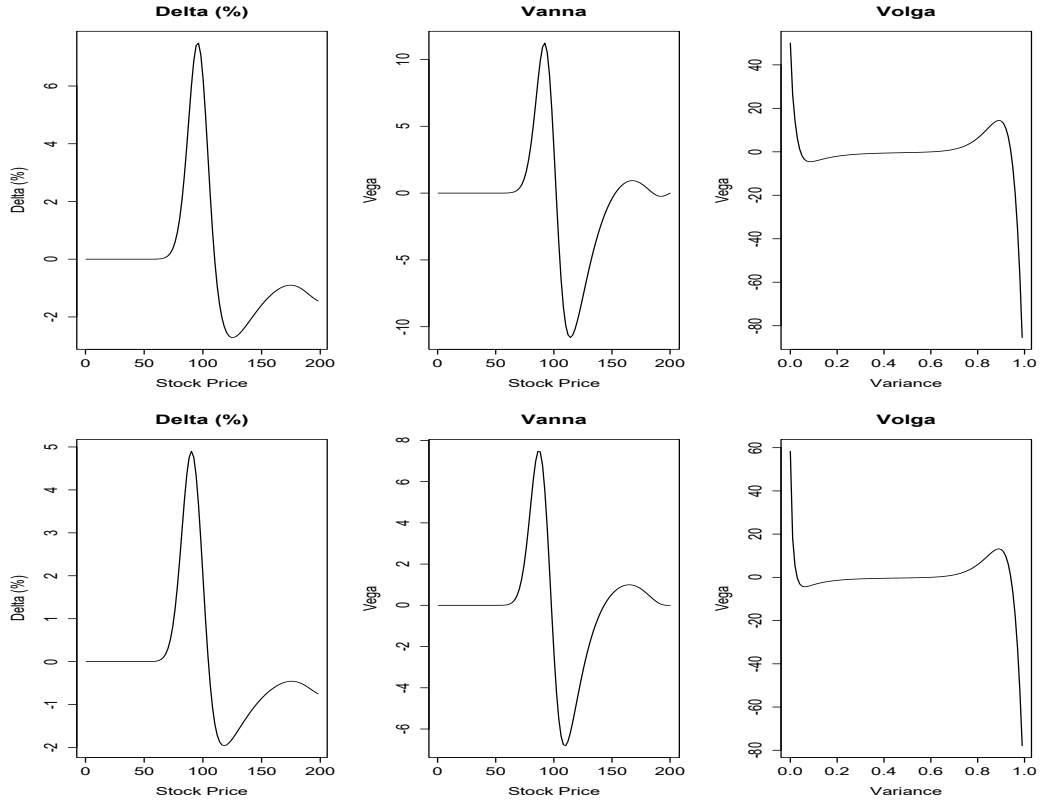


Figure 2.4: The differences plotted between the values in the new model and the Heston model from Figure 2.3.

| Risks | Value | Delta | Vega | Vanna | Volga |
|-----------|--------|---------|--------|---------|----------|
| Heston | 11.299 | 74.117% | 79.238 | -0.5666 | -543.263 |
| New Model | 10.841 | 71.868% | 73.393 | -0.4005 | -281.226 |

Table 2.6: Summary for at-the-money (ATM) call at $S = 98.255$ and $v = 0.030049$.

| | 120 Call | ATM Call |
|------------|----------|----------|
| Heston | 17.335% | 17.335% |
| New Model | 15.342% | 15.578% |
| Difference | -1.993% | -1.757% |

Table 2.7: Implied volatility calculated based on the risk calculated in the Heston model.

The premium and risks of the market driver is shown in Table 2.5 and those of the ATM call in Table 2.6. The results show that the prices of the plain vanilla calls are now lower than those in the Heston model. We also see in Table 2.7 that

the implied volatility is lower under the new model.

2.6.3 PIA on the Example in Subsection 2.6.1

We now see what happens when we apply the PIA to the semilinear case in Subsection 2.6.1 in calculating the value of the 120 call. We take $\pi_0 \equiv 0$ so that the solution of 0th iteration matches with the one from the Heston model. The result is shown in Figure 2.5. We tried up to 4th iteration as it implies convergence in numerical solution at this point as shown in Table 2.8.

| Iteration | 0th | 1st | 2nd | 3rd | 4th |
|------------|--------|--------|-----------------------|-------|-------|
| Difference | 2.3177 | 0.0322 | 7.72×10^{-6} | 0.000 | 0.000 |

Table 2.8: Largest differences in absolute value between the numerical solutions of the approximated linear PDE and the original semilinear PDE. The figures could be regarded as the differences in percentage against the initial price of the stock as it is set to 100.

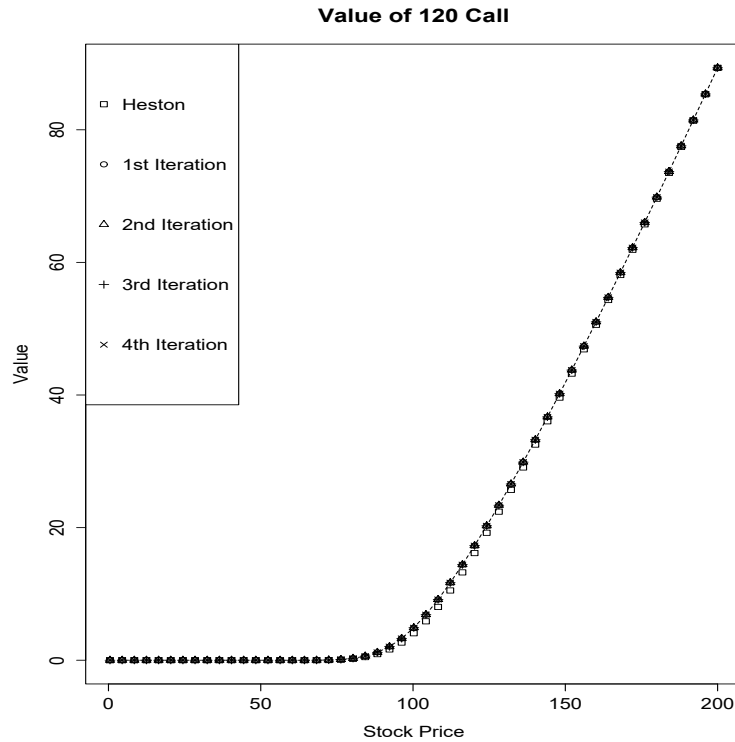


Figure 2.5: PIA results for the 120 call. Dotted line is the solution using Finite Difference Method (FDM) directly on the semilinear PDE. v is taken as $v = 0.040048$.

In Figure 2.6, we show a magnification of Figure 2.5 centered around the stock price where we saw the largest difference, which happened to be at-the-money.

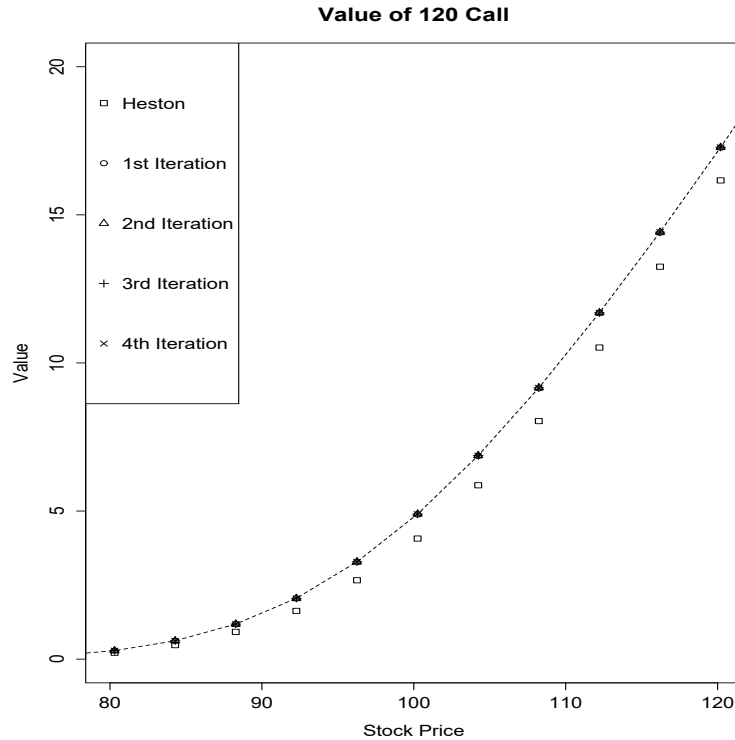


Figure 2.6: Magnification around at-the-money of Figure 2.5. We see that the first iteration already approximates well the numerical solution to the semilinear PDE.

We see in Figure 2.6 that the numerical solution of the semilinear PDE is different from that of the Heston model (0th iteration), but the 1st iteration in the PIA already brings the solution very close to that of the semilinear PDE. This is also implied by the result in Table 2.8. This means that the numerical solution of the semilinear PDE is well approximated by a series of linear PDEs. This is good news as we do not have to create a separate program to calculate the solution to the new model, but can just reuse the same program for the Heston model with modified coefficients. The PIA also appears to have better convergence compared to the explicit FDM on a Dirichlet boundary value problem of a second order semilinear elliptic PDE as will be explored in the next chapter.

2.7 Conclusions

We introduced a new model which reflects the impact of a large position that is skewing the volatility market. We also introduced the Policy Improvement Algorithm. The algorithm lets us handle a semilinear PDE as a series of linear PDEs and at the same time keep the calculation load similar to that when we run the FDM on the original semilinear problem, thanks to the fast convergence of the iterations. This enables us to easily implement the new model in practice by reusing the resources used for the Heston model which has already been widely used in the industry.

We only used a single product as a market driver, but we might try to extend this to the case when it is of a portfolio of several products. We only used a plain vanilla option as the market driver, but we should also be able to extend the model to be used for more exotic options. The difficulty then is to show the existence and uniqueness of the solution to the semilinear PDE (2.8) and to check if the solution satisfies the positive variance condition (2.6). If so, by substituting this solution in the coefficient of the linear PDE (2.7), we can solve for the values of other derivatives products as in the case of the Heston model. It only takes relatively small effort to allow for the market asymmetry and to get the correct risks driven by the market driver. The numerical calculations when the market driver is an autocallable are shown in Appendix C.

The other difficulty in applying the model to actual trading appears in the calibration process. We assumed that we knew all the parameters including the detail of the market driver, but it may be challenging to recover these in the actual market, especially with more freedom in the model than in the Heston model and with limited market information.

Chapter 3

Quadratic Local Convergence of the PIA

3.1 Introduction

In Chapter 2, we introduced a new model for pricing derivatives products when we have a position concentration in the over-the-counter market. The model requires us to solve a nonlinear partial differential equation (PDE) and this may prevent traders from using it in practice due to possible difficulties in implementing a solution in their pricing models. To overcome this difficulty, we used the policy improvement algorithm (PIA) to enable us to approximate the nonlinear PDE by a series of linear ones parameterized by a control. The solutions of the linear PDEs converge to that of the original semilinear PDE as we iteratively solve the linear PDEs under the algorithm. Since their stochastic volatility pricing models can solve linear PDEs (as in Heston's model), the traders can now implement the new model. We further showed that the PIA approximated solutions show *quadratic local convergence* (QLC) to the analytic solution. This provides an explanation of why the convergence happens so fast.

The natural question to ask is how general this QLC is in the PIA framework. In this chapter, we consider a general infinite time horizon problem and calculate the rate of convergence of the PIA-derived approximations to that of the corresponding semilinear elliptic PDE. We give three conditions which enable us to show the QLC. These assumptions are indeed satisfied by the problem considered in Chapter 2. We describe in Remark 10 how some of these assumptions can be relaxed.

The rest of the paper is organized as follows: Section 3.2 briefly explains the setup. In Section 3.3, we state the main theorem about QLC of the approximated

solutions to the semilinear PDE. We give a numerical example in Section 3.4 and give some concluding questions in Section 3.5.

3.2 Setup

We briefly explain our setup. Let $(\Omega, \mathcal{F}, (\mathcal{F}_t)_{t \geq 0}, \mathbf{P})$ be a filtered probability space. We assume that \mathcal{E} is a simply connected, convex, and bounded subset of \mathbb{R}^n that has $C^{2,\beta}$ boundary. We define

$$\tau_{\mathcal{E}}(\mathcal{Y}) := \inf\{t \geq 0; \mathcal{Y}_t \notin \mathcal{E}\} \quad (3.1)$$

for any continuous process $\mathcal{Y} = (\mathcal{Y}_t)_{t \geq 0}$.

For a control Π and starting point z , we wish to define the controlled process $Z^{z,\Pi}$ by

$$Z_t^{z,\Pi} = z + \int_0^t \sigma(Z_s^{z,\Pi}, \Pi_s) dB_s + \int_0^t \mu(Z_s^{z,\Pi}, \Pi_s) ds, \quad 0 \leq t \leq \tau_{\mathcal{E}}(Z^{z,\Pi}), \quad (3.2)$$

where $\sigma : \mathbb{R}^n \times \mathbb{R}^d \rightarrow \mathbb{R}^{n \times n}$ and $\mu : \mathbb{R}^n \times \mathbb{R}^d \rightarrow \mathbb{R}^n$ are measurable mappings, B is an n -dimensional Wiener process and Π takes values in $A = \mathbb{R}^d$.

For any $z \in \mathbb{R}^n$ define $\mathcal{A}(z)$, the set of admissible control at z , as

$$\begin{aligned} \mathcal{A}(z) := \{ & \Pi = (\Pi_t)_{t \geq 0}; \Pi \text{ is adapted to } (\mathcal{F}_t)_{t \geq 0}, \Pi_t(\omega) \in \mathbb{R}^d \\ & \text{for every } t \geq 0 \text{ and } \omega \in \Omega, \text{ and there exists a process} \\ & Z^{z,\Pi} = (Z_t^{z,\Pi})_{t \geq 0} \text{ that satisfies (3.2) and is unique in law} \}. \end{aligned} \quad (3.3)$$

A measurable function $\pi : \Omega \times (0, \infty] \rightarrow \mathbb{R}^d$ is a *Markov policy* if for every $z \in \Omega$ and $\forall T > 0$ there exists a process $Z_t^{z,\pi}$ that is unique in law and satisfies the following:

$$\begin{aligned} Z_t^{z,\pi} &= z + \int_0^t \sigma(Z_s^{z,\pi}, \pi(Z_s^{z,\pi}, s)) dB_s + \int_0^t \mu(Z_s^{z,\pi}, \pi(Z_s^{z,\pi}, s)) ds \\ &= z + \int_0^t \sigma_{\pi}(Z_s^{z,\pi}) dB_s + \int_0^t \mu_{\pi}(Z_s^{z,\pi}) ds, \quad 0 \leq t \leq T \wedge \tau_{\mathcal{E}}. \end{aligned} \quad (3.4)$$

We define the payoff function V^{Π} for any admissible Π as

$$\begin{aligned}
V^\Pi(z) &:= \mathbf{E} \left(\int_0^{\tau_\mathcal{E}} e^{-\alpha t} f(Z_t^{z,\Pi}, \Pi_t) dt + e^{-\alpha(\tau_\mathcal{E})} g(Z_{\tau_\mathcal{E}}^{z,\Pi}) \right) \\
&= \mathbf{E} \left(\int_0^{\tau_\mathcal{E}} e^{-\alpha t} f^{\Pi_t}(Z_t^{z,\Pi}) dt + e^{-\alpha(\tau_\mathcal{E})} g(Z_{\tau_\mathcal{E}}^{z,\Pi}) \right),
\end{aligned} \tag{3.5}$$

where α is some positive constant and $f : \mathbb{R}^n \times \mathbb{R}^d \rightarrow \mathbb{R}$ and $g : \mathbb{R}^n \rightarrow \mathbb{R}$. We assume that f^π is C^2 with respect to π and g is continuous. The problem is to find the value function V defined as

$$V := \sup_{\Pi \in \mathcal{A}} V^\Pi. \tag{3.6}$$

For any Markov policy π that is Lipschitz continuous on $\bar{\mathcal{E}}$, define $L^\pi : C^2 \rightarrow C$ by

$$L^\pi \phi := \frac{1}{2} \text{Tr} \{ \sigma_\pi^T (H\phi) \sigma_\pi \} + \mu_\pi^T \nabla \phi = \sum_{i,j} a_{ij}^\pi \frac{\partial^2 \phi}{\partial x_i \partial x_j} + \sum_i b_i \frac{\partial \phi}{\partial x_i}, \tag{3.7}$$

where $H\phi$ is the Hessian of ϕ .

From [32], V^π satisfies the PDE

$$L^\pi V^\pi - \alpha V^\pi + f^\pi = 0. \tag{3.8}$$

Starting from a Markov policy π_0 , the PIA defines successive controls by the recursion

$$\pi_{i+1} = \arg \max_{a \in \mathcal{A}} (L^a V^{\pi_i} - \alpha V^{\pi_i} + f^a). \tag{3.9}$$

Note that we assume that $\exists \nu > 0$ such that the differential operator L^π is uniformly elliptic, i.e.,

$$\frac{1}{\nu} |\xi|^2 \leq a_{ij}^\pi \xi_i \xi_j \leq \nu |\xi|^2 \quad \forall \xi_i, \xi_j \in \mathcal{E}, \forall \pi \in \mathbb{R}^d. \tag{3.10}$$

We define the distance at a point x from $\partial\mathcal{E}$ as

$$d_x = \min_{\xi \in \mathcal{E}} |x - \xi|, \tag{3.11}$$

and the distance between points x and y as

$$d_{xy} = \min(d_x, d_y). \tag{3.12}$$

We define the norm $\|u\|_{2,\beta}$ as

$$\|u\|_{2,\beta} = \langle u \rangle_\beta + \sum \langle dD_x u \rangle_\beta + \sum \langle d^2 D_x^2 u \rangle_\beta, \quad (3.13)$$

where

$$\begin{aligned} \langle d^m u \rangle_0 &= \sup_{x \in \bar{\mathcal{E}}} d_x^m |u(x)|, \\ H_\beta(u) &= \sup_{x,y \in \bar{\mathcal{E}}} d_{xy}^{m+\alpha} \frac{|u(x) - u(y)|}{d_{xy}^\beta}, \\ \langle d^m u \rangle_\beta &= \langle d^m u \rangle_0 + H_\beta(d^m u). \end{aligned} \quad (3.14)$$

$C^{2,\beta}(\bar{\mathcal{E}})$ is the Banach space of functions $u(x)$ that are continuous in $\bar{\mathcal{E}}$ with $\|u\|_{2,\beta}$ finite (Section 3.8, [22]).

3.3 Main Results

We make the following assumptions in this section.

Assumption 1. μ_π is in the form of $\mathbf{M}\pi + \mathbf{b}$ for some constant $n \times d$ matrix \mathbf{M} and n dimensional vector \mathbf{b} .

Assumption 2. σ_π is independent of π .

Assumption 3. f^π is strictly and uniformly concave in π , i.e. $\exists \lambda > 0$ such that $\mathbf{x}^T (H_\pi f^\pi) \mathbf{x} \leq -\lambda \|\mathbf{x}\|^2 < 0$ for all $\mathbf{x} \in \bar{\mathcal{E}}$, where $H_\pi f^\pi$ represents the Hessian of f^π with respect to π .

With these assumptions, we show the following:

Theorem 3.3.1. Under Assumptions 1, 2, and 3, there exists a $C > 0$ such that

$$\|V^{\pi_{i+1}} - V^{\pi_i}\|_{2,\beta} \leq C \|V^{\pi_i} - V^{\pi_{i-1}}\|_{2,\beta}^2, \quad (3.15)$$

where C only depends on the domain \mathcal{E} , the ellipticity constant ν from (3.10), and the bounds on the coefficients of the differential operator L^π .

Remark 9. Applying (3.15) iteratively, we obtain

$$\|V^{\pi_{i+1}} - V^{\pi_i}\|_{2,\beta} \leq \frac{\{C \|V^{\pi_1} - V^{\pi_0}\|_{2,\beta}\}^{2^i}}{C}. \quad (3.16)$$

Therefore, once $\|V^{\pi_{i+1}} - V^{\pi_i}\|_{2,\beta} < 1/C$, convergence is extremely fast.

Remark 10. Suppose that A , the action space (the value space for π) is not \mathbb{R}^d . We may replace it by its image under $\mu(x, \cdot)$, provided we simultaneously replace f by \tilde{f} given by

$$\tilde{f}(x, m) = \sup_{\pi \in (x, \cdot)^{-1}(m)} f(x, \pi),$$

since we wish to maximise V^π . Suppose that this image is \mathcal{M} . By allowing relaxed controls (see for example [1]) we can replace this by $\mathcal{N} := \bar{co}(\mathcal{M})$, the closure of the convex hull of \mathcal{M} . This will have the effect of simultaneously replacing $\tilde{f}(x, \cdot)$ by \bar{f} , the smallest concave majorant of \tilde{f} . If \bar{f} is strictly uniformly concave and \mathcal{N} is an affine set in \mathbb{R}^n then we recover Assumptions 1 and 3.

As we shall see, the proof of Theorem 3.3.1 relies heavily on Taylor's theorem and the disappearance of $\nabla_a(L^\alpha V^{\pi_i} - \alpha V^{\pi_i} + f^\alpha)$ at its maximum, where ∇_a denotes the gradient with respect to a . So, if \mathcal{N} is a compact subset of \mathbb{R}^d then we hit a problem when the maximizer μ lies on the boundary of \mathcal{N} .

We should still be able to obtain good approximations to V with QLC by extending the action space to $\tilde{\mathcal{N}}$ and extending \bar{f}^μ to $f^{*,\mu}$ in such a way that $\bar{f}^\mu = f^{*,\mu}$ in \mathcal{N} , $f^{*,\mu}$ always takes its maximum, \hat{f} in the interior of $\tilde{\mathcal{N}}$ and $\hat{f} - \sup_{\mu \in \mathcal{N}} \bar{f}^\mu \leq \epsilon$.

Remark 11. We considered the elliptic case, but the parabolic case follows in exactly the same fashion. We have the following theorem:

Theorem 3.3.2. Under the same assumptions as in Theorem 3.3.1 with a given initial condition, (3.16) holds in the parabolic case.

This is a generalization of Proposition 2.5.3 in Chapter 2. The proof of Theorem 3.3.1 is deferred to Appendix D.

3.4 Numerical Example

We apply the PIA in solving numerically a semilinear elliptic PDE. We take $\mathcal{E} \subset \mathbb{R}^2$ to be $[0.5, 2.0] \times [0.5, 2.0]$ with its corners smoothed in a $C^{2,\beta}$ fashion (this is needed to apply the boundary estimate in Theorem 3.3.1).

3.4.1 First Example

The SDEs we consider are

$$\begin{cases} dx = \pi x dt + \sigma x dW^1, \\ dy = \pi y dt + \eta y dW^2, \\ \langle dW^1, dW^2 \rangle = 0, \end{cases} \quad (3.17)$$

where W^1 and W^2 are 1-dimensional Wiener processes and $\pi \in \mathbb{R}$. Thus

$$\mu_\pi = \begin{pmatrix} \pi x \\ \pi y \end{pmatrix} \quad \text{and} \quad \sigma_\pi = \begin{pmatrix} \sigma x & 0 \\ 0 & \eta y \end{pmatrix}. \quad (3.18)$$

We take f^π to be

$$f^\pi = 1 - \frac{1}{2}\pi^2. \quad (3.19)$$

We define V^π as in (3.5) with $g \equiv 0$ on $\partial\mathcal{E}$. Then, V^{π_i} satisfies the elliptic PDE:

$$\frac{1}{2}\sigma^2 x^2 \frac{\partial^2 V^{\pi_i}}{\partial x^2} + \frac{1}{2}\eta^2 y^2 \frac{\partial^2 V^{\pi_i}}{\partial y^2} + \pi_i x \frac{\partial V^{\pi_i}}{\partial x} + \pi_i y \frac{\partial V^{\pi_i}}{\partial y} - \alpha V^{\pi_i} + 1 - \frac{1}{2}\pi_i^2 = 0, \quad (3.20)$$

where π_i is determined by

$$\pi_i = x \frac{\partial V^{\pi_{i-1}}}{\partial x} + y \frac{\partial V^{\pi_{i-1}}}{\partial y}. \quad (3.21)$$

Note that if V^{π_i} converges, the limit function V satisfies a semilinear elliptic PDE

$$\frac{1}{2}\sigma^2 x^2 \frac{\partial^2 V}{\partial x^2} + \frac{1}{2}\eta^2 y^2 \frac{\partial^2 V}{\partial y^2} - \alpha V + 1 - \frac{1}{2} \left(x \frac{\partial V}{\partial x} + y \frac{\partial V}{\partial y} \right)^2 = 0. \quad (3.22)$$

The variables we use are in Table 3.1.

Table 3.1: Parameters we use for the numerical calculation.

| parameter | value |
|----------------------|---------|
| α | 0.03 |
| σ | 2.0 |
| η | 0.2 |
| x_{max} | 2.0 |
| x_{min} | 0.50 |
| y_{max} | 2.0 |
| y_{min} | 0.50 |
| ToleranceLevel1 | 0.00001 |
| ToleranceLevel2 | 0.001 |
| discretization nodes | 100 |

We use the explicit finite difference method (FDM) to see the convergence

starting at $\pi_0 \equiv 0$ with the boundary condition $V^{\pi_i}|_{\partial\mathcal{E}} \equiv 0$. We discretize (3.20) and obtain

$$\begin{aligned}
& \frac{1}{2} \left(\frac{\sigma^2 x_j^2}{\Delta x^2} + \frac{\pi_i(j, k) x_j}{\Delta x} \right) V(j+1, k) + \frac{1}{2} \left(\frac{\sigma^2 x_j^2}{\Delta x^2} - \frac{\pi_i(j, k) x_j}{\Delta x} \right) V(j-1, k) \\
& + \frac{1}{2} \left(\frac{\eta^2 y_k^2}{\Delta y^2} + \frac{\pi_i(j, k) y_k}{\Delta y} \right) V(j, k+1) + \frac{1}{2} \left(\frac{\eta^2 y_k^2}{\Delta y^2} - \frac{\pi_i(j, k) y_k}{\Delta y} \right) V(j, k-1) \\
& - \left(\frac{\sigma^2 x_j^2}{\Delta x^2} + \frac{\eta^2 y_k^2}{\Delta y^2} + \alpha \right) V(j, k) + 1 - \frac{1}{2} \pi_i^2(j, k) \\
& = p_{j+1, k} V(j+1, k) + p_{j-1, k} V(j-1, k) + p_{j, k+1} V(j, k+1) \\
& + p_{j, k-1} V(j, k-1) + p_{j, k} V(j, k) + q_i(j, k) = 0,
\end{aligned} \tag{3.23}$$

where x_j and y_j represent coordinates of the mesh points, $V(j, k)$ and $\pi_i(j, k)$ are corresponding values at the mesh points, and Δx and Δy are corresponding mesh sizes. We therefore can write (3.23) in the form

$$\begin{aligned}
V(j, k) = & -\frac{1}{p_{j, k}} \{ p_{j+1, k} V(j+1, k) + p_{j-1, k} V(j-1, k) \\
& + p_{j, k+1} V(j, k+1) + p_{j, k-1} V(j, k-1) + q_i(j, k) \}.
\end{aligned} \tag{3.24}$$

We use the Gauss-Seidel method [58] together with the PIA to solve (3.22). The procedure is as follows:

1. Set $V^0(j, k) = 0$ and $\pi_0(j, k) = 0 \quad \forall(j, k)$.
2. Assume that we have π_i and V^ℓ for all the mesh points. Use (3.24) to calculate the values $V^{\ell+1}(j, k)$. That is, use

$$\begin{aligned}
V^{\ell+1}(j, k) = & -\frac{1}{p_{j, k}} \{ p_{j+1, k} V^\ell(j+1, k) + p_{j-1, k} V^\ell(j-1, k) \\
& + p_{j, k+1} V^\ell(j, k+1) + p_{j, k-1} V^\ell(j, k-1) + q_i(j, k) \}
\end{aligned} \tag{3.25}$$

to calculate $V^{\ell+1}(j, k)$.

3. Iteratively solve for $V^{\ell+1}$ from V^ℓ and stop when $\max_{j, k} |V^{\ell+1}(j, k) - V^\ell(j, k)| <$

ToleranceLevel1. Calculate $\pi_{i+1}(j, k)$ by

$$\pi_{i+1}(j, k) = \frac{V^{\ell+1}(j+1, k) - V^{\ell+1}(j-1, k)}{2\Delta x} x_j + \frac{V^{\ell+1}(j, k+1) - V^{\ell+1}(j, k-1)}{2\Delta y} y_k. \quad (3.26)$$

4. Repeat Procedure 3 and end the program when $\max_{j,k} |\pi_i(j, k) - \pi_{i+1}(j, k)| < \text{ToleranceLevel2}$. The numerical solution to (3.22) is $V^{\ell+1}(j, k)$.

The method converges if the diagonal terms of the matrix are greater than the sum of the absolute values of the off-diagonal terms (Theorem 4.4.5, [9]). That is, on (3.24), the method converges if

$$|p_{j,k}| > |p_{j+1,k}| + |p_{j-1,k}| + |p_{j,k+1}| + |p_{j,k-1}|. \quad (3.27)$$

With π_i small enough, the condition of the cited theorem is satisfied with the parameters we have chosen.

To compare the calculation load, we also numerically solved the corresponding linear PDE

$$\frac{1}{2}yx^2 \frac{\partial^2 V}{\partial x^2} + \frac{1}{2}y\eta^2 \frac{\partial^2 V}{\partial y^2} - \alpha V - 1 = 0. \quad (3.28)$$

The only difference between (3.22) and (3.28) is the existence of the term $-(1/2)\{x(\partial V/\partial x) + y(\partial V/\partial y)\}^2$.

Table 3.2 shows the numerical results in both linear and semilinear cases. For the linear case (3.28), we used Gauss-Seidel method with the tolerance level equal to ToleranceLevel1 in Table 3.1. We see that the linear and semilinear cases have similar order in terms of the number of calculations to approximate to the specified tolerance level.

Table 3.2: Calculation load comparison for successful convergence. One calculation here means solving the difference equation (3.25) once at one point.

| Problem Type | Method | # of calculations |
|--------------|--------------------|-------------------|
| Linear | FDM (Gauss-Seidel) | 24,541,704 |
| Semilinear | PIA & Gauss-Seidel | 34,372,107 |

Table 3.3 shows the result in more detail.

Table 3.3: Detail of the calculations in the PIA.

| PIA steps | Max Difference in $ \pi_i - \pi_{i-1} $ | Max Difference in $ V^{\pi_i} - V^{\pi_{i-1}} $ | # of calculations | Calculation time in hours |
|-----------|---|---|-------------------|---------------------------|
| 0 | 2.15455038 | | 24,541,704 | 0:16 |
| 1 | 1.55932909 | 0.02563695 | 8,017,218 | 0:05 |
| 2 | 0.16986263 | 0.00372773 | 1,744,578 | 0:01 |
| 3 | 0.00400477 | 0.00006031 | 58,806 | 0:00 |
| 4 | 0.00066038 | 0.00000995 | 9,801 | 0:00 |

Table 3.3 shows that the first step in the PIA already decreases the number of calculation to get the convergence in the Gauss-Seidel method. The data is plotted in Figure 3.1.

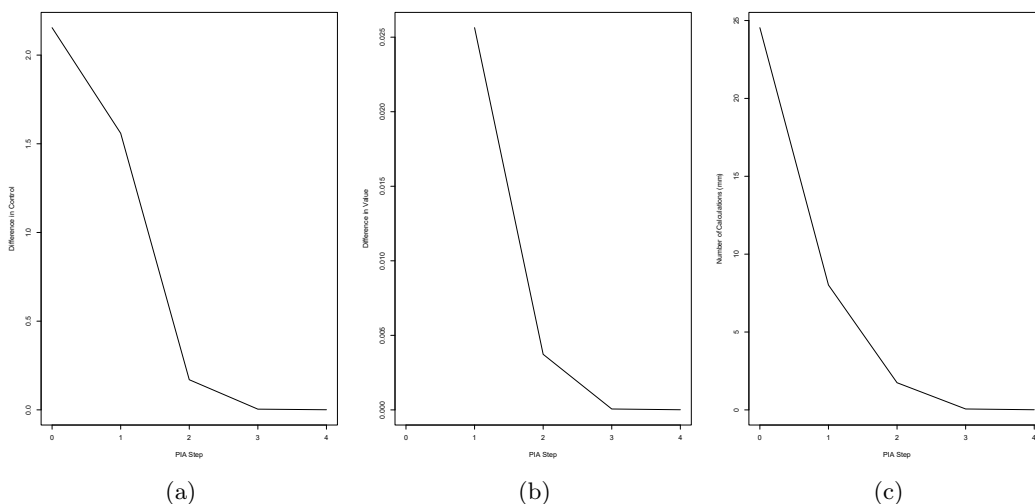


Figure 3.1: Graphs of the data in Table 3.3. (a) the maximum of $|\pi_i - \pi_{i-1}|$ in each step, (b) the maximum of $|V^{\pi_i} - V^{\pi_{i-1}}|$ in each step, and (c) the number of calculations in each step.

Remark 12. We did try applying the FDM directly to the differential equation (3.22), but could not get the convergence in the Gauss-Seidel method as fast as applying the PIA. Time taken for the calculation was 1:08 and number of calculations performed was 54,434,754 compared to 0:22 and 34,372,107 respectively with the PIA as shown in Table 3.2 and Table 3.3.

3.4.2 Second Example

We provide another example.

The SDEs we consider are

$$\begin{cases} dx = \sigma x dW^1, \\ dy = \pi dt + \eta y dW^2, \\ \langle dW^1, dW^2 \rangle = 0, \end{cases} \quad (3.29)$$

where W^1 and W^2 are 1-dimensional Wiener processes and $\pi \in \mathbb{R}$. Thus

$$\mu_\pi = \begin{pmatrix} 0 \\ \pi \end{pmatrix} \quad \text{and} \quad \sigma_\pi = \begin{pmatrix} \sigma x & 0 \\ 0 & \eta y \end{pmatrix}. \quad (3.30)$$

We take f^π to be

$$f^\pi = -\cosh(\pi). \quad (3.31)$$

We define V^π as in (3.5) with $g \equiv 0$ on $\partial\mathcal{E}$. Then, V^{π_i} satisfies the elliptic PDE:

$$\frac{1}{2}\sigma^2 x^2 \frac{\partial^2 V^{\pi_i}}{\partial x^2} + \frac{1}{2}\eta^2 y^2 \frac{\partial^2 V^{\pi_i}}{\partial y^2} + \pi_i \frac{\partial V^{\pi_i}}{\partial y} - \alpha V^{\pi_i} - \cosh(\pi_i) = 0, \quad (3.32)$$

where π_i is determined by

$$\pi_i = \text{arc sinh} \left(\frac{\partial V^{\pi_{i-1}}}{\partial y} \right). \quad (3.33)$$

Note that if V^{π_i} converges, the limit function V satisfies a semilinear elliptic PDE

$$\frac{1}{2}\sigma^2 x^2 \frac{\partial^2 V}{\partial x^2} + \frac{1}{2}\eta^2 y^2 \frac{\partial^2 V}{\partial y^2} + \frac{\partial V}{\partial y} \text{arc sinh} \left(\frac{\partial V}{\partial y} \right) - \sqrt{1 + \left(\frac{\partial V}{\partial y} \right)^2} - \alpha V = 0. \quad (3.34)$$

The variables we use are in Table 3.4.

As in Section 3.4.1, we use the explicit FDM to see the convergence starting at $\pi_0 \equiv 0$ with the boundary condition $V^{\pi_i}|_{\partial\mathcal{E}} \equiv 0$. We discretize (3.32) and obtain

Table 3.4: Parameters we use for the numerical calculation.

| parameter | value |
|----------------------|---------|
| α | 0.03 |
| σ | 2.0 |
| η | 0.2 |
| x_{max} | 2.0 |
| x_{min} | 0.50 |
| y_{max} | 2.0 |
| y_{min} | 0.50 |
| ToleranceLevel1 | 0.00001 |
| ToleranceLevel2 | 0.001 |
| discretization nodes | 100 |

$$\begin{aligned}
& \frac{1}{2} \left(\frac{\sigma^2 x_j^2}{\Delta x^2} \right) V(j+1, k) + \frac{1}{2} \left(\frac{\sigma^2 x_j^2}{\Delta x^2} \right) V(j-1, k) \\
& + \frac{1}{2} \left(\frac{\eta^2 y_k^2}{\Delta y^2} + \frac{\pi_i(j, k)}{\Delta y} \right) V(j, k+1) + \frac{1}{2} \left(\frac{\eta^2 y_k^2}{\Delta y^2} - \frac{\pi_i(j, k)}{\Delta y} \right) V(j, k-1) \\
& - \left(\frac{\sigma^2 x_j^2}{\Delta x^2} + \frac{\eta^2 y_k^2}{\Delta y^2} + \alpha \right) V(j, k) - \cosh(\pi_i(j, k)) \\
& = p_{j+1, k} V(j+1, k) + p_{j-1, k} V(j-1, k) + p_{j, k+1} V(j, k+1) \\
& + p_{j, k-1} V(j, k-1) + p_{j, k} V(j, k) + q'_i(j, k) = 0,
\end{aligned} \tag{3.35}$$

where x_j , y_j , $V(j, k)$, $\pi_i(j, k)$, Δx , and Δy are as defined in the previous subsection at (3.23). We write (3.35) in the form

$$\begin{aligned}
V(j, k) = -\frac{1}{p_{j, k}} \{ & p_{j+1, k} V(j+1, k) + p_{j-1, k} V(j-1, k) \\
& + p_{j, k+1} V(j, k+1) + p_{j, k-1} V(j, k-1) + q'_i(j, k) \}.
\end{aligned} \tag{3.36}$$

We use the Gauss-Seidel method together with the PIA to solve (3.34). The procedure of the algorithm is as follows:

1. Set $V^0(j, k) = 0$ and $\pi_0(j, k) = 0 \quad \forall(j, k)$.
2. Assume that we have π_i and V^ℓ for all the mesh points. Use (3.36) to calculate

the values $V^{\ell+1}(j, k)$. That is, use

$$V^{\ell+1}(j, k) = -\frac{1}{p_{j,k}} \{p_{j+1,k}V^{\ell}(j+1, k) + p_{j-1,k}V^{\ell}(j-1, k) + p_{j,k+1}V^{\ell}(j, k+1) + p_{j,k-1}V^{\ell}(j, k-1) + q'_i(j, k)\} \quad (3.37)$$

to calculate $V^{\ell+1}(j, k)$.

- Iteratively solve for $V^{\ell+1}$ from V^{ℓ} and stop when $\max_{j,k} |V^{\ell+1}(j, k) - V^{\ell}(j, k)| < \text{ToleranceLevel1}$. Calculate $\pi_{i+1}(j, k)$ by

$$\pi_{i+1}(j, k) = \text{arc sinh} \left(\frac{V^{\ell+1}(j, k+1) - V^{\ell+1}(j, k-1)}{2\Delta y} \right). \quad (3.38)$$

- Repeat Procedure 3 and end the program when $\max_{j,k} |\pi_i(j, k) - \pi_{i+1}(j, k)| < \text{ToleranceLevel2}$. The numerical solution to (3.34) is $V^{\ell+1}(j, k)$.

The method converges if (3.27) is satisfied.

To compare the calculation load, we also numerically solved the corresponding linear PDE (3.28), where the only difference from (3.34) is the existence of the terms $(\partial V/\partial y) \text{arc sinh}(\partial V/\partial y) - \sqrt{1 + (\partial V/\partial y)^2} + 1$.

Table 3.5 shows the numerical results in both linear and semilinear cases. For the linear case (3.28), we used Gauss-Seidel method with the tolerance level equal to ToleranceLevel1 in Table 3.4. We see that the linear and semilinear cases have similar order in terms of the number of calculations to approximate to the specified tolerance level.

Table 3.5: Calculation load comparison for successful convergence. One calculation here means solving the difference equation (3.37) once at one point.

| Problem Type | Method | # of calculations |
|--------------|--------------------|-------------------|
| Linear | FDM (Gauss-Seidel) | 24,541,704 |
| Semilinear | PIA & Gauss-Seidel | 37,537,830 |

Table 3.6 shows the result in more detail.

Table 3.6 shows that the first step in the PIA already decreases the number of calculation to get the convergence in the Gauss-Seidel method. The data is plotted in Figure 3.2.

Table 3.6: Detail of the calculations in the PIA.

| PIA steps | Max Difference in $ \pi_i - \pi_{i-1} $ | Max Difference in $ V^{\pi_i} - V^{\pi_{i-1}} $ | # of calculations | Calculation time |
|-----------|---|---|-------------------|------------------|
| 0 | 1.707439 | | 24,541,704 | 0:14 |
| 1 | 0.609614 | 0.0343466 | 8,703,288 | 0:05 |
| 2 | 0.156637 | 0.00676332 | 4,087,017 | 0:02 |
| 3 | 0.00503 | 0.00020391 | 196,020 | 0:00 |
| 4 | 0.000246 | 0.00000997 | 9,801 | 0:00 |

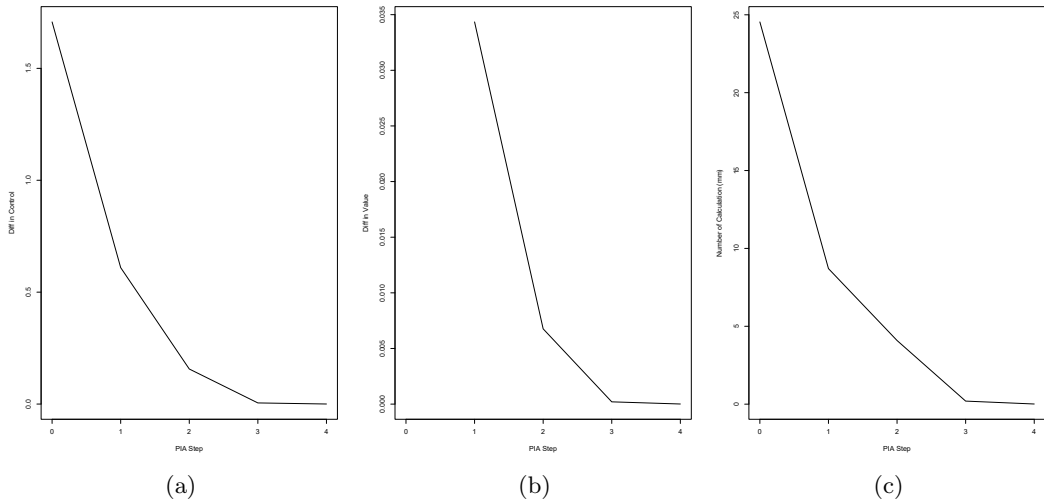


Figure 3.2: Graphs of the data in Table 3.6. (a) the maximum of $|\pi_i - \pi_{i-1}|$ in each step, (b) the maximum of $|V^{\pi_i} - V^{\pi_{i-1}}|$ in each step, and (c) the number of calculations in each step.

3.5 Conclusion and Open Questions

We have shown that the PIA has the QLC property in a fairly general framework. The natural questions to ask are

1. Can we show QLC under weaker conditions?

and

2. Can we show some convergence rate outside the “local quadratic region” (see Remark 9)? We know that the QLC holds, so when the norm of the difference of the type $\|V^{\pi_{i+1}} - V^{\pi_i}\|_{2,\beta}$ becomes small enough, we know that it converges with order 2 to the original solution from (3.15). However, this does not tell us

with what order the difference $\|V^{\pi_{i+1}} - V^{\pi_i}\|_{2,\beta}$ becomes small enough starting from arbitrary V^{π_0} .

Chapter 4

Modeling Technical Analysis

4.1 Introduction

Many traders base their trading strategies on technical analysis (TA). The analysis uses heavily the visual shape of historical price graphs (which traders call 'charts') to determine whether the asset is a good buy or not. One of the basic analyses in the field is that of a support and resistance line. In this method, the traders obtain a horizontal line called a support (resistance) line that they believe is a local support (roof) of the asset price. The analysis is that if the stock price crosses a support line from above and goes lower than the level by 'a lot', then it is considered that the stock has moved into a recession regime in which case traders should sell, or at least, not be long of the stock. On the other hand, if the asset price spikes up crossing a resistance line from below, the asset is considered to have shifted to a boom regime and the method asks the traders to buy the asset or to cover the short.

Remark 13. *The method of support/resistance level can be applied to any assets as long as their historical prices are available. In the thesis, we focus on the case when the asset is a stock.*

We note here that the support/resistance level is not a hard limit. Therefore, the stock can go lower (higher) than the support (resistance) level, but it is expected to correct in a short period of time if the regime has not changed. We also note that there may be several support/resistance levels in one chart.

A level could, in theory, be a support level but not a resistance level and vice versa. However, the level is where the stock-price regime changes and it is natural to consider it to be both a support and resistance level in the following way. From one regime, the other regime is relatively 'better' or 'worse'. Hence, if we are in the 'better' regime, the level which lies around the lower end of the regime is considered

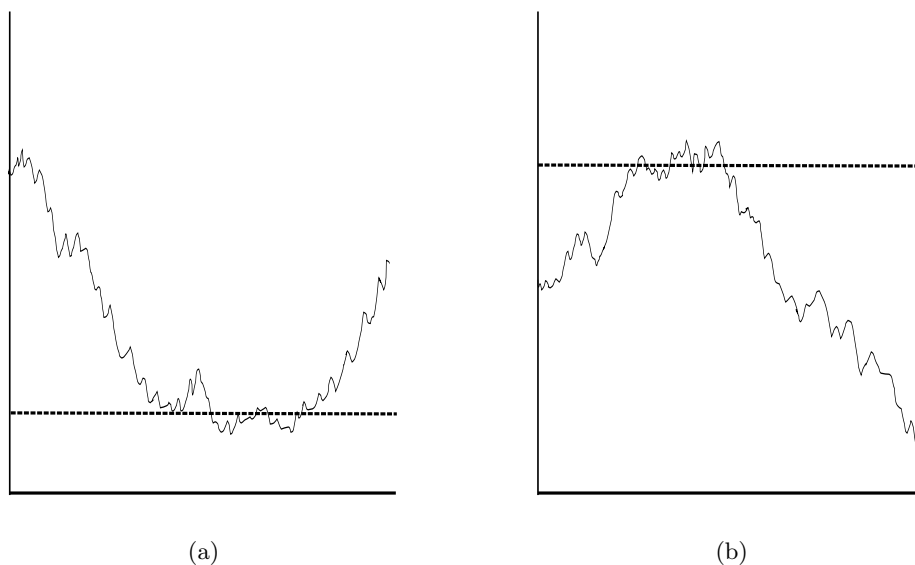


Figure 4.1: Example of (a) the support and (b) the resistance levels. Note that the levels are not hard limits, and the price can fluctuate around the levels.

to be a support line; if we are in the ‘worse’ regime, the same level which now lies around the upper end of the regime is considered to be a resistance line. When a support level becomes a resistance level or vice versa, we say that the stock has a *regime transition*. This is in line with how traders think of the level.

Methods in TA are based on historical behaviour of stocks. They are not currently supported by any theory, though they may be partially explained using behavioural science. Nevertheless, many traders believe they are useful and powerful. One reason is that the methods in TA are free from human emotions. Traders are consistently affected by the present performance of their portfolios and psychological stresses. Even if their trading instinct is sharp, the performance of their portfolios may deteriorate due to other non-trading factors. The decisions that TA makes are believed not to be affected by these factors.

Another reason why many traders support TA is that they believe in the strong form of the efficient market hypothesis (EMH). They believe that the stock price reflects not only the information publicly available, but even the information that is not disclosed in public. For example, if an investor has some insider information that potentially pushes the stock price lower, he might want to sell the stock before other people do to take advantage of possessing the information. He can only extract benefit for himself by selling the stock in the market, which pushes the

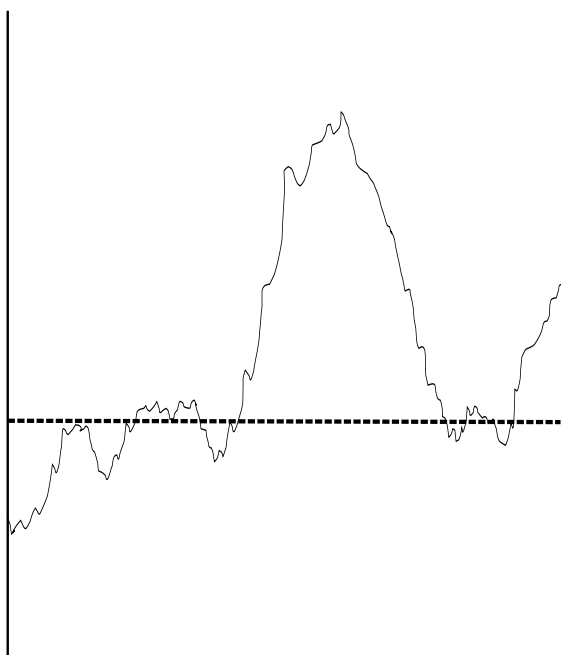


Figure 4.2: An example of a line being both the support and resistance level.

stock price lower. Even though the information is not publicly available, it is thus reflected in the price chart of the stock.

Remark 14. *Instead of selling the stock directly in the market, the investor with insider information can seek other methods of benefiting himself from the expected stock performance. For example, he can buy naked puts on the stock. Then, the counterparty who sold the option to the investor has to sell the stock to hedge the position (unless the counterparty is happy holding it without any hedges). In either case, the investor with insider information will make the market sell the stock.*

Some studies on TA have been performed, but they mainly focus on how to detect the sign of the regime transition as quickly as possible and checking by comparing what the performance would have been if a trader adopted TA in his trading strategies. Some examples of research that focus on these points are [8] and [48]. We know of no literature attempting to model and justify TA methods mathematically.

In order to model the method of support/resistance level, we initially considered several approaches. One is to use stochastic delay differential equations

(SDDEs; [7], [49], [53], [83]). This makes sense as TA is the method we use to forecast dynamics of the future stock price from analysing historical prices, and SDDEs are stochastic differential equations (SDEs) with coefficients that depend on the historical levels. However, this method requires many parameters and does not imply the optimal trading strategy traders should adopt under the setup.

The other method we considered was using a skew Brownian motion to model the price process. This has different probabilities of positive and negative excursions from the support/resistance level. Skew Brownian motion is the process in which the negative excursions from the origin of the standard Brownian motion are flipped with the probability $1 - \alpha$. It is described in [29]. Using this process to describe the underlying stock price process under our setup requires a lot less parameters than using SDDEs. However, as [57] and [67] show, the model with skew Brownian motion has arbitrage opportunities. It is discussed in [57] that we can get an arbitrage-free and complete market within the class of simple strategies, but not in a more general setup.

Remark 15. *We think it is still possible to approach using skew Brownian motion in modeling the method of supply/resistance level by using approximated skew Brownian motion. From [25], skew Brownian motion satisfies the SDE*

$$dX_t = dW_t + (2\alpha - 1)dL_0^X(t), \quad (4.1)$$

where $L_0^X(\cdot)$ is the local time at zero defined by

$$L_0^X(t) = \lim_{\epsilon \downarrow 0} \frac{1}{2\epsilon} \int_0^t \mathbb{1}_{[-\epsilon, \epsilon]}(X_s) ds. \quad (4.2)$$

We can approximate the process X by Y_ϵ defined as

$$dY_\epsilon(t) = dW_t + (2\alpha - 1)d\ell_0^{Y_\epsilon}(t), \quad (4.3)$$

with some $\epsilon > 0$ with

$$\ell_0^{Y_\epsilon}(t) = \frac{1}{2\epsilon} \int_0^t \mathbb{1}_{[-\epsilon, \epsilon]}(Y_\epsilon) ds. \quad (4.4)$$

From now on we adopt a different model: we assume that there are only two regimes in the stock price which correspond to different log normal diffusion processes. We then define criteria for deciding on buying/selling the stock via optimal control theory.

One of the things that makes our setup special is that these two regimes are not distinguishable based on the current stock price, i.e. there is a region where

the stock price can have dynamics corresponding to either of the two SDEs. This feature provides some “room” for the process in each regime to move around the support/resistance level without switching to the other regime.

The rest of the chapter is organized as follows: Section 4.2 presents the setup we use for the model with a support/resistance level. We first solve for the optimal selling problem given that we already hold the stock at time $t = 0$ in Section 4.3. Using the results from the optimal selling problem, we then solve the optimal purchasing problem in Section 4.4. We derive our conclusions and refer to possible future research topics in Section 4.5.

4.2 Setup

We assume that there are levels L and H ($0 < L < H$) at which the regimes change. We define the *positive region* as the domain $[L, \infty)$ and the *negative region* as the domain $(0, H]$. Note that the two regions have non-empty intersection $[L, H]$.

We assume that there are only two regimes in the price process; the positive regime and the negative regime.

Under the positive regime, the process lies in the positive region and has dynamics

$$dS_t = \mu_+ S_t dt + \sigma_+ S_t dW_t, \quad (4.5)$$

where μ_+ and $\sigma_+ > 0$ are constants and W_t is a one dimensional Brownian motion. The transition from the positive to the negative regime occurs when the positive regime is in place and S exits the positive region.

On the other hand, under the negative regime, the process lies in the negative region and has dynamics

$$dS_t = \mu_- S_t dt + \sigma_- S_t dW_t. \quad (4.6)$$

where μ_- and $\sigma_- > 0$ are constants. The transition from the negative to the positive regime occurs when the negative regime is in place and S exits the negative region.

Let $r > 0$ denote the interest rate and we assume

$$\mu_- < r < \mu_+. \quad (4.7)$$

The condition (4.7) implies the discounted price process is a supermartingale under the negative regime and a submartingale in the positive regime up to the time of the first regime transition.

To keep track of which regime currently holds, we define the flag process F_t which takes values in $\{-1, +1\}$ as

$$F_t = \begin{cases} +1 & \text{if the dynamics correspond to the positive regime} \\ -1 & \text{if the dynamics correspond to the negative regime} \end{cases}. \quad (4.8)$$

The flag process F_t indicates under which regime the price process S_t is at time t . From the definition of the regime transition, F_t jumps from one value to the other only in the following cases:

$$\begin{cases} F_{t-} = +1 \text{ and } S_t = L, \text{ then } F_t = -1 \\ F_{t-} = -1 \text{ and } S_t = H, \text{ then } F_t = +1 \end{cases}. \quad (4.9)$$

Remark 16. *We have the following proposition:*

Proposition 4.2.1. *The model we introduced in Section 4.2 is arbitrage-free.*

The proof of Proposition 4.2.1 is deferred to Section E.3.2 in Appendix E.

We set M as the level of the asset price at which the trader is happy to take profit. In other words, the asset that the trader held at the price below M will be sold upon breaching the level M . We therefore assume that the initial price is below M . For each $a \leq M$, we define the time T_a as

$$T_a := \inf\{t | S_t = a\}. \quad (4.10)$$

We set \mathcal{T}_M as the set of all stopping times that are not greater than T_M . We set X_t as S_t stopped at T_M .

4.3 Selling Problem

First, we assume that we already hold the asset and think of the optimal selling strategy. We find the selling strategy that enables us to sell at the best value among the expectations of all the future prices discounted to today. The problem is mathematically equivalent to solving the following optimal stopping problem:

$$V(x, f) = \sup_{\tau \in \mathcal{T}_M} \mathbf{E}_{x, f}[e^{-r\tau} X_\tau]. \quad (4.11)$$

We want to characterize the optimal stopping time τ^* that leads to

$$V(x, f) = \mathbf{E}_{x,f}[e^{-r\tau^*} X_{\tau^*}]. \quad (4.12)$$

In order to find the candidates for τ^* , we define the continuation region \mathcal{C} and the stopping region \mathcal{D} as

$$\mathcal{C} = \{V(x, f) > x\}, \quad \mathcal{D} = \{V(x, f) = x\}, \quad (4.13)$$

and set τ_m as

$$\tau_m = \inf\{t | X_t = m; t \leq T_M\}. \quad (4.14)$$

We hypothesise that the optimal policy is to sell when X reaches m or M for a suitable value of m to be determined. We think of the set of τ_m as the candidate for the solution to the optimal stopping problem (4.11). If we define $V_m = \mathbf{E}[e^{-r\tau_m} X_{\tau_m}]$, then V_m is the solution to the following ODEs:

$$\begin{cases} \frac{1}{2}\sigma_+^2 x^2 V_m''(x, +1) + \mu_+ x V_m'(x, +1) - rV_m(x, +1) = 0, & x \in [L, M] \\ \frac{1}{2}\sigma_-^2 x^2 V_m''(x, -1) + \mu_- x V_m'(x, -1) - rV_m(x, -1) = 0, & x \in [m, H] \end{cases}. \quad (4.15)$$

In order to solve the optimal selling problem (4.11), we use the following theorem.

Theorem 4.3.1. ([59])

Consider the optimal stopping problem

$$V_t^T = \sup_{t \leq \tau \leq T} \mathbf{E}G_\tau \quad (4.16)$$

under the assumption that the condition $\mathbf{E}(\sup_{0 \leq t \leq T} |G_t|) < \infty$ holds. Furthermore, consider the process

$$\mathcal{S}_t = \operatorname{ess\,sup}_{\tau \geq t} \mathbf{E}(G_\tau | \mathcal{F}_t) \quad (4.17)$$

and the stopping time

$$\tau_t = \inf\{s \geq t | \mathcal{S}_s = G_s\}. \quad (4.18)$$

Then for all $t \geq 0$ we have:

$$\begin{aligned}\mathcal{S}_t &\geq \mathbf{E}(G_\tau|\mathcal{F}_t) \quad \text{for each } \tau \in \mathfrak{M}_t, \\ \mathcal{S}_t &= \mathbf{E}(G_{\tau_t}|\mathcal{F}_t)\end{aligned}\tag{4.19}$$

where \mathfrak{M}_t denotes the family of all stopping times τ satisfying $\tau \geq t$. Moreover, if $t \geq 0$ is given and fixed, then we have:

- The stopping time τ_t is optimal in (4.16).
- If τ^* is optimal stopping time in (4.16), then $\tau_t \leq \tau^*$ \mathbf{P} -a.s.
- The process $(\mathcal{S}_t)_{s \geq t}$ is the smallest right-continuous supermartingale which dominates $(G_s)_{s \geq t}$.
- The stopped process $(\mathcal{S}_{s \wedge \tau_t})_{s \geq t}$ is a right-continuous martingale.

The process \mathcal{S}_t is called the Snell envelope of the process G_t . The plan of solving the optimal selling problem is as follows:

1. Find the maximizer \hat{m} of $V_m(x, f)$.
2. Show that the process $e^{-rt}V_{\hat{m}}(X_t, F_t)$ is a supermartingale that dominates the gains process $e^{-rt}X_t$.

The fact that $e^{-rt}V_{\hat{m}}(X_t, F_t)$ is minimal comes from the Optional Sampling Theorem. Then Theorem 4.3.1 proves that the optimal stopping time of the problem (4.11) is the first time when $e^{-rt}V_{\hat{m}}(X_t, F_t) = e^{-rt}X_t$, hence when $V_{\hat{m}}(X_t, F_t) = X_t$. In other words, the optimal stopping time is the first time the process X_t enters the domain \mathcal{D} . Finally, this stopping time is equivalent to the first time X_t hits the level \hat{m} when $F_{t-} = -1$ and when the process hits M when $F_{t-} = +1$.

We let $\alpha_1 < \alpha_2$ be the two solutions to the characteristic equation

$$\frac{1}{2}\sigma_+^2\alpha^2 + \mu_+\alpha - r = 0,\tag{4.20}$$

and $\beta_1 < \beta_2$ the solutions to

$$\frac{1}{2}\sigma_-^2\beta^2 + \mu_-\beta - r = 0.\tag{4.21}$$

What we know right away from the equations (4.7), (4.20), and (4.21) is that

$$\alpha_1, \beta_1 < 0\tag{4.22}$$

and

$$\alpha_2 < 1 < \beta_2. \quad (4.23)$$

With some constants $A, B, C,$ and D which are determined from boundary conditions, $V_m(x, +1)$ and $V_m(x, -1)$ can be written as

$$\begin{cases} V_m(x, +1) = Ax^{\alpha_1} + Bx^{\alpha_2} \\ V_m(x, -1) = Cx^{\beta_1} + Dx^{\beta_2} \end{cases}. \quad (4.24)$$

We now solve for $A, B, C,$ and D in (4.24) in the following two cases: the case when $m \leq L$ and when $m > L$.

4.3.1 The Case Where $m \leq L$

In the case when $m \leq L,$ $V_m(x, f)$ satisfies (4.15) with the boundary conditions

$$\begin{cases} V_m(m, -1) = m \leq L \\ V_m(L, -1) = V_m(L, +1) \\ V_m(H, +1) = V_m(H, -1) \\ V_m(M, +1) = M \end{cases}, \quad (4.25)$$

and set $V_m(x, -1) = x$ for $x \in (0, m).$ Define $P(x) = x^{\alpha_2} - M^{\alpha_2 - \alpha_1}x^{\alpha_1},$ $Q(x) = x^{\beta_2} - m^{\beta_2 - \beta_1}x^{\beta_1},$ and $R(x) = m^{1 - \beta_1}x^{\beta_1} - M^{1 - \alpha_1}x^{\alpha_1}.$ We solve (4.25) for $A, B, C,$ and D in (4.24) and obtain:

$$\begin{cases} A = M^{1 - \alpha_1} - BM^{\alpha_2 - \alpha_1} \\ B = \frac{R(L)Q(H) - R(H)Q(L)}{P(L)Q(H) - P(H)Q(L)} \\ C = m^{1 - \beta_1} - Dm^{\beta_2 - \beta_1} \\ D = \frac{R(L)P(H) - R(H)P(L)}{Q(H)P(L) - Q(L)P(H)} \end{cases}. \quad (4.26)$$

4.3.2 $m \geq L$ Case

In the case when $m \geq L,$ $V_m(x, f)$ solves (4.15) with the boundary conditions

$$\begin{cases} V_m(m, -1) = m \geq L \\ V_m(H, -1) = V_m(H, +1) \\ V_m(L, +1) = L \\ V_m(M, +1) = M \end{cases}. \quad (4.27)$$

We do not consider $m > H$ here as then the problem will be an optimal stopping problem under one regime (i.e. the positive regime).

The condition $V_m(L, -1) = V_m(L, +1)$ is replaced with $V_m(L, +1) = L$ since the process is stopped when it goes below the level m . We solve for the coefficients in (4.24) and obtain

$$\begin{cases} A = \frac{L^{1-\alpha_1} M^{1-\alpha_1} (M^{\alpha_2-1} - L^{\alpha_2-1})}{M^{\alpha_2-\alpha_1} - L^{\alpha_2-\alpha_1}} \\ B = \frac{M^{1-\alpha_2} - L^{1-\alpha_2}}{M^{\alpha_2-\alpha_1} - L^{\alpha_2-\alpha_1}} \\ C = \frac{m^{1-\beta_1} H^{-\beta_1} (H^{\beta_2} - m^{\beta_2-1} V_m(H, +1))}{H^{\beta_2-\beta_1} - m^{\beta_2-\beta_1}} \\ D = \frac{H^{-\beta_1} V_m(H, +1) - m^{1-\beta_1}}{H^{\beta_2-\beta_1} - m^{\beta_2-\beta_1}} \end{cases} \quad (4.28)$$

Note that $V_m(x, +1)$ does not depend on m .

4.3.3 Solving the Optimal Stopping Problem

In Subsection 4.3.1 and Subsection 4.3.2, we solved for $V_m(x, f)$. We now have the candidates for the solution of the optimal stopping problem (4.11) with the stopping rule "stop the asset price process X_t when it first hits the level m or M if this is earlier (since we are required to sell at level M)". In other words, we have candidates of m that satisfy

$$\tau^* = \tau_m. \quad (4.29)$$

What we want to do next is to verify which choice of m actually works and enables us to solve the optimal stopping problem (4.11) with (4.29). If we guessed the right form of the optimal policy, the optimal m should be the one that maximizes $V_m(x, f)$. We now solve for the maximizer of $V_m(x, f)$.

4.3.4 Maximizer in the Case of $m \leq L$

We calculate the maximizer in the case when $m \leq L$. For that, it is sufficient to maximize $V_m(L, -1)$.

Defining

$$\begin{cases} G_1 = (L^{\beta_1} H^{\alpha_2} - L^{\alpha_2} H^{\beta_1}) + M^{\alpha_2 - \alpha_1} (L^{\alpha_1} H^{\beta_1} - L^{\beta_1} H^{\alpha_1}) \\ G_2 = M^{1 - \alpha_1} (L^{\alpha_2} H^{\alpha_1} - L^{\alpha_1} H^{\alpha_2}) < 0 \\ G_3 = (H^{\beta_2} L^{\alpha_2} - L^{\beta_2} H^{\alpha_2}) + M^{\alpha_2 - \alpha_1} (H^{\alpha_1} L^{\beta_2} - L^{\alpha_1} H^{\beta_2}) \\ G_4 = (L^{\alpha_2} - M^{\alpha_2 - \alpha_1} L^{\alpha_1}) (L^{\beta_1} H^{\beta_2} - L^{\beta_2} H^{\beta_1}) < 0 \\ G_5 = M^{1 - \alpha_1} L^{\beta_1} (L^{\alpha_1} H^{\alpha_2} - L^{\alpha_2} H^{\alpha_1}) > 0 \\ G_6 = M^{1 - \alpha_1} L^{\beta_2} (L^{\alpha_2} H^{\alpha_1} - L^{\alpha_1} H^{\alpha_2}) = L^{\beta_2} G_2 < 0 \end{cases}, \quad (4.30)$$

$V_m(L, -1)$ is expressed as

$$V_m(L, -1) = \frac{G_4 m^{1 - \beta_1} + G_5 m^{\beta_2 - \beta_1} + G_6}{G_1 m^{\beta_2 - \beta_1} + G_3}. \quad (4.31)$$

We further define

$$f_M(m) = (1 - \beta_2) G_1 m^{\beta_2 - \beta_1} - (\beta_2 - \beta_1) G_2 m^{\beta_2 - 1} + (1 - \beta_1) G_3. \quad (4.32)$$

We calculate the derivative of $V_m(L, -1)$ with respect to m and obtain

$$\begin{aligned} & (G_1 m^{\beta_2 - \beta_1} + G_3)^2 \frac{dV_m(L, -1)}{dm} \\ &= G_4 \left[(1 - \beta_2) \left\{ G_1 m^{\beta_2 - 2\beta_1} + G_2 m^{\beta_2 - \beta_1 - 1} \right\} \right. \\ & \quad \left. + (1 - \beta_1) \left\{ G_3 m^{-\beta_1} - G_2 m^{\beta_2 - \beta_1 - 1} \right\} \right] \\ &= G_4 m^{-\beta_1} f_M(m). \end{aligned} \quad (4.33)$$

Let us define \hat{m} as m such that $f_M(m) = 0$ and \hat{M} as M such that $f_M(L) = 0$. In order to find the maximizer of $V_m(L, -1)$ with respect to $m \in (0, L]$, we show that $V_m(L, -1)$ is strictly concave in $m \in (0, L]$ and show that there is a unique maximizer \hat{m} that is characterized by $dV_m(L, -1)/dm = 0$. Then we can find the maximizer of $V_m(L, -1)$ when $m \in (0, L]$ by checking whether $\hat{m} \in (0, L]$.

Thanks to (4.33), this is equivalent in showing the following lemma on $f_M(m)$:

Lemma 4.3.2. *$f_M(m)$ satisfies the following 3 conditions:*

1. $f_M(0) < 0$.

2. $f'_M(m) > 0$.

3.

$$\begin{aligned} f_M(L) &\geq 0 \quad \text{when } M \geq \hat{M} \\ f_M(L) &< 0 \quad \text{when } M < \hat{M}. \end{aligned} \quad (4.34)$$

Proof. First, we check $f_M(0) = (1 - \beta_1)G_3 < 0$. Since $\beta_1 < 1$ from (4.22), we only need to check if $G_3 < 0$. Indeed,

$$\begin{aligned} G_3 &= (H^{\beta_2}L^{\alpha_2} - L^{\beta_2}H^{\alpha_2}) + M^{\alpha_2 - \alpha_1}(H^{\alpha_1}L^{\beta_2} - L^{\alpha_1}H^{\beta_2}) \\ &< (H^{\beta_2}L^{\alpha_2} - L^{\beta_2}H^{\alpha_2}) + H^{\alpha_2 - \alpha_1}(H^{\alpha_1}L^{\beta_2} - L^{\alpha_1}H^{\beta_2}) \\ &= L^{\alpha_1}H^{\beta_2}(L^{\alpha_2 - \alpha_1} - H^{\alpha_2 - \alpha_1}) < 0. \end{aligned} \quad (4.35)$$

Second, we check if $f'_M(m) > 0$ in $m \in [0, L]$.

$$f'_M(m) = -(\beta_2 - \beta_1)(\beta_2 - 1)m^{\beta_2 - 2} \left\{ G_1 m^{1 - \beta_1} + G_2 \right\}. \quad (4.36)$$

We define $P(m, M) := G_1 m^{1 - \beta_1} + G_2$. Since $P(0, M) < 0$ and $P(m, M)$ is monotone in m , if we show that $P(L, M) < 0$, then we obtain the conclusion $f'_M(m) > 0$.

$$\begin{aligned} P(L, M) &= (L^{\beta_1}H^{\alpha_2} - H^{\beta_1}L^{\alpha_2})L^{1 - \beta_1} \\ &+ L^{1 - \beta_1}M^{\alpha_2 - \alpha_1}(L^{\alpha_1}H^{\beta_1} - L^{\beta_1}H^{\alpha_1}) + M^{1 - \alpha_1}(L^{\alpha_2}H^{\alpha_1} - L^{\alpha_1}H^{\alpha_2}). \end{aligned} \quad (4.37)$$

Denoting the derivative with respect to M by d_M , we calculate $d_MP(L, M)$:

$$\begin{aligned} d_MP(L, M) &= (\alpha_2 - \alpha_1)L^{1 - \beta_1}M^{\alpha_2 - \alpha_1 - 1}(L^{\alpha_1}H^{\beta_1} - L^{\beta_1}H^{\alpha_1}) \\ &+ (1 - \alpha_1)M^{-\alpha_1}(L^{\alpha_2}H^{\alpha_1} - L^{\alpha_1}H^{\alpha_2}) \\ &= M^{\alpha_2 - \alpha_1 - 1} \left\{ (\alpha_2 - \alpha_1)L^{1 - \beta_1}(L^{\alpha_1}H^{\beta_1} - L^{\beta_1}H^{\alpha_1}) \right. \\ &\quad \left. + (1 - \alpha_1)M^{1 - \alpha_2}(L^{\alpha_2}H^{\alpha_1} - L^{\alpha_1}H^{\alpha_2}) \right\}. \end{aligned} \quad (4.38)$$

If $\beta_1 \leq \alpha_1$, then it is obvious from (4.38) that

$$d_MP(L, M) < 0. \quad (4.39)$$

We now assume $\beta_1 > \alpha_1$. Define

$$\begin{aligned} Q(M) &= (\alpha_2 - \alpha_1)L^{1-\beta_1}(L^{\alpha_1}H^{\beta_1} - L^{\beta_1}H^{\alpha_1}) \\ &\quad + (1 - \alpha_1)M^{1-\alpha_2}(L^{\alpha_2}H^{\alpha_1} - L^{\alpha_1}H^{\alpha_2}). \end{aligned} \quad (4.40)$$

We see from (4.40) that $Q(M)$ is monotonically decreasing with respect to M . Therefore, we calculate $d_M P(L, M)$ at $M = H$ and obtain

$$\begin{aligned} d_M P(L, M) &= M^{\alpha_2 - \alpha_1 - 1} Q(M) \\ &< M^{\alpha_2 - \alpha_1 - 1} Q(H) \\ &= M^{\alpha_2 - \alpha_1 - 1} \left\{ (\alpha_2 - \alpha_1)L^{1-\beta_1}(L^{\alpha_1}H^{\beta_1} - L^{\beta_1}H^{\alpha_1}) \right. \\ &\quad \left. + (1 - \alpha_1)H^{1-\alpha_2}(L^{\alpha_2}H^{\alpha_1} - L^{\alpha_1}H^{\alpha_2}) \right\} \\ &= M^{\alpha_2 - \alpha_1 - 1} \left[(\alpha_2 - \alpha_1)LH^{\alpha_1} \left\{ \left(\frac{H}{L} \right)^{\beta_1 - \alpha_1} - 1 \right\} \right. \\ &\quad \left. - (1 - \alpha_1)L^{\alpha_2}H^{1+\alpha_1-\alpha_2} \left\{ \left(\frac{H}{L} \right)^{\alpha_2 - \alpha_1} - 1 \right\} \right] \\ &< 0. \end{aligned} \quad (4.41)$$

We again proved

$$d_M P(L, M) < 0. \quad (4.42)$$

As a consequence of (4.39) and (4.42),

$$\begin{aligned} P(L, M) &\leq P(L, M)|_{M=H} \\ &= -L^{\alpha_1}H(H^{\alpha_2 - \alpha_1} - L^{\alpha_2 - \alpha_1}) \left\{ 1 - \left(\frac{L}{H} \right)^{1-\beta_1} \right\} \\ &< 0, \end{aligned} \quad (4.43)$$

hence we have

$$f'_M(m) > 0, \quad m \in [0, L]. \quad (4.44)$$

Finally, we check $f_M(L)$. Let us define

$$q_\alpha(x) = (1 - \beta_1)x^{\beta_2 - \beta_1} - (\beta_2 - \beta_1)x^{\alpha - \beta_1} + (\beta_2 - 1) \quad (\alpha < 1). \quad (4.45)$$

Then, we can calculate $f_M(L)$ as

$$\begin{aligned} f_M(L) &= (1 - \beta_2)(G_1 L^{\beta_2 - \beta_1} + G_3) + (\beta_2 - \beta_1)(G_3 - G_6 L^{-1}) \\ &= (\beta_2 - \beta_1)L^{\beta_2 - 1}(L^{\alpha_1} H^{\alpha_2} - L^{\alpha_2} H^{\alpha_1})M^{1 - \alpha_1} \\ &\quad - L^{\alpha_1 + \beta_2 - \beta_1} H^{\beta_1} q_{\alpha_1} \left(\frac{H}{L} \right) M^{\alpha_2 - \alpha_1} + L^{\beta_2 - \beta_1 + \alpha_2} H^{\beta_1} q_{\alpha_2} \left(\frac{H}{L} \right). \end{aligned} \quad (4.46)$$

We have

$$q'_\alpha(x) = (1 - \beta_1)(\beta_2 - \beta_1)x^{\alpha - \beta_1 - 1} \left(x^{\beta_2 - \alpha} - \frac{\alpha - \beta_1}{1 - \beta_1} \right) > 0 \quad (x \geq 1), \quad (4.47)$$

hence

$$q_\alpha(x) \geq q_\alpha(1) = 0. \quad (4.48)$$

The derivative of $f_M(L)$ with respect to M is calculated as

$$\begin{aligned} d_M f_M(L) &= (\beta_2 - \beta_1)(1 - \alpha_1)L^{\beta_2 - 1}(L^{\alpha_1} H^{\alpha_2} - L^{\alpha_2} H^{\alpha_1})M^{-\alpha_1} \\ &\quad - (\alpha_2 - \alpha_1)L^{\alpha_1 - \beta_1 + \beta_2} H^{\beta_1} q_{\alpha_1} \left(\frac{H}{L} \right) M^{\alpha_2 - \alpha_1 - 1}. \end{aligned} \quad (4.49)$$

We note here that the coefficient of $M^{-\alpha_1}$ in (4.49), which is the higher order term in M , is positive.

Calculating the value $f_M(L)$ when $M = H$,

$$\begin{aligned} f_M(L)|_{M=H} &= L^{\alpha_1}(H^{\alpha_2 - \alpha_1} - L^{\alpha_2 - \alpha_1}) \\ &\quad \times \{(\beta_2 - \beta_1)L^{\beta_2 - 1}H + (\beta_1 - 1)H^{\beta_2} + (1 - \beta_2)L^{\beta_2 - \beta_1}H^{\beta_1}\}. \end{aligned} \quad (4.50)$$

However, we have

$$(\beta_2 - \beta_1)L^{\beta_2 - 1}H + (\beta_1 - 1)H^{\beta_2} + (1 - \beta_2)L^{\beta_2 - \beta_1}H^{\beta_1} < 0, \quad (4.51)$$

hence

$$f_M(L)|_{M=H} < 0. \quad (4.52)$$

Therefore, $f_M(L) \geq 0$ when $M \geq \hat{M}$ and $f_M(L) < 0$ when $M < \hat{M}$. \square

We obtain the following proposition directly from Lemma 4.3.2:

Proposition 4.3.3. *When $m \leq L$, the value of m that maximizes $V_m(x, f)$ is*

$$\begin{cases} \hat{m} & \text{when } M \geq \hat{M} \\ L & \text{when } M < \hat{M} \end{cases}. \quad (4.53)$$

Remark 17. *Proposition 4.3.3 says that if M is not as large as \hat{M} , the point where $V_m(x, f)$ takes its maximum is when $m = L$, which is the largest m possible in the range of m considered. However, if M is large enough, $V_m(x, f)$ takes its maximum at $\hat{m} \in (0, L)$. This is in line with the intuition that if M is too low, we cannot expect much profit by holding on to the stock in the negative regime, hence it is optimal to sell the position right away. However, if M is large enough, even if the stock price is currently in the negative regime, there is a hope that the stock enters the positive regime in the near future and generates a large profit. Therefore, it is optimal to hold on to the position in this case until the process breaches the level \hat{m} .*

4.3.5 Maximizer in the Case where $m \geq L$

In the case when $m \geq L$, the solution $V_m(x, f)$ is calculated (4.24) with A, B, C , and D in (4.28). We solve for the maximizer of $V_m(x, f)$ over $m \geq L$.

Defining

$$E = m^{-\beta_1} H^{\beta_2 - \beta_1} \left\{ (1 - \beta_1) H^{\beta_2 - \beta_1} + (\beta_2 - 1) m^{\beta_2 - \beta_1} - (\beta_2 - \beta_1) m^{\beta_2 - 1} H^{-\beta_1} V_m(H, +1) \right\}, \quad (4.54)$$

we can calculate the derivative of $V_m(x, -1)$ with respect to m as

$$\begin{aligned} (H^{\beta_2 - \beta_1} - m^{\beta_2 - \beta_1})^2 \frac{dV_m(x, -1)}{dm} &= E x^{\beta_1} - \frac{E}{H^{\beta_2 - \beta_1}} x^{\beta_2} \\ &= E x^{\beta_1} \left\{ 1 - \left(\frac{x}{H} \right)^{\beta_2 - \beta_1} \right\} \quad x \in [m, H]. \end{aligned} \quad (4.55)$$

The sign of the derivative dV_m/dm matches with that of E , so we focus on the sign of E . The sign is the same as that of g defined by

$$g(m) := (1 - \beta_1)H^{\beta_2 - \beta_1} + (\beta_2 - 1)m^{\beta_2 - \beta_1} - (\beta_2 - \beta_1)m^{\beta_2 - 1}H^{-\beta_1}V_m(H, +1). \quad (4.56)$$

Remark 18. From (4.55), we see that the m that maximizes $V_m(x, -1)$ maximizes $V_m(H, -1)$ and vice versa. For that, it is sufficient to maximize $V_m(H, -1)$ over m .

We show a few lemmas we need for later use.

Lemma 4.3.4. $V_m(H, +1) \geq H$.

Proof. $e^{-rt}(V_m(X_t, +1) - X_t)$ is a supermartingale. This is because before we stop X_t upon reaching L or M , $e^{-rt}V_m(X_t, +1)$ is a martingale (as it satisfies the ODE (4.15)) and $e^{-rt}X_t$ is a submartingale in the positive regime, hence $-e^{-rt}X_t$ is a supermartingale. Upon reaching the level L or M , $e^{-rt}(V_m(X_t, +1) - X_t) = 0$ due to the boundary conditions (4.27) and it will be zero thereafter as we stop the process X_t upon reaching the level L or M . Then, it follows from the Optional Sampling Theorem,

$$V_m(X_0, +1) - X_0 \geq 0. \quad (4.57)$$

Hence, considering the price process starting at H , we have the desired result. \square

Lemma 4.3.5. $V_m(H, +1)$ is continuous in M . Furthermore, it is strictly and monotonically increasing in M .

Proof. The continuity of $V_m(H, +1)$ with respect to M is obvious from the expression in (4.24) and (4.28). The second half of the lemma can also be verified from the expression in (4.24) and (4.28), but we can also verify it as follows. Let τ_{LM} be the first exit time of the process from the domain $[L, M]$. $V_m(H, +1)$ is the expected value of $e^{-rt}X_t$ at the first exit time τ_{LM} . If we make M larger, τ_{LM} gets larger. In the positive regime, since $e^{-rt}X_t$ is a submartingale, this shows that $V_m(H, +1)$ is monotonically increasing in M . \square

If we take the derivative of g with respect to m , we obtain

$$g'(m) = (\beta_2 - \beta_1)(\beta_2 - 1)m^{\beta_2 - \beta_1 - 1} \left\{ 1 - \left(\frac{m}{H} \right)^{\beta_1} \frac{V_m(H, +1)}{m} \right\} < 0, \quad (4.58)$$

where we used Lemma 4.3.4 in the last inequality. Therefore,

$$g(L) > g(m) > g(H). \quad (4.59)$$

Again from Lemma 4.3.4, we have

$$g(H) = (\beta_2 - \beta_1)H^{\beta_2 - \beta_1} \left(1 - \frac{V_m(H, +1)}{H} \right) < 0. \quad (4.60)$$

We now calculate $g(L)$.

$$\begin{aligned} g(L) &= (1 - \beta_1)H^{\beta_2 - \beta_1} \left\{ 1 - \left(\frac{L}{H} \right)^{\beta_2} \frac{V_m(H, +1)}{L} \right\} \\ &\quad + (\beta_2 - 1)L^{\beta_2 - \beta_1} \left\{ 1 - \left(\frac{L}{H} \right)^{\beta_1} \frac{V_m(H, +1)}{L} \right\}. \end{aligned} \quad (4.61)$$

From (4.61), $g(L)$ is a decreasing function of $V_m(H, +1)$. In case $V_m(H, +1) = H$, we have

$$\begin{aligned} g(L)|_{V_m(H, +1) = H} &= (1 - \beta_1)H^{\beta_2 - \beta_1} \left\{ 1 - \left(\frac{L}{H} \right)^{\beta_2 - 1} \right\} \\ &\quad + (\beta_2 - 1)L^{\beta_2 - \beta_1} \left\{ 1 - \left(\frac{L}{H} \right)^{\beta_1 - 1} \right\}. \end{aligned} \quad (4.62)$$

We define

$$p(x) := 2 - x^{\beta_2 - 1} - x^{\beta_1 - 1}, \quad x \leq 1. \quad (4.63)$$

We first note that $p(1) = 0$. We take the derivative of p with respect to x and get

$$\begin{aligned} p'(x) &= -(\beta_2 - 1)x^{\beta_2 - 2} - (\beta_1 - 1)x^{\beta_1 - 2} \\ &= (\beta_2 - 1)x^{\beta_1 - 2} \left(\frac{1 - \beta_1}{\beta_2 - 1} - x^{\beta_2 - \beta_1} \right) > 0. \end{aligned} \quad (4.64)$$

Therefore,

$$p(x) \leq p(1) = 0. \quad (4.65)$$

From (4.65), we have

$$1 - x^{\beta_2 - 1} \leq x^{\beta_1 - 1} - 1 \quad (x \leq 1). \quad (4.66)$$

Substituting $x = L/H$ in (4.66), we have

$$1 - \left(\frac{L}{H}\right)^{\beta_2-1} \leq \left(\frac{L}{H}\right)^{\beta_1-1} - 1. \quad (4.67)$$

Let us define

$$q(y) = (1 - \beta_1)y^{\beta_2-\beta_1} - (\beta_2 - \beta_1)y^{1-\beta_1} + (\beta_2 - 1). \quad (4.68)$$

Coming back to (4.62), reordering the terms, we equivalently have

$$\begin{cases} g(L)|_{V_m(H,+1)=H} > L^{\beta_2-\beta_1}q(y) \\ K := H/L > 1 \end{cases}. \quad (4.69)$$

We note that $q(1) = 0$ and

$$q'(y) = y^{-\beta_1}(\beta_2 - \beta_1)(1 - \beta_1)(y^{\beta_2-1} - 1) \geq 0 \quad y \geq 1, \quad (4.70)$$

so we have

$$q(K) \geq q(1) = 0, \quad y \geq 1. \quad (4.71)$$

From (4.69) and (4.71), we have

$$g(L)|_{V_m(H,+1)=H} > 0. \quad (4.72)$$

As a conclusion, from (4.59), (4.60), and (4.72), there exists some value of $V_m(H, +1)$ which makes $g(L) = 0$. Since $g(L)$ is monotonically decreasing with respect to $V_m(H, +1)$ and (from Lemma 4.3.5) $V_m(H, +1)$ is monotonically increasing with respect to M , there exists a unique M that satisfies $g(L) = 0$.

We define \tilde{m} as m that satisfies $g(m) = 0$ and \tilde{M} as M that satisfies $g(L) = 0$. Then, we have the following proposition:

Proposition 4.3.6. *When $m \geq L$, the value of m that maximizes $V_m(x, f)$ is*

$$\begin{cases} \tilde{m} & \text{when } M \leq \tilde{M} \\ L & \text{when } M > \tilde{M} \end{cases}. \quad (4.73)$$

Remark 19. *We have \hat{M} in Proposition 4.3.3 and \tilde{M} in Proposition 4.3.6. We note that although we introduced it in different ways, $\hat{M} = \tilde{M}$. We can verify this easily by checking the boundary conditions when we have $M = \hat{M}$ and $M = \tilde{M}$ in each case. Therefore, we use $\bar{M} = \hat{M} = \tilde{M}$.*

4.3.6 Optimal Stopping Problem

We define \bar{m} as

$$\bar{m} = \begin{cases} \hat{m}, & M \geq \bar{M} \\ \tilde{m}, & M \leq \bar{M} \end{cases}. \quad (4.74)$$

We show the following theorem:

Theorem 4.3.7. *The solution to the optimal stopping problem (4.11) τ^* is equal to $\tau_{\bar{m}}$.*

Proof. We first show the theorem in the case when $M \geq \bar{M}$. We start by showing the following:

1. $e^{-rt}V_{\hat{m}}(X_t, -1)$ is a supermartingale;
2. $e^{-rt}V_{\hat{m}}(X_t, -1)$ dominates the gains process $e^{-rt}X_t$.

For the first point, $V_{\hat{m}}(\cdot, -1)$ satisfies the ODE which enables us to show that its discounted process $e^{-rt}V_{\hat{m}}(t, -1)$ is a martingale up to the time when the price process breaches the level \hat{m} . After it breaches the level, the process $e^{-rt}V_{\hat{m}}(X_t, -1)$ will just be $e^{-rt}X_t$ thereafter, which is a supermartingale in the regime.

We now focus on the second part, to show that $e^{-rt}V_{\hat{m}}(X_t, -1) \geq e^{-rt}X_t$, hence to show $V_{\hat{m}}(x, -1) \geq x$. We define ζ as

$$\zeta(x) = V_{\hat{m}}(x, -1) - x = Cx^{\beta_1} + Dx^{\beta_2} - x. \quad (4.75)$$

We investigate this function in the domain $[\hat{m}, L]$. First, note that $\zeta(\hat{m}) = 0$. We calculate first and second derivatives of $\zeta(x)$ with respect to x :

$$\zeta'(x) = \beta_1 Cx^{\beta_1-1} + \beta_2 Dx^{\beta_2-1} - 1 \quad (4.76)$$

and

$$\zeta''(x) = \beta_1(\beta_1 - 1)Cx^{\beta_1-2} + \beta_2(\beta_2 - 1)Dx^{\beta_2-2}. \quad (4.77)$$

Substituting C and D , and using $f_M(\hat{m}) = 0$, we can further calculate

$$\zeta''(x) = \frac{(\beta_2 - 1)(1 - \beta_1)(\beta_2 x^{\beta_2 - \beta_1} - \beta_1 \hat{m}^{\beta_2 - \beta_1})x^{\beta_1 - 2}}{(\beta_2 - \beta_1)\hat{m}^{\beta_2 - 1}} > 0. \quad (4.78)$$

We calculate $\zeta'(\hat{m})$.

$$\begin{aligned}
\zeta'(\hat{m}) &= \beta_1 C \hat{m}^{\beta_1-1} + \beta_2 D \hat{m}^{\beta_2-1} - 1 \\
&= \beta_1 C \hat{m}^{\beta_1-1} + \beta_2 D \hat{m}^{\beta_2-1} - (C \hat{m}^{\beta_1-1} + D \hat{m}^{\beta_2-1}) \\
&= C \hat{m}^{\beta_1-1} (\beta_1 - 1) + (\beta_2 - 1) D \hat{m}^{\beta_2-1},
\end{aligned} \tag{4.79}$$

where the second equality comes from the boundary condition at $x = \hat{m}$. We substitute the values of C and D in (4.79) and obtain

$$\begin{aligned}
&\{(1 - \beta_1)G_1 \hat{m}^{\beta_2 - \beta_1} + (1 - \beta_1)G_3\} \zeta'(\hat{m}) \\
&= [(\beta_2 - 1)G_2 \hat{m}^{\beta_2 - \beta_1} - (1 - \beta_2)G_1 \hat{m}^{\beta_2 - 2\beta_1 + 1}] (\beta_1 - 1) \hat{m}^{\beta_1 - 1} \\
&+ [(1 - \beta_1)G_1 \hat{m}^{1 - \beta_1} + (1 - \beta_1)G_2] (\beta_2 - 1) \hat{m}^{\beta_1 - 1} \\
&= 0.
\end{aligned} \tag{4.80}$$

From $\zeta(\hat{m}) = 0$, (4.78), and (4.80), we have $\zeta(x) = V_{\hat{m}}(x, -1) - x \geq 0$ in $x \in [\hat{m}, L]$.

In order to solve the optimal stopping problem (4.11), we want to show that $e^{-rt}V_{\hat{m}}(X_t, F_t)$ is the Snell envelope of $e^{-rt}X_t$.

The fact that $e^{-rt}V_{\hat{m}}(X_t, F_t)$ is a supermartingale is shown similarly as we showed that $e^{-rt}V_{\hat{m}}(X_t, -1)$ is a supermartingale.

We further have to show that $e^{-rt}V_{\hat{m}}(X_t, +1) - e^{-rt}X_t \geq 0$ in $x \in [L, M]$. For this, we use the fact that since $e^{-rt}V_{\hat{m}}(X_t, +1) - e^{-rt}X_t$ is a supermartingale, we can use the Optional Sampling Theorem to deduce that

$$\begin{aligned}
e^{-rt}\{V_{\hat{m}}(X_t, +1) - X_t\} &\geq e^{-r\tau_+} \min\{V_{\hat{m}}(L, +1) - L, 0\} \\
&= e^{-r\tau_+} \min\{V_{\hat{m}}(L, -1) - L, 0\} \geq 0,
\end{aligned} \tag{4.81}$$

where τ_+ is the first stopping time the process goes out of the region $[L, M]$. Note that we've replaced $V_{\hat{m}}(L, +1)$ with $V_{\hat{m}}(L, -1)$ thanks to the boundary condition (4.25). Therefore, in the case $M \geq \hat{M}$, the Snell envelope of $e^{-rt}X_t$ is $e^{-rt}V_{\hat{m}}(X_t, F_t)$ and the optimal stopping time is the first time when the process X_t hits the level M or \hat{m} .

The argument in the case when $M \leq \bar{M}$ will be similar, and we show that $e^{-rt}V_{\hat{m}}(X_t, -1) \geq e^{-rt}X_t$, hence to show $V_{\hat{m}}(x, -1) \geq x$. We define the function $\zeta(x)$ as (4.75). We evaluate this function in the domain $[\tilde{m}, H]$.

First, note that $\zeta(\tilde{m}) = 0$. We calculate first and second derivatives of $\zeta(x)$

with respect to x and they are the same as in (4.76) and (4.77) respectively.

Since $g(\tilde{m}) = 0$, we have

$$\begin{aligned} (1 - \beta_1)H^{-\beta_1}\{H^{\beta_2} - \tilde{m}^{\beta_2-1}V_+(H, M)\} \\ = (\beta_2 - 1)H^{-\beta_1}\{\tilde{m}^{\beta_2-1}V_+(H, M) - H^{\beta_1}\tilde{m}^{\beta_2-\beta_1}\}. \end{aligned} \quad (4.82)$$

Substituting C and D , and using (4.82), we can further calculate

$$\begin{aligned} \zeta''(x) &= (\beta_2 - 1)H^{-\beta_1} \frac{(V_+(H, M) - \tilde{m}^{1-\beta_1}H^{\beta_1})}{H^{\beta_2-\beta_1} - \tilde{m}^{\beta_2-\beta_1}} (\beta_2 x^{\beta_2-1} - \beta_1 \tilde{m}^{\beta_2-\beta_1} x^{\beta_1-2}) \\ &> 0. \end{aligned} \quad (4.83)$$

We calculate $\zeta'(\tilde{m})$.

$$\begin{aligned} \zeta'(\tilde{m}) &= \beta_1 C \tilde{m}^{\beta_1-1} + \beta_2 D \tilde{m}^{\beta_2-1} - 1 \\ &= \beta_1 C \tilde{m}^{\beta_1-1} + \beta_2 D \tilde{m}^{\beta_2-1} - (C \tilde{m}^{\beta_1-1} + D \tilde{m}^{\beta_2-1}) \\ &= C \tilde{m}^{\beta_1-1}(\beta_1 - 1) + (\beta_2 - 1)D \tilde{m}^{\beta_2-1}, \end{aligned} \quad (4.84)$$

where the second equality comes from the boundary condition at $x = \tilde{m}$. We substitute the values of C and D in (4.84) and obtain

$$\begin{aligned} (H^{\beta_2-\beta_1} - \tilde{m}^{\beta_2-\beta_1})\zeta'(\tilde{m}) \\ = (\beta_1 - 1)H^{-\beta_1}(H_2^\beta - \tilde{m}^{\beta_2-1}V_{\tilde{m}}(H, +1)) \\ + (\beta_2 - 1)\tilde{m}^{\beta_2-1}(H^{-\beta_1}V_{\tilde{m}}(H, +1) - \tilde{m}^{1-\beta_1}) \\ = 0, \end{aligned} \quad (4.85)$$

where we used (4.82) in the last equality. From $\zeta(\tilde{m}) = 0$, (4.83), and (4.85), we have $\zeta(x) = V_{\tilde{m}}(x, -1) - x \geq 0$ in $x \in [\tilde{m}, H]$. \square

4.4 Optimal Timing of Buying

Up to the previous section, we were dealing with the optimal selling problem. We now think of the optimal timing to purchase the shares. We assume that we introduce the capital to purchase the asset only at the time of purchase, and seek to maximise our discounted profit.

We solve the following optimal stopping problem:

$$U(x, f) = \sup_{\tau \in \mathcal{T}_M} \mathbf{E}_{x,f}[e^{-r\tau} \{V(X_\tau, F_\tau) - X_\tau\}]. \quad (4.86)$$

We show the following theorem:

Theorem 4.4.1. *It is optimal to purchase the shares when and only when the underlying process is in the positive regime.*

Proof. We define the gains process

$$G(X_t, F_t) = e^{-rt} \{V(X_t, F_t) - X_t\}. \quad (4.87)$$

We further define $\mathcal{U}(X_t, F_t)$ as

$$\mathcal{U}(X_t, F_t) = \begin{cases} e^{-r(\min\{t, \tau_H\})} \{V(X_{\min\{t, \tau_H\}}, +1) - X_{\min\{t, \tau_H\}}\}, & F_t = +1 \\ \mathbf{E}_x[e^{-r\tau_H} \{V(H, +1) - H\}], & F_t = -1. \end{cases} \quad (4.88)$$

In the positive regime, $e^{-rt}V(X_t, +1)$ is a martingale while $e^{-rt}X_t$ is a submartingale. Hence, $G(X_t, +1)$ is a local* supermartingale. Therefore, $G(X_t, +1)$ is itself the Snell envelope that dominates $G(X_t, +1)$ and so it is optimal to stop the process right away.

In the negative regime, $e^{-rt}V(X_t, -1)$ is a martingale and $e^{-rt}X_t$ is a supermartingale. Hence, $G(X_t, -1)$ is a local submartingale. Since the process X_t will hit the level H almost surely, from the Optional Sampling Theorem, it is therefore optimal to run the process as long as possible, which corresponds to running the process until it leaves the negative regime.

We also see that

$$\begin{aligned} \mathcal{U}(X_t, -1) &= \mathbf{E}_x[e^{-r\tau_H} \{V(H, +1) - H\}] = \mathbf{E}_x[e^{-r\tau_H} \{V(H, -1) - H\}] \\ &\geq e^{-rt}(V(X_t, -1) - X_t) = G(X_t, -1). \end{aligned} \quad (4.89)$$

The first line in (4.89) uses the boundary condition and the second line uses the fact that $G(X_t, -1)$ is a submartingale and the Optional Sampling Theorem. Therefore, $\mathcal{U}(X_t, F_t)$ is a supermartingale that dominates the gains process $G(X_t, F_t)$. We then use Theorem 4.3.1 and the solution to the optimal stopping problem (4.86) is the first time the process (X_t, F_t) enters the stopping region, i.e.

*Here, the terminology "local" means 'locally in space'.

the region where $\mathcal{U}(x, \pm 1) = G(x, \pm 1)$. This corresponds to the first time when $F_t = +1$ or when $F_{t-} = -1$ and $(X_t, F_t) = (H, +1)$. \square

4.5 Conclusions

We started with a simple setup where we only have one support/resistance level and fully showed the optimal level to sell the shares. We also considered the optimal timing to purchase the shares and found out that it is only optimal to do so in the positive regime given that the investors borrow money upon buying the shares.

A possible extension of the problem considered in this section is to have the price process follow more general SDEs where μ 's and σ 's are functions of the price. We believe we can follow the same calculation as we did in this thesis using a general theory of ODEs.

Another possible problem to consider is to use different cost functions for the gains processes. For example, in considering the optimal purchasing problem, we assumed that the investors borrow money at the time they decided to purchase the shares. Instead, we can consider the case where the investors already have cash in hand at time $t = 0$ and for this, we need to consider different gains process.

Bibliography

- [1] ANDERSON, D., AND DJEHICHE, B. A maximum principle for relaxed stochastic control of linear sdes with application to bond portfolio optimization. *Math. Methods Oper. Res.* 72, 2 (Oct. 2010), 273–310.
- [2] ANG, C. S. *Analyzing Financial Data and Implementing Financial Models Using R*. Springer International Publishing Switzerland, Cham, Switzerland, 2015.
- [3] ARRIOJAS, M., HU, Y., MOHAMMED, S.-E., AND PAP, G. A delayed Black and Scholes formula. *Stoch. Anal. Appl.* 25, 2 (2007), 471 – 492.
- [4] AVELLANEDA, M., AND LIPKIN, M. D. A market-induced mechanism for stock pinning. *Quant. Finance* 3, 6 (2003), 417 – 425.
- [5] AZIMZADEH, P., FORSYTH, P. A., AND VETZAL, K. R. Hedging costs for variable annuities under regime-switching. In *Hidden Markov Models in Finance: Further Developments and Applications, Volume II*, R. S. Mamon and R. J. Elliott, Eds. Springer Science+Business Media, 2014, ch. 6.
- [6] BANK FOR INTERNATIONAL SETTLEMENTS. Semiannual OTC derivatives statistics, sep 2015.
- [7] BAO, J., AND YUAN, C. Comparison theorem for stochastic differential delay equations with jumps. *Acta Appl. Math.* 116 (2011), 119 – 132.
- [8] BLANCHET-SCALLIET, C., DIOP, A., GIBSON, R., TALAY, D., AND TANRÉ, E. Technical analysis compared to mathematical models based methods under parameter mis-specification. *J. Bank. Finance* 31 (2007), 1351 – 1373.
- [9] BLUM, E. K. *Numerical Analysis and Computation: Theory and Practice*. Addison–Wesley, Reading, MA, 1972.

- [10] BRITTEN-JONES, M., AND NEUBERGER, A. Arbitrage pricing with incomplete markets. *Appl. Math. Finance* 3 (1996), 347 – 363.
- [11] CAMERON, M. 'No panic' as Nikkei volatility spikes, dealers say. *Risk magazine* (May 2013).
- [12] CAMERON, M. Uridashi losses put at \$ 500 million after Nikkei rebounds. *Structured Products* (Mar. 2013).
- [13] CORNS, T. R. A., AND SATCHELL, S. E. Skew brownian motion and pricing European options. *The European Journal of Finance* 13, 6 (2007), 523 – 544.
- [14] DE ANGELIS, T., AND PESKIR, G. A probabilistic approach to the reduite in optimal stopping. *Appl. Math. Finance* 23, 6 (2016), 465 – 483.
- [15] DENG, G., MALLET, J., AND MCCANN, C. Modeling autocallable structured products. *Journal of Derivatives & Hedge Funds* 17, 4 (2011), 326–340.
- [16] DUFFY, D. J. *Finite Difference Methods in Financial Engineering: A Partial Differential Equation Approach*. John Wiley & Sons, Chichester, West Sussex, 2006.
- [17] EL KAROUI, N., LEPELTIER, J.-P., AND MILLET, A. A probabilistic approach to the reduite in optimal stopping. *Probab. Math. Statist* 13, 1 (1992), 97 – 121.
- [18] EVANS, L. C. *Partial Differential Equations*, second ed. AMS, Providence, RI, 2010.
- [19] FLEMING, W. H., AND SONER, H. M. *Controlled Markov Processes and Viscosity Solutions*, second ed. Springer Science+Business Media Inc., New York, NY, 2006.
- [20] FORST, W., AND HOFFMANN, D. *Optimization – Theory and Practice*. Springer, New York, NY, 2010.
- [21] FREY, R., AND STREMME, A. Market volatility and feedback effects from dynamic hedging. *Math. Finance* 7, 4 (1997), 351–374.
- [22] FRIEDMAN, A. *Partial Differential Equations of Parabolic Type*. Princeton–Hall, Englewood Cliffs, NJ, 1964.
- [23] GILBARG, D., AND TRUDINGER, N. S. *Elliptic Partial Differential Equations of Second Order*. Springer, Berlin, 2001.

- [24] HABA, F., AND JACQUIER, A. Asymptotic arbitrage in the Heston model. *Int. J. Theor. Appl. Finance* 18, 8 (2015).
- [25] HARRISON, J. M., AND SHEPP, L. A. On skew brownian motion. *Ann. Probab.* 9, 2 (1981), 309 – 313.
- [26] HESTON, S. L. A closed-form solution for options with stochastic volatility with applications to bond and currency options. *Rev. Financial Stud.* 6, 2 (1993), 327–343.
- [27] HULL, J. C. *Options, Futures, and Other Derivatives*, ninth ed. Pearson Education Inc., Upper Saddle River, NJ, 2015.
- [28] IKEDA, N., AND WATANABE, S. *Stochastic Differential Equations and Diffusion Processes*. Elsevier North–Holland Inc., New York, NY, 1981.
- [29] ITÔ, K., AND HENRY P. MCKEAN, J. *Diffusion Processes and Their Sample Paths*. Springer-Verlag, Berlin, 1965.
- [30] JACKA, S. D., AND MIJATOVIĆ, A. On the policy improvement algorithm in continuous time. *Stochastics* 89, 1 (2017), 348–359.
- [31] JACKA, S. D., MIJATOVIĆ, A., AND ŠIRAJ, D. Policy improvement algorithm for continuous finite horizon problem.
- [32] JACKA, S. D., MIJATOVIĆ, A., AND ŠIRAJ, D. Policy improvement algorithm for controlled multidimensional diffusion processes.
- [33] JEANBLANC, M., YOR, M., AND CHESNEY, M. *Mathematical Methods for Financial Markets*. Springer–Verlag, London, United Kingdom, 2009.
- [34] JEANNIN, M., IORI, G., AND SAMUEL, D. Modeling stock pinning. *Quant. Finance* 8, 8 (2008), 823 – 831.
- [35] KARATZAS, I., AND SHREVE, S. E. *Brownian Motion and Stochastic Calculus*, second ed. Springer Science + Business Inc., New York, NY, 1998.
- [36] KARATZAS, I., AND SHREVE, S. E. *Methods of Mathematical Finance*. Springer-Verlag, New York, NY, 1998.
- [37] KARLIN, S., AND TAYLOR, H. M. *A Second Course in Stochastic Processes*. Academic Press, New York, NY, 1981.

- [38] KELLEY, C. T. *Iterative Methods for Linear and Nonlinear Equations*. SIAM, Philadelphia, PA, 1995.
- [39] KELLEY, C. T. *Solving Nonlinear Equations with Newton's Method*. SIAM, Philadelphia, PA, 2003.
- [40] LADYŽENSKAJA, O. A., SOLONNIKOV, V. A., AND URAL'CEVA, N. N. *Linear and Quasi-linear Equations of Parabolic Type*. American Mathematical Society, Providence, RI, 1968.
- [41] LADYZHENSKAYA, O. A., AND URAL'TSEVA, N. N. *Linear and Quasilinear Elliptic Equations*. Academic Press, New York, NY, 1968.
- [42] LANGTANGEN, H. P. *A Primer on Scientific Programming with Python*, fourth ed. Springer-Verlag, Berlin, 2014.
- [43] LE GALL, J.-F. *Brownian Motion, Martingales, and Stochastic Calculus*. Springer, Switzerland, 2016.
- [44] LEJAY, A. On the constructions of the skew Brownian motion. *Probab. Surv.* 3 (2006), 413 – 466.
- [45] LIEBERMAN, G. M. *Second Order Parabolic Differential Equations*. World Scientific Publishing Co. Pte. Ltd., Singapore, 1996.
- [46] LIN, S. Finite difference schemes for Heston model. Master's thesis, University of Oxford, 2008.
- [47] LINDVALL, T., AND ROGERS, L. C. G. Coupling of multidimensional diffusions by reflection. *Ann. Probab.* 14, 3 (1986), 860–872.
- [48] LO, A. W., MAMAYSKY, H., AND WANG, J. Foundations of technical analysis: Computational algorithms, statistical inference, and empirical implementation. *J. Finance* 55, 4 (2000), 1705 – 1765.
- [49] LONGTIN, A. Stochastic delay-differential equations. In *Complex Time-Delay Systems: Theory and Applications*, F. M. Atay, Ed. Springer-Verlag, 2010, ch. 6.
- [50] LORD, R., KOEKKOEK, R., AND DIJK, D. V. A comparison of biased simulation schemes for stochastic volatility models. *Quant. Finance* 10, 2 (2010), 177–194.
- [51] LORIG, M., ZHOU, Z., AND ZOU, B. A mathematical analysis of technical analysis, Oct. 2017. arXiv:1710.09476.

- [52] MANGAT, J. Structured shift for Japanese investment products. *Asia Risk* (December 2010).
- [53] MAO, X. *Stochastic Differential Equations & Applications*. Horwood Publishing Ltd., 1997.
- [54] MAO, X., AND YUAN, C. *Stochastic Differential Equations with Markovian Switching*. Imperial College Press, London, UK, 2006.
- [55] MARRAY, M. German agency KfW maintains its €75bn issuance target for 2010. *Credit* (July 2010).
- [56] MOHAMMED, S. E. A. *Stochastic Functional Differential Equations*. Pitman Publishing Inc., 1984.
- [57] NILSEN, W., AND SAYIT, H. No arbitrage in markets with bounces and sinks. *International Review of Applied Financial Issues and Economics* 3, 4 (2011), 696 – 699.
- [58] ORTEGA, J. M., AND RHEINBOLDT, W. C. *Iterative Solution of Nonlinear Equations in Several Variables*. Academic Press, New York, NY, 1970.
- [59] PESKIR, G., AND SHIRYAEV, A. *Optimal Stopping and Free-Boundary Problems*. Birkhäuser Verlag, Basel, Switzerland, 2006.
- [60] PETERSEIL, Y. Equity derivatives house of the year: Credit Suisse. *Structured Products* (August 2014).
- [61] PLATEN, E., AND SCHWEIZER, M. On feedback effects from hedging derivatives. *Math. Finance* 8, 1 (1998), 67–84.
- [62] PROTTER, P. E. *Stochastic Integration and Differential Equations: A New Approach*. Springer-Verlag, 1990.
- [63] PUCCI, P., AND SERRIN, J. *The Maximum Principle*. Birkhäuser, Basel, Switzerland, 2007.
- [64] REUTERS LTD. *Introduction to Technical Analysis*. John Wiley & Sons, Singapore, 1999.
- [65] ROCKAFELLAR, R. T. *Convex Analysis*. Princeton University Press, Princeton, NJ, 1970.

- [66] ROGERS, L. C. G., AND WILLIAMS, D. *Diffusions, Markov Processes and Martingales Volume 2: Itô Calculus*, second ed. Cambridge University Press, Cambridge, UK, 2000.
- [67] ROSSELLO, D. Arbitrage in skew brownian motion models. *Insurance: Mathematics and Economics* 50 (2012), 50 – 56.
- [68] SHREVE, S. E. *Stochastic Calculus for Finance II: Continuous-Time Models*. Springer, New York, NY, 2004.
- [69] ŠIRAJ, D. *Coupling and the policy improvement algorithm for controlled diffusion processes*. PhD thesis, University of Warwick, 2015.
- [70] SIRCAR, K. R., AND PAPANICOLAOU, G. General Black-Scholes models accounting for increased market volatility from hedging strategies. *Appl. Math. Finance* 5, 1 (1998), 45–82.
- [71] SMITH, G. D. *Numerical Solution of Partial Differential Equations: Finite Difference Methods*, third ed. Clarendon Press, Oxford, 1985.
- [72] SONER, H. M. Stochastic representations for nonlinear parabolic pdes. In *Handbook of Differential Equations: Evolutionary Equations*, C. M. Dafermos and E. Feireisl, Eds., vol. 3. Elsevier B. V., 2007, ch. 6.
- [73] TAVELLA, D., AND RANDALL, C. *Pricing Financial Instruments: The Finite Difference Method*. John Wiley & Sons, New York, NY, 2000.
- [74] THOMPSON, H. Equity structuring resurfaces as Japanese investors hunt for yield. *Asia Risk* (March 2011).
- [75] THOMPSON, H. Structured product investors hit by sharp fall in Japanese equities. *Asia Risk* (Mar. 2011).
- [76] VAGHELA, V. Hedging drives demand for Japan dividend futures. *Asia Risk* (September 2012).
- [77] VAGHELA, V. Japan dividend futures in virtuous circle. *Structured Products* (Oct. 2012).
- [78] VAGHELA, V. Uridashi knockouts push Japan dividend futures to outperform Nikkei. *Asia Risk* (May 2013).
- [79] VAGHELA, V. Credit Suisse prospers despite low volatility environment. *Asia Risk* (Oct. 2014).

- [80] VAGHELA, V. Plunging Nikkei brings \$ 40m vega losses to Japan dealers. *Asia Risk* (Feb. 2014).
- [81] VAGHELA, V. HSCEI Korea structured product losses spark regulatory fears. *Asia Risk* (October 2015).
- [82] VAGHELA, V. Low rates enhance appeal of autocallables beyond core Asia market. *Asia Risk* (July 2015).
- [83] YANG, Z., MAO, X., AND YUAN, C. Comparison theorem of one-dimensional stochastic hybrid delay systems. *Systems Control Lett.* 57 (2008), 56 – 63.

Appendix A

Derivation of Heston's PDE (2.3)

We derive Heston's PDE (2.3). For price of an arbitrary derivative structure V , using Ito's Lemma and substituting (2.1),

$$\begin{aligned}
 dV &= \left\{ \frac{\partial V}{\partial t} + \mu S \frac{\partial V}{\partial S} + \kappa(\bar{v} - v) \frac{\partial V}{\partial v} + \frac{1}{2} v S^2 \frac{\partial^2 V}{\partial S^2} + \frac{1}{2} v \eta^2 \frac{\partial^2 V}{\partial v^2} \right. \\
 &\quad \left. + v S \eta \rho \frac{\partial^2 V}{\partial S \partial v} \right\} dt + \sqrt{v} S \frac{\partial V}{\partial S} dW^1 + \eta \sqrt{v} \frac{\partial V}{\partial v} dW^2 \quad (\text{A.1}) \\
 &= \Phi(V) dt + \sqrt{v} S \frac{\partial V}{\partial S} dW^1 + \eta \sqrt{v} \frac{\partial V}{\partial v} dW^2.
 \end{aligned}$$

Let us think of a portfolio $U = V_1 + \delta S + \gamma V_2$, where V_1 and V_2 are arbitrary derivatives structures. Then, from the variation principle, since the portfolio U should make $rU dt$ in infinitesimal time dt , the following should hold:

$$dU = dV_1 + \delta dS + \gamma dV_2 = r(V_1 + \delta S + \gamma V_2) dt. \quad (\text{A.2})$$

We substitute (A.1) in (A.2) and obtain

$$\begin{aligned}
 &\left(\Phi(V_1) dt + \sqrt{v} S \frac{\partial V_1}{\partial S} dW^1 + \eta \sqrt{v} \frac{\partial V_1}{\partial v} dW^2 \right) + \delta(\mu S dt + \sqrt{v} S dW^1) \\
 &+ \gamma \left(\Phi(V_2) dt + \sqrt{v} S \frac{\partial V_2}{\partial S} dW^1 + \eta \sqrt{v} \frac{\partial V_2}{\partial v} dW^2 \right) = r(V_1 + \delta S + \gamma V_2) dt \quad (\text{A.3})
 \end{aligned}$$

Comparing the coefficients of dW^1 and dW^2 terms on both sides of (A.3), we obtain

$$\delta = \frac{(\partial V_1/\partial v)(\partial V_2/\partial S) - (\partial V_1/\partial S)(\partial V_2/\partial v)}{\partial V_2/\partial v} \quad (A.4)$$

$$\gamma = -\frac{\partial V_1/\partial v}{\partial V_2/\partial v}$$

Finally, we compare the coefficients of the dt term in (A.3) and derive

$$\Phi(V_1) - rV_1 + \delta(\mu - r)S = -\gamma(\Phi(V_2) - rV_2). \quad (A.5)$$

Substituting δ and γ from (A.4) to (A.3),

$$\frac{\partial V_2}{\partial v} \left(\Phi(V_1) - rV_1 - \frac{\partial V_1}{\partial S}(\mu - r)S \right) = \frac{\partial V_1}{\partial v} \left(\Phi(V_2) - rV_2 - \frac{\partial V_2}{\partial S}(\mu - r)S \right). \quad (A.6)$$

Since V_1 and V_2 were arbitrary, with the introduction of a function $\Lambda(S, v, t)$ that depends only on S , v , and t (and independent of the derivatives structure), for the value of any derivative structure V , we have

$$\Phi(V) - rV - \frac{\partial V}{\partial S}(\mu - r)S = \Lambda(S, v, t) \frac{\partial V}{\partial v}. \quad (A.7)$$

We substitute back the function $\Phi(\cdot)$ introduced in (A.1) and obtain

$$\begin{aligned} \frac{\partial V}{\partial t} + rS \frac{\partial V}{\partial S} + \left\{ \kappa(\bar{v} - v) - \Lambda(S, v, t) \right\} \frac{\partial V}{\partial v} \\ + \frac{1}{2}vS^2 \frac{\partial^2 V}{\partial S^2} + \frac{1}{2}v\eta^2 \frac{\partial^2 V}{\partial v^2} + vS\eta\rho \frac{\partial^2 V}{\partial S\partial v} - rV = 0. \end{aligned} \quad (A.8)$$

If we take $\Lambda(S, v, t) = \lambda v$ with a constant λ as in [26], we derive (2.3).

Appendix B

Lemmas for Chapter 2

The lemmas stated here are more or less those in [31], [32], and [69]. We only modify them to fit our problem. We show them here, however, so that this paper is self-contained.

A property that forms the basis of the following lemmas is that processes controlled by Markov policies are strong Markov processes (Theorem 4.20 in [35]).

Lemma B.1. *For every Markov policy π , $z \in \mathcal{E}$, $0 < t < T$, and any stopping time \mathcal{S} that is almost surely less than $t \wedge \tau_\Omega$,*

$$\begin{aligned} \mathbf{E} \left(\int_0^{t \wedge \tau} e^{-rs} f^\pi(Z_s^{z, \pi}, t-s) ds + e^{-r(t \wedge \tau)} g(Z_{t \wedge \tau}^{z, \pi}, t \wedge \tau) \middle| \mathcal{F}_\mathcal{S} \right) \\ = \int_0^\mathcal{S} e^{-rs} f^\pi(Z_s^{z, \pi}, t-s) ds + e^{-r\mathcal{S}} V^{g, \mathcal{E}, \pi}(Z_\mathcal{S}^{z, \pi}, t - \mathcal{S}). \end{aligned} \quad (\text{B.1})$$

In particular, the process $(\int_0^{T'} e^{-rs} f^\pi(Z_s^{z, \pi}, t-s) ds + e^{-rT'} V^{g, \mathcal{E}, \pi}(Z_{T'}^{z, \pi}, T'))_{T' \leq T}$ is a uniformly integrable martingale.

Proof. Let $\tau = \tau_\mathcal{E}(Z^{z, \pi})$ and $\tau_\mathcal{S} := \tau \circ \theta_\mathcal{S} = \tau_\mathcal{E}(Z_{\cdot + \mathcal{S}}^{z, \pi})$, where θ is the shift operator. Then $\tau_\mathcal{S} = \tau - \mathcal{S}$ holds almost surely, and we obtain

$$\begin{aligned} \mathbf{E} \left(\int_0^{t \wedge \tau} e^{-rs} f^\pi(Z_s^{z, \pi}, t-s) ds + e^{-r(t \wedge \tau)} g(Z_{t \wedge \tau}^{z, \pi}, t \wedge \tau) \middle| \mathcal{F}_\mathcal{S} \right) \\ = \int_0^\mathcal{S} e^{-rs} f^\pi(Z_s^{z, \pi}, t-s) ds \\ + \mathbf{E} \left(\int_\mathcal{S}^{t \wedge \tau} e^{-rs} f^\pi(Z_s^{z, \pi}, t-s) ds + e^{-r(t \wedge \tau)} g(Z_{t \wedge \tau}^{z, \pi}, t \wedge \tau) \middle| \mathcal{F}_\mathcal{S} \right) \end{aligned}$$

$$\begin{aligned}
&= \int_0^{\mathcal{S}} e^{-rs} f^\pi(Z_s^{z,\pi}, t-s) ds + \mathbf{E} \left(\int_0^{t \wedge \tau - \mathcal{S}} e^{-r(s+\mathcal{S})} f^\pi(Z_{s+\mathcal{S}}^{z,\pi}, t-(s+\mathcal{S})) ds \right. \\
&\quad \left. + e^{-r((t-\mathcal{S}) \wedge (\tau-\mathcal{S}) + \mathcal{S})} g(Z_{(t-\mathcal{S}) \wedge (\tau-\mathcal{S}) + \mathcal{S}}^{z,\pi}, (t-\mathcal{S}) \wedge (\tau-\mathcal{S}) + \mathcal{S}) \middle| \mathcal{F}_{\mathcal{S}} \right) \\
&= \int_0^{\mathcal{S}} e^{-rs} f^\pi(Z_s^{z,\pi}, t-s) ds + e^{-r\mathcal{S}} \mathbf{E} \left(\int_0^{(t-\mathcal{S}) \wedge \tau_{\mathcal{S}}} e^{-rs} f^\pi(Z_{s+\mathcal{S}}^{z,\pi}, t-(s+\mathcal{S})) ds \right. \\
&\quad \left. + e^{-r((t-\mathcal{S}) \wedge \tau_{\mathcal{S}})} g(Z_{(t-\mathcal{S}) \wedge \tau_{\mathcal{S}} + \mathcal{S}}^{z,\pi}, (t-\mathcal{S}) \wedge \tau_{\mathcal{S}} + \mathcal{S}) \middle| \mathcal{F}_{\mathcal{S}} \right) \\
&= \int_0^{\mathcal{S}} e^{-rs} f^\pi(Z_s^{z,\pi}, t-s) ds + e^{-r\mathcal{S}} \mathbf{E}_x \left(\left\{ \int_0^{(t-\mathcal{S}) \wedge \tau} e^{-rs} f^\pi(Z_s^{z,\pi}, t-(s+\mathcal{S})) ds \right. \right. \\
&\quad \left. \left. + e^{-r(t-\mathcal{S}) \wedge \tau} g(Z_{(t-\mathcal{S}) \wedge \tau}^{z,\pi}, (t-\mathcal{S}) \wedge \tau) \right\} \circ \theta_{\mathcal{S}} \middle| \mathcal{F}_{\mathcal{S}} \right) \\
&= \int_0^{\mathcal{S}} e^{-rs} f^\pi(Z_s^{z,\pi}, t-s) ds + e^{-r\mathcal{S}} \mathbf{E}_{Z_{\mathcal{S}}^{z,\pi}} \left(\int_0^{(t-\mathcal{S}) \wedge \tau} e^{-rs} f^\pi(Z_s^{z,\pi}, t-(s+\mathcal{S})) ds \right. \\
&\quad \left. + e^{-r(t-\mathcal{S}) \wedge \tau} g(Z_{(t-\mathcal{S}) \wedge \tau}^{z,\pi}, (t-\mathcal{S}) \wedge \tau) \right) \\
&= \int_0^{\mathcal{S}} e^{-rs} f^\pi(Z_s^{z,\pi}, t-s) ds + e^{-r\mathcal{S}} V^{g,\mathcal{E},\pi}(Z_{\mathcal{S}}^{z,\pi}, t-\mathcal{S})
\end{aligned}$$

□

By taking expectation on both sides of (B.1), we retrieve a corollary which is so-called Bellman's principle.

Corollary B.2. *For every Markov policy π , $z \in \mathcal{E}$, $0 < t < T$, and stopping time \mathcal{S} which is almost surely less than or equal to $t \wedge \tau_{\Omega}$,*

$$V^{g,\mathcal{E},\pi}(z, t) = \mathbf{E} \left(\int_0^{\mathcal{S}} e^{-rs} f^\pi(Z_s^{z,\pi}, t-s) ds \right) + e^{-r\mathcal{S}} \mathbf{E}(V^{g,\mathcal{E},\pi}(Z_{\mathcal{S}}^{z,\pi}, t-\mathcal{S})). \quad (\text{B.2})$$

We now use the method of mirror coupling [47].

Lemma B.3. *For every Lipschitz Markov control and small enough $\epsilon > 0$, there exists $\delta > 0$ such that the following holds for every $z_1, z_2 \in \mathcal{E}$: if $\|z_1 - z_2\| < \delta$ then there exist processes $\tilde{Z}^{z_1,\pi}$ and $\tilde{Z}^{z_2,\pi}$ that have the same laws as $Z^{z_1,\pi}$ and $Z^{z_2,\pi}$ respectively such that*

$$\|\tilde{Z}_t^{z_1,\pi} - \tilde{Z}_t^{z_2,\pi}\| \leq G_{\tau_t} \quad \text{on } t < \rho\delta$$

and

$$\tilde{Z}_t^{z_1, \pi} = \tilde{Z}_t^{z_2, \pi} \quad \text{on } t \geq \rho_0$$

for every $t \geq 0$, where

$$\rho_c := \inf \{t \geq 0; \|\tilde{Z}^{z_1, \pi} - \tilde{Z}^{z_2, \pi}\| = c\} \quad , \quad (\inf \phi = \infty)$$

for any $c \geq 0$, G is the squared Bessel process of dimension $1 + \epsilon$ started at $\|z_1 - z_2\|$, and $(\tau_t)_{t \geq 0}$ is a stochastic time change with the property

$$\tau_t \leq \frac{t}{\nu_1}, \quad t \geq 0.$$

For the proof of Lemma B.3, we refer to [31] and [69].

Lemma B.4. *For every Lipschitz Markov policy π , the function $V^{g, \mathcal{E}, \pi}(\cdot, t)$ is continuous with bounded initial condition.*

Proof. Let $\epsilon > 0$ and $\hat{\delta} \leq \delta$. For $\|z_1 - z_2\| \leq \hat{\delta}$, we calculate $|V^{g, \mathcal{E}, \pi}(z_1, t) - V^{g, \mathcal{E}, \pi}(z_2, t)|$.

$$\begin{aligned} & |V^{g, \mathcal{E}, \pi}(z_1, t) - V^{g, \mathcal{E}, \pi}(z_2, t)| \\ &= \left| \mathbf{E} \left(\int_0^{t \wedge \tau_{z_1}} e^{-rs} f^\pi(\tilde{Z}_s^{z_1, \pi}, t-s) ds + e^{-r(t \wedge \tau_{z_1})} g(\tilde{Z}_{t \wedge \tau_{z_1}}^{z_1, \pi}, t \wedge \tau_{z_1}) \right) \right. \\ &\quad \left. - \mathbf{E} \left(\int_0^{t \wedge \tau_{z_2}} e^{-rs} f^\pi(\tilde{Z}_s^{z_2, \pi}, t-s) ds + e^{-r(t \wedge \tau_{z_2})} g(\tilde{Z}_{t \wedge \tau_{z_2}}^{z_2, \pi}, t \wedge \tau_{z_2}) \right) \right| \\ &< \left| \mathbf{E} \left(\int_0^{\rho_0} e^{-rs} \{f^\pi(\tilde{Z}_s^{z_1, \pi}, t-s) - f^\pi(\tilde{Z}_s^{z_2, \pi}, t-s)\} ds \middle| I_{\rho_0 \leq \rho_\delta} \right) \right| \\ &+ \left| \mathbf{E} \left(\int_{\rho_0}^t e^{-rs} \{f^\pi(\tilde{Z}_s^{z_1, \pi}, t-s) - f^\pi(\tilde{Z}_s^{z_2, \pi}, t-s)\} ds \right. \right. \\ &\quad \left. \left. + e^{-rt} \{g(\tilde{Z}_t^{z_1, \pi}, t) - g(\tilde{Z}_t^{z_2, \pi}, t)\} \middle| I_{\rho_0 \leq \rho_\delta} \right) \right| \\ &+ \left| \mathbf{E} \left(\int_0^t e^{-rs} \{f^\pi(\tilde{Z}_s^{z_1, \pi}, t-s) - f^\pi(\tilde{Z}_s^{z_2, \pi}, t-s)\} ds \right. \right. \\ &\quad \left. \left. + e^{-rt} \{g(\tilde{Z}_t^{z_1, \pi}, t) - g(\tilde{Z}_t^{z_2, \pi}, t)\} \middle| I_{\rho_0 > \rho_\delta} \right) \right| \\ &= B_1 + B_2 + B_3. \end{aligned} \tag{B.3}$$

For B_1 , since f^π is Lipschitz continuous, we can take $\delta_1 \in (0, \delta)$ small enough such that

$$B_1 < C \|\tilde{Z}_s^{z_1, \pi} - \tilde{Z}_s^{z_2, \pi}\| < \epsilon/2. \quad (\text{B.4})$$

For B_2 , due to the definition of \tilde{Z} , the processes $\tilde{Z}_t^{z_1, \pi}$ and $\tilde{Z}_t^{z_2, \pi}$ take the same values in this time frame in consideration, so $B_2 = 0$.

Due to the boundedness of f^π and g , the last term B_3 could be bounded by some constant multiplied by $\mathbf{P}(\rho_0 > \rho_\delta)$. If we denote by $\rho_\delta(\mathcal{Y})$ and $\rho_0(\mathcal{Y})$ the first hitting times of the levels δ and 0 respectively for any process \mathcal{Y} , we have from Lemma B.3

$$\mathbf{P}(\rho_\delta < \rho_0) \leq \mathbf{P}\left(\rho_\delta(G_\tau) < \rho_0(G_\tau)\right) \leq \mathbf{P}\left(\rho_\delta\left(G_{\frac{1}{\nu_1}}\right) < \rho_0\left(G_{\frac{1}{\nu_1}}\right)\right). \quad (\text{B.5})$$

Using the scale property of the squared Bessel process we get

$$\begin{aligned} \mathbf{P}\left(\rho_\delta\left(G_{\frac{1}{\nu_1}}\right) < \rho_0\left(G_{\frac{1}{\nu_1}}\right)\right) &= \mathbf{P}\left(\rho_\delta\left(\frac{1}{\nu_1}G\right) < \rho_0\left(\frac{1}{\nu_1}G\right)\right) \\ &= \mathbf{P}(\rho_{\nu_1\delta}(G) < \rho_0(G)). \end{aligned} \quad (\text{B.6})$$

Recall that the scale function of the Bessel process with dimension $1 + \epsilon$ is given by $s(z) := z^{\frac{1-\epsilon}{2}}$, and that the process G starts at $\|z_1 - z_2\| < \hat{\delta}$. Hence we obtain

$$\mathbf{P}(\rho_{\nu_1\delta}(G) < \rho_0(G)) = \frac{s(\|z_1 - z_2\|) - s(0)}{s(\nu_1\delta)} \leq \left(\frac{\hat{\delta}}{\nu_1\delta}\right)^{\frac{1-\epsilon}{2}}. \quad (\text{B.7})$$

We set $\delta = \delta_1$ and take $\hat{\delta} \in (0, \delta)$ small enough so that

$$2C \left(\frac{\hat{\delta}}{\nu_1\delta}\right)^{\frac{1-\epsilon}{2}} < \frac{\epsilon}{2}. \quad (\text{B.8})$$

Collecting what we calculated, we have proved that $\|z_1 - z_2\| < \hat{\delta}$ implies $|V^{g, \mathcal{E}, \pi}(z_1, t) - V^{g, \mathcal{E}, \pi}(z_2, t)| < \epsilon$, so we have uniform continuity of $V^{g, \mathcal{E}, \pi}(\cdot, t)$. \square

Lemma B.5. *For every Lipschitz Markov policy π , the function $V^{g, \mathcal{E}, \pi}$ is continuous.*

Proof. If we proved the continuity of $V^{g, \mathcal{E}, \pi}$ with respect to t for fixed z , the statement is proved using the triangle inequality and Lemma B.4. Therefore, we prove the continuity in t with fixed z . Due to Corollary B.2, we have

$$\begin{aligned}
V^{g,\mathcal{E},\pi}(z, t + \delta) - V^{g,\mathcal{E},\pi}(z, t) &= \mathbf{E} \left(\int_0^\delta e^{-rs} f^\pi(Z_s^{z,\pi}, t - s) ds \right) \\
&\quad + e^{-r\delta} \mathbf{E} \left(V^{g,\mathcal{E},\pi}(Z_\delta^{z,\pi}, t) - e^{r\delta} V^{g,\mathcal{E},\pi}(z, t) \right).
\end{aligned} \tag{B.9}$$

Applying Lemma B.4, we obtain

$$|V^{g,\mathcal{E},\pi}(z, t + \delta) - V^{g,\mathcal{E},\pi}(z, t)| \leq C\delta + C' \mathbf{E}(\|Z_\delta^{z,\pi} - z\|). \tag{B.10}$$

The SDE for $Z_\delta^{z,\pi}$ yields

$$Z_\delta^{z,\pi} - z = \int_0^\delta \mu_\pi(Z_s^{z,\pi}, s) ds + \int_0^\delta \sigma_\pi(Z_s^{z,\pi}, s) dW_s. \tag{B.11}$$

Therefore, we have

$$\begin{aligned}
|V^{g,\mathcal{E},\pi}(z, t + \delta) - V^{g,\mathcal{E},\pi}(z, t)| &\leq C\delta \\
&\quad + C' \mathbf{E} \left(\left| \int_0^\delta \mu_\pi(Z_s^{z,\pi}, s) ds \right| \right) + C'' \mathbf{E} \left(\left| \int_0^\delta \sigma_\pi(Z_s^{z,\pi}, s) dW_s \right| \right).
\end{aligned} \tag{B.12}$$

The second term on RHS can be bounded by some multiple of δ as μ_π is bounded. For the last term, using Jensen's inequality and Burkholder-Davis-Gundy inequality,

$$\begin{aligned}
\mathbf{E} \left(\left| \int_0^\delta \sigma_\pi(Z_s^{z,\pi}, s) dW_s \right| \right) &\leq \left(\mathbf{E} \left(\int_0^\delta \sigma_\pi(Z_s^{z,\pi}, s) dW_s \right)^2 \right)^{\frac{1}{2}} \\
&\lesssim \left(\mathbf{E} \left(\int_0^\delta \sigma_\pi^2(Z_s^{z,\pi}, s) ds \right) \right)^{\frac{1}{2}}.
\end{aligned} \tag{B.13}$$

This proves the continuity of $V^{g,\mathcal{E},\pi}$ with respect to t with fixed z . Therefore, the continuity of $V^{g,\mathcal{E},\pi}$ is proved. \square

Appendix C

Numerical Calculations on Autocallables under Market Driver Model

C.1 Pricing Autocallable as the Market Driver

Since our motivation of constructing the new model with concentration effect in Chapter 2 was to price autocallables in such an environment, we numerically calculate the price of an autocallable in the market driver model. We also price a straddle under the concentration by the autocallable and see how the concentration affects other products.

The detail of the autocallable we price in concentration is listed in Table C.1.

| Parameter | Value |
|-----------|----------|
| K | 105% |
| c | 85% |
| k | 70% |
| T | 3 Years |
| h | 3% |
| l | 0.01% |
| q | 3 months |
| Q | 0.00005 |

Table C.1: Detail of the autocallable structure in concentration.

We price the autocallable under the PDE of the Heston model (2.3) and that of the new model (2.8). The premiums and the risks of the product under the models are

shown in Table C.2 and in Figure C.1.

| Risks | Value | Delta | Vega | Vanna | Volga |
|-----------|--------|---------|---------|--------|----------|
| Heston | 93.561 | 55.247% | -29.240 | 0.4676 | -130.155 |
| New Model | 93.772 | 53.730% | -30.002 | 0.5431 | -195.48 |

Table C.2: Summary for the autocallable that is the market driver at $S = 98.255$ and $v = 0.030001$.

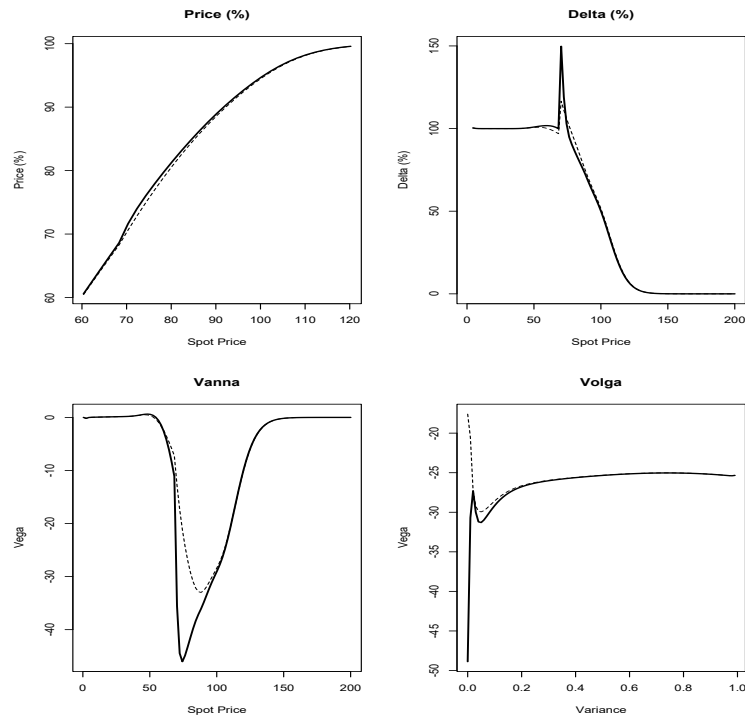


Figure C.1: Premiums and risks of the concentrated autocallable at time $t = 0$. Solid lines indicate those in the new model and dotted lines those in the Heston model.

Note that the price of the autocallable is higher in the new model as the option that the structure is short of is priced cheaper now with the volatility offered in the market.

C.2 Pricing Straddle under the Concentration in Autocallable

We first price a straddle described in Table C.3 given the concentration in the autocallable given in Table C.1. The premiums and risks of the straddle in the Heston model and our model are shown in Table C.4 and in Figure C.2

| | |
|-----------|---------|
| Structure | Stradle |
| Tenor | 3 years |
| Strike | 100% |

Table C.3: Detail of the straddle we price.

| Risks | Value | Delta | Vega | Vanna | Volga |
|-----------|--------|---------|--------|---------|----------|
| Heston | 24.936 | 32.519% | 51.703 | 0.5346 | 1710.885 |
| New Model | 24.515 | 36.231% | 52.050 | -0.2208 | 1101.994 |

Table C.4: Summary for the straddle given the existence of the autocallable described in Section C.1 as the market driver at $S = 98.255$ and $v = 0.030001$.

Since the volatility is offered from the concentration in the autocallable, the straddle is priced cheaper under the new model.

C.3 Pricing Another Autocallable under the Concentration in Autocallable

Finally, we price another autocallable structure with detail given in Table C.5 given the existence of the autocallable in Table C.1 as the market driver.

| Parameter | Value |
|-----------|----------|
| K | 95% |
| c | 75% |
| k | 60% |
| T | 3 Years |
| h | 4% |
| l | 0.01% |
| q | 3 months |

Table C.5: Detail of a different autocallable to be priced given the concentration of the structure given in Table C.1.

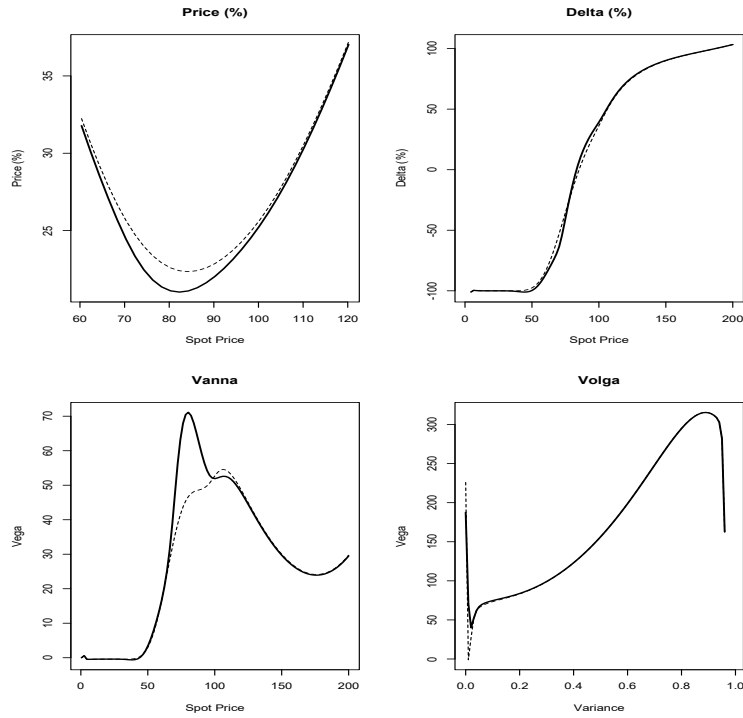


Figure C.2: Premiums and risks of the straddle under the risk concentration in the autocallable. Solid lines indicate those in the new model and dotted lines those in the Heston model without any assumptions on risk concentration.

The premiums and risks of the autocallable are shown in Table C.6 and in Figure C.3.

| Risks | Value | Delta | Vega | Vanna | Volga |
|-----------|--------|---------|---------|--------|----------|
| Heston | 98.486 | 26.176% | -21.175 | 1.3033 | -244.708 |
| New Model | 98.574 | 24.881% | -21.194 | 1.3607 | -273.463 |

Table C.6: Summary for the autocallable in Table C.5 given another autocallable described in Section C.1 as the market driver at $S = 98.255$ and $v = 0.030001$.

As in the case of the market driver in Section C.1, the different autocallable structure considered in this section is also priced higher under the new model.

C.4 Summary

Calculating the corresponding volatility level in the new model for each product, we obtain the result shown in Table C.7.

From this table, we see that the model indeed takes into account the concentration

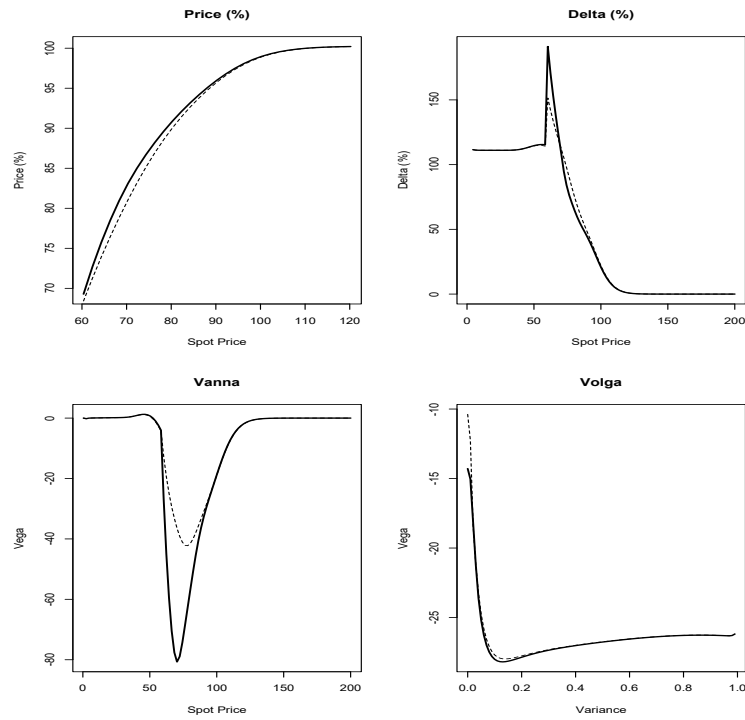


Figure C.3: Premiums and risks of the autocallable described in Table C.6 under the concentration of another autocallable specified in Table C.1. Solid lines indicate those in the new model and dotted lines those in the Heston model without any concentrations.

| | Autocallable (Market Driver) | Straddle | Autocallable (Not the Market Driver) |
|------------|---------------------------------|----------|--|
| Heston | 17.321% | 17.321% | 17.321% |
| New Model | 15.102% | 14.780% | 16.069% |
| Difference | -2.219% | -2.541% | -1.252% |

Table C.7: Implied volatilities calculated based on the risk figures from the Heston model.

effect of the autocallable and shifts the volatility lower. Even if the market driver is of exotic type like an autocallable, we see that the new model reflects the impact of the market driver in price and risks.

Appendix D

Proof of Theorem 3.3.1

In this Appendix, we give a proof of Theorem 3.3.1.

Proof: V^{π_i} satisfies

$$\frac{1}{2}\text{Tr}\{\sigma^T(HV^{\pi_i})\sigma\} + \mu_{\pi_i}^T \cdot \nabla V^{\pi_i} - \alpha V^{\pi_i} + f^{\pi_i} = 0, \quad (\text{D.1})$$

and since Assumption 2 is that σ does not depend on π , π_i is determined by the iteration:

$$\begin{aligned} \pi_{i+1} &= \arg \max_{\pi \in \mathcal{A}} \left(\frac{1}{2}\text{Tr}\{\sigma^T(HV^{\pi_i})\sigma\} + \mu_{\pi}^T \cdot \nabla V^{\pi_i} + f^{\pi} \right) \\ &= \arg \max_{\pi \in \mathcal{A}} \left(\mu_{\pi}^T \cdot \nabla V^{\pi_i} + f^{\pi} \right). \end{aligned} \quad (\text{D.2})$$

From Assumption 1, we can write

$$\mu_{\pi} = \mathbf{M}\pi + \mathbf{b}. \quad (\text{D.3})$$

It then follows from (D.2) that

$$\mathbf{M}^T \nabla V^{\pi_n} + \nabla_{\pi} f^{\pi}|_{\pi=\pi_{n+1}} = \mathbf{0}. \quad (\text{D.4})$$

Subtracting (D.4) with $n = i - 1$ from the same equation with $n = i$, and setting $W_i := V^{\pi_{i+1}} - V^{\pi_i}$, we obtain

$$\mathbf{M}^T \nabla W_{i-1} + \nabla_{\pi} f^{\pi}|_{\pi=\pi_{i+1}} - \nabla_{\pi} f^{\pi}|_{\pi=\pi_i} = \mathbf{0}. \quad (\text{D.5})$$

Using the Mean Value Theorem, we can then write (D.5) as

$$\mathbf{M}^T \nabla W_{i-1} + (H_\pi f^\pi)|_{\pi'}^T \cdot (\pi_{i+1} - \pi_i) = \mathbf{0} \quad (\text{D.6})$$

for some $\pi' \in \mathbb{R}^d$.

It follows from Assumption 3 that $H_\pi f^\pi$ is negative definite, hence invertible, so we can rewrite (D.6) as

$$\pi_{i+1} - \pi_i = -\{(H_\pi f^\pi)|_{\pi'}^T\}^{-1} \mathbf{M}^T \nabla W_{i-1}. \quad (\text{D.7})$$

Comparing (D.1) for i and $i+1$,

$$\begin{cases} \frac{1}{2} \text{Tr}\{\sigma^T (H V^{\pi_{i+1}}) \sigma\} + (\mathbf{M}\pi_{i+1} + \mathbf{b})^T \cdot \nabla V^{\pi_{i+1}} - \alpha V^{\pi_{i+1}} + f^{\pi_{i+1}} = 0, \\ \frac{1}{2} \text{Tr}\{\sigma^T (H V^{\pi_i}) \sigma\} + (\mathbf{M}\pi_i + \mathbf{b})^T \cdot \nabla V^{\pi_i} - \alpha V^{\pi_i} + f^{\pi_i} = 0, \end{cases} \quad (\text{D.8})$$

and subtracting, we get

$$\begin{aligned} & \frac{1}{2} \text{Tr}\{\sigma^T (H W_i) \sigma\} + (\mathbf{M}\pi_{i+1} + \mathbf{b})^T \cdot \nabla W_i - \alpha W_i \\ & + \{\mathbf{M}(\pi_{i+1} - \pi_i)\}^T \cdot \nabla V^{\pi_i} + (f^{\pi_{i+1}} - f^{\pi_i}) = 0. \end{aligned} \quad (\text{D.9})$$

We define \mathcal{R}_i as

$$\mathcal{R}_i = (\pi_{i+1} - \pi_i)^T \mathbf{M} \nabla V^{\pi_i} + (f^{\pi_{i+1}} - f^{\pi_i}), \quad (\text{D.10})$$

then we obtain, from Taylor's theorem,

$$\begin{aligned} \mathcal{R}_i &= (\pi_{i+1} - \pi_i)^T \cdot \left\{ \mathbf{M} \nabla V^{\pi_i} + \nabla_\pi f^\pi|_{\pi=\pi_{i+1}} - \frac{1}{2} H_\pi f^\pi|_{\pi'} \cdot (\pi_{i+1} - \pi_i) \right\} \\ &= -\frac{1}{2} (\pi_{i+1} - \pi_i)^T (H_\pi f^\pi)|_{\pi'}^T \cdot (\pi_{i+1} - \pi_i) \text{ from (D.4)}. \end{aligned} \quad (\text{D.11})$$

Using (D.7), we can write (D.11) as

$$\mathcal{R}_i = -\frac{1}{2} (\mathbf{M}^T \nabla W_{i-1})^T (H_\pi f^\pi|_{\pi'})^{-1} (\mathbf{M}^T \nabla W_{i-1}), \quad (\text{D.12})$$

and then we can rewrite (D.9) as

$$\frac{1}{2} \text{Tr}\{\sigma^T (H W_i) \sigma\} + (\mathbf{M}\pi_{i+1} + \mathbf{b})^T \nabla W_i - \alpha W_i + \mathcal{R}_i = 0. \quad (\text{D.13})$$

We have the same Dirichlet condition on the boundary of the domain for each V^π ,

therefore $W_i \equiv 0$ on $\partial\mathcal{E}$. From Schauder's estimate on second order linear elliptic partial differential equations [23, pg. 108], we conclude that

$$\|W_i\|_{2,\beta} \leq C\|\mathcal{R}_i\|_{0,\beta} = C\|\nabla W_{i-1}\|_{0,\beta}^2 \leq C\|W_{i-1}\|_{2,\beta}^2, \quad (\text{D.14})$$

where the constant C depends only on the domain \mathcal{E} , the ellipticity constant ν , and the bounds on the coefficients of the elliptic differential operator. \square

Appendix E

Arbitrage-free Markets

E.1 Introduction

We recall that the existence of a risk neutral measure implies that there is no arbitrage opportunity in the market [33]. Hence, we show the existence of such a measure in the new model proposed in Chapter 2 and in the setup in Chapter 4.

E.2 No Arbitrage for the New Model

We show that the new model (2.4) in Chapter 2 has a risk neutral measure, hence that the market is arbitrage-free. We refer to [33] (pg. 393) for further reference.

We recall the new model:

$$\begin{cases} dS = \mu S dt + \sqrt{v} S dW^1 \\ dv = \kappa(\bar{v} - v + Q \frac{\partial F}{\partial v}) dt + \eta \sqrt{v} dW^2 \\ d\langle W^1, W^2 \rangle_t = \rho dt \end{cases}, \quad (\text{E.1})$$

with some coefficient Q and some function F . Note that from the theory of partial differential equations, the term $\partial F / \partial v$ is continuous and bounded with continuous initial and boundary conditions.

Let \tilde{W}^2 be a Brownian motion that is independent of W^2 such that $W^2 = \rho W_1 + \sqrt{1 - \rho^2} \tilde{W}^2$. Any $\sigma(W_s^1, W_s^2, s \leq t) = \sigma(W_s^1, \tilde{W}_s^2, s \leq t)$ -martingale can be written as stochastic integrals with respect to the pair (W^1, \tilde{W}^2) . Therefore, any Radon-Nykodým density satisfies

$$dZ_t = Z_t(\phi_t dW_t^1 + \gamma_t d\tilde{W}_t^2), \quad (\text{E.2})$$

for some predictable processes ϕ and γ .

Since we need to find a risk neutral measure, we focus on the case when $\gamma = 0$, when $dZ_t = \phi_t Z_t dW^1$. We want to look for a measure which makes $e^{-rt} S_t$ a martingale under the measure $\mathbf{Q} = Z\mathbf{P}$, hence $Ze^{-rt} S_t$ a local martingale under the measure \mathbf{P} . $Ze^{-rt} S_t$ satisfies the SDE:

$$\begin{aligned} d(Ze^{-rt} S_t) &= (e^{-rt} S) dZ + Z d(e^{-rt} S) + dZ \cdot d(e^{-rt} S) \\ &= Ze^{-rt} S \{(-r + \mu_t + \sqrt{v} \phi_t) dt + (\phi_t + \sqrt{v}) dW^1\}, \end{aligned} \tag{E.3}$$

where the first equality is derived from integration by parts. From (E.3), $Ze^{-rt} S_t$ is a local martingale under the measure \mathbf{P} if and only if $-r + \mu_t + \sqrt{v} \phi_t = 0$. With this ϕ , we found a risk neutral measure and therefore the market is arbitrage-free. This proves Proposition 2.2.1.

Remark 20. *The positive variance condition (2.6) guarantees $v > 0$ a.s..*

E.3 No Arbitrage in the Technical Analysis Setup

E.3.1 Technical Analysis Setup

We first review the setup for the technical analysis model. We assume that there are levels L and H ($0 < L < H$) at which the regimes change. We define the *positive region* as the domain $[L, \infty)$ and the *negative region* as the domain $(0, H]$. Note that the two regions have non-empty intersection $[L, H]$.

We assume that there are only two regimes in the price process; the positive regime and the negative regime.

Under the positive regime, the process lies in the positive region and has dynamics

$$dS_t = \mu_+ S_t dt + \sigma_+ S_t dW_t, \tag{E.4}$$

where μ_+ and $\sigma_+ > 0$ are constants and W_t is a one dimensional Brownian motion. The transition from the positive to the negative regime occurs when the positive regime is in place and S exits the positive region.

On the other hand, under the negative regime, the process lies in the negative region and has dynamics

$$dS_t = \mu_- S_t dt + \sigma_- S_t dW_t. \tag{E.5}$$

where μ_- and $\sigma_- > 0$ are constants. The transition from the negative to the positive regime occurs when the negative regime is in place and S exits the negative region.

Let $r > 0$ denote the interest rate and we assume

$$\mu_- < r < \mu_+. \quad (\text{E.6})$$

The condition (E.6) implies the discounted price process is a supermartingale under the negative regime and a submartingale in the positive regime up to the time of the first regime transition.

To keep track of which regime currently holds, we define the flag process F_t which takes values in $\{-1, +1\}$ as

$$F_t = \begin{cases} +1 & \text{if the dynamics correspond to the positive regime} \\ -1 & \text{if the dynamics correspond to the negative regime} \end{cases}. \quad (\text{E.7})$$

The flag process F_t indicates under which regime the price process S_t is at time t . From the definition of the regime transition, F_t jumps from one value to the other only in the following cases:

$$\begin{cases} F_{t-} = +1 \text{ and } S_t = L, \text{ then } F_t = -1 \\ F_{t-} = -1 \text{ and } S_t = H, \text{ then } F_t = +1 \end{cases}. \quad (\text{E.8})$$

E.3.2 No Arbitrage

Let S be the process determined by the SDE $dS = \mu S dt + \sigma S dW$ with a Wiener process W under the measure \mathbf{P} . We introduce θ as

$$\theta = \frac{\mu - r}{\sigma}. \quad (\text{E.9})$$

Then we have the following proposition:

Proposition E.1. ([33]) *If Z is the process defined by*

$$Z(t) = \exp\left(-\int_0^t \theta(s) dW(s) - \frac{1}{2} \int_0^t \theta(s)^2 ds\right), \quad (\text{E.10})$$

then the measure $\tilde{\mathbf{P}} = \tilde{\mathbf{P}}_T$ defined by $d\tilde{\mathbf{P}} = Z(T)d\mathbf{P}$ is a risk neutral measure.

We define θ_+ and θ_- to be

$$\theta_+ = \frac{\mu_+ - r}{\sigma_+}, \quad \theta_- = \frac{\mu_- - r}{\sigma_-}. \quad (\text{E.11})$$

From Proposition E.1, we construct the risk neutral measure as

$$Z'(t) = \exp \left(- \sum_i \int_{\tau_i}^{\tau_{i+1}} \theta'(s) dW(s) - \frac{1}{2} \sum_i \int_{\tau_i}^{\tau_{i+1}} \theta'(s)^2 ds \right), \quad (\text{E.12})$$

where τ_i 's are stopping times when regime switching happens and θ' is defined as

$$\theta' = \begin{cases} \theta_+, & \text{when } S_t \text{ is in the positive regime between } \tau_i \text{ and } \tau_{i+1} \\ \theta_-, & \text{when } S_t \text{ is in the negative regime between } \tau_i \text{ and } \tau_{i+1} \end{cases}, \quad (\text{E.13})$$

or equivalently,

$$\theta' = \begin{cases} \theta_+, & \text{when } F_t = +1 \text{ between } \tau_i \text{ and } \tau_{i+1} \\ \theta_-, & \text{when } F_t = -1 \text{ between } \tau_i \text{ and } \tau_{i+1} \end{cases}. \quad (\text{E.14})$$

θ' is a predictable process and it is bounded, so from Novikov's condition, Z' is a martingale. Therefore, this is a risk neutral measure and the market is arbitrage-free. This proves Proposition 4.2.1.